CHALMERS

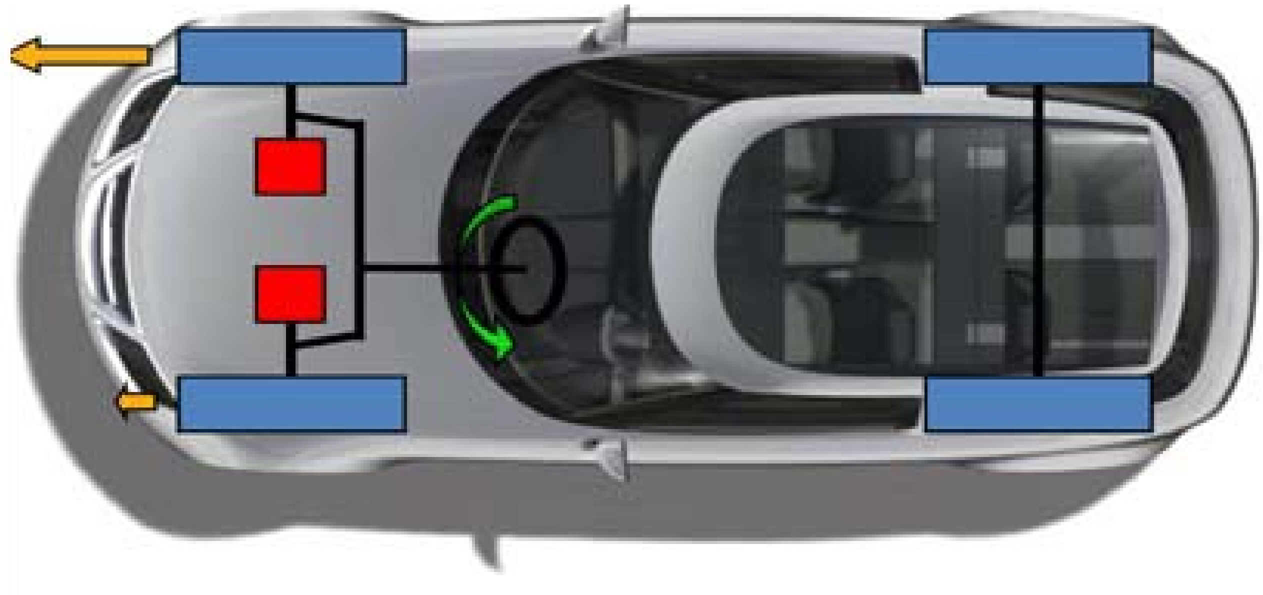

New Vehicle Functionality Using Electric Propulsion

Master's thesis in Automotive Engineering

ADITHYA ARIKERE

Department of Applied Mechanics
Division of Vehicle Engineering & Autonomous Systems
Vehicle Dynamics Group
CHALMERS UNIVERSITY OF TECHNOLOGY
Gothenburg, Sweden 2012
Master's thesis 2012:20

MASTER'S THESIS IN AUTOMOTIVE ENGINEERING

New Vehicle Functionality Using Electric Propulsion

ADITHYA ARIKERE

Department of Applied Mechanics
Division of Vehicle Engineering & Autonomous Systems
Vehicle Dynamics Group
CHALMERS UNIVERSITY OF TECHNOLOGY

Gothenburg, Sweden 2012

New Vehicle Functionality Using Electric Propulsion
ADITHYA ARIKERE

Master's thesis 2012:20
ISSN 1652-8557
Department of Applied Mechanics
Division of Vehicle Engineering & Autonomous Systems
Vehicle Dynamics Group
Chalmers University of Technology
SE-412 96 Gothenburg
Sweden
Telephone: +46 (0)31-772 1000

Cover:
A Saab concept car showing a two motor front wheel drive electric drivetrain layout

Chalmers Reproservice
Gothenburg, Sweden 2012

New Vehicle Functionality Using Electric Propulsion
Master's thesis in Automotive Engineering
ADITHYA ARIKERE
Department of Applied Mechanics
Division of Vehicle Engineering & Autonomous Systems
Vehicle Dynamics Group
Chalmers University of Technology

Abstract

More stringent emission and fuel efficiency requirements for cars are leading to increased electrification of drivetrains. There arises a need to be able to justify the significantly increased costs associated with the electrification. One way to do this is to achieve new or improved functions using the new electric actuators available at our disposal.

Significant number of publications are available that study making use of electrification to do basic functions such as propulsion, regenerative braking and in some cases, direct yaw control. This project aims to go beyond such basic functions, identify new functions and develop one of them with high potential.

First, brainstorming was done to identify new functions. These functions were subjected to detailed analysis and rating to select the one with the highest potential. The vehicle configurations (location of motors, engine and the wheels/axles they drive) were also analysed to identify the best among them. The selection process yielded "Customise feel" as the best function.

Next, the function was developed to tune the transient yaw dynamics of the vehicle using an empirical feed forward controller and the steering torque feedback using a model based controller. The steering torque controller was rudimentary in design and was a proof of concept to show that effective control of steering torque can be done. The yaw response controller on the other hand was a more comprehensive controller. The controller parameters were determined through optimisation by `Matlab`'s *Genetic Algorithm*. The controller optimisation was done for step steer manoeuvres at different speeds. The tuned controller was then validated for different manoeuvres and scenarios.

The results of simulations run with these controllers on a comprehensive 9 degree of freedom vehicle model are presented and it is seen that a yaw response time reduction of between 30% to 60% and a yaw overshoot reduction of between 15% to 80% can be achieved in the step steer manoeuvres at different speeds. The steering torque was also reduced by the targeted 30% effectively.

It is seen that the torque vectoring capability is very effective in controlling both the lateral dynamics and the steering torque of the vehicle. This capability of torque vectoring therefore opens up new possibilities in effective control of vehicle motion and hence in future active safety systems.

Keywords: customer functions, drivetrain electrification, torque vectoring, yaw response, steering torque

Preface

This master thesis project was carried out as part of the PhD project titled "Improved Stability and Manoeuvrability using Electric Propulsion" which is being executed in partnership with e-AAM driveline systems, Autoliv, Leannova, Innovatum and Chalmers. The project is funded by FFI (Strategic Vehicle Research and Innovation) platform of Vinnova which is a Swedish governmental agency aimed at increasing the competitiveness of Swedish researchers and companies.

This master thesis project was aimed to be a broader but less in-depth version of the PhD project, i.e., while the PhD project focuses only on and goes in depth into active safety functions, the master thesis project considers all types of functions and develops only one of them as much as time allows. Large parts of this master thesis work will be carried forward into the PhD project.

The master thesis project was fully carried out at Chalmers.

Acknowledgements

I would like to thank my adviser Gunnar Olsson and my examiner Bengt Jacobson for their invaluable support and continuous feedback throughout the project.

I am also grateful toward my colleague Matthijs Klomp for always being available for a technical discussion and whose experience and feedback were of great help in improving the project.

Lastly, I would like to thank my other colleagues at the Vehicle Dynamics Group, especially Mathias Lidberg, for their feedback during presentations and help with the brainstorming session.

Göteborg, June 2012,
Adithya Arikere

Nomenclature

Symbol	Description	Units
m	Total vehicle mass	kg
m_s	Sprung mass	kg
I_{zz}	Moment of inertia about $\mathcal{Z}$ axis (Yaw moment of inertia)	kgm^2
I_{yy}	Moment of inertia about $\mathcal{Y}$ axis (Pitch moment of inertia)	kgm^2
I_{xx}	Moment of inertia about $\mathcal{X}$ axis (Roll moment of inertia)	kgm^2
l	Wheel base	m
l_i	Distance of axle i from vehicle center of gravity	m
s_i	Half track width of axle i	m
R_w	Wheel radius	m
ω_i	Angular velocity of wheel i	rad/s
u_i	Longitudinal velocity of wheel i	m/s
v_i	Lateral velocity of wheel i	m/s
δ	Road wheel angle	rad
$a_{x,y}$	Longitudinal (x) or lateral (y) acceleration	m/s^2
$h_{0,r}$	Height of center of gravity above roll axis	m
$h_{0,p}$	Height of center of gravity above pitch axis	m
$h_{i,r}$	Height of roll center of axle i	m
$h_{i,p}$	Height of pitch center of axle i	m
ϕ	Roll angle	rad
θ	Pitch angle	rad
$k_{\phi,i}$,k_ϕ	Roll stiffness of axle i and total roll stiffness	N/rad
$c_{\phi,i}$,c_ϕ	Roll damping of axle and total roll damping i	Ns/rad
k_θ	Pitch stiffness	N/rad
c_θ	Pitch damping	Ns/rad
$\alpha_{\{f,r\}\{l,r\}}$	Slip angle of the left or right wheel on the front or rear axle	rad
$F_{\{x,y\},\{f,r\}\{l,r\}}$	Longitudinal (x) or lateral (y) force of the left or right wheel on the front or rear axle	N
ΔT	Difference in torques being supplied across an axle	Nm
B,C,c_0,c_1,μ_0,μ_1	Tyre and road parameters for *Magic formula*	-
κ_i	Longitudinal slip of wheel i	-
α_i	Lateral slip angle of wheel i	-
$\sigma_{x,i}$	Normalised longitudinal slip of wheel i	-
$\sigma_{y,i}$	Normalised lateral slip of wheel i	-
σ_i	Combined slip of wheel i	-
γ	Castor angle	rad
β	Kingpin inclination	rad
d_{kpo}	Kingpin offset at wheel hub center	m
u	Longitudinal velocity	m/s
v	Lateral velocity	m/s
r	Yaw rate	rad
Single track model		
a	Distance of front axle from vehicle center of gravity	m
b	Distance of rear axle from vehicle center of gravity	m
C_f	Front axle stiffness	N/rad
C_r	Rear axle stiffness	N/rad
α_f	Front axle slip angle	rad
α_r	Rear axle slip angle	rad
F_{fy}	Front axle lateral force	N
F_{yr}	Rear axle lateral force	N

Contents

1 Introduction

Increasing pressure from governments and environmentally aware customers to make more eco-friendly and sustainable cars has led to the electrification of the drivetrain in recent decades. One of the early adopters of this practice was the Toyota Prius and the Honda Insight. These cars were focused on mainly improving efficiency over their pure fossil-fuel based counterparts.

While the Toyota Prius became quite successful, the Honda Insight failed to capture significant market share. One of the reasons for this - and the reason why most hybrids are not very popular - is the cost. Adding a heavy electric drivetrain and battery in addition to the existing engine significantly increases the weight which in turn hampers handling, performance and fuel efficiency. To counter-act these effects, more expensive lightweight and stiffer materials, more efficient batteries, etc. are required, which increase cost even further. Due to this, it becomes hard to justify the large increase in cost for limited improvement in fuel efficiency.

However, over the years, due to even more pressure from legislation, there has been rapid drive to electrify cars. So far, manufacturers have only been using a single motor electric/hybrid drive to power their cars. The main advantage in these vehicles is the capability to perform regenerative braking which is to recuperate energy from the moving vehicle by braking using the electric motor. This energy is otherwise wasted as heat from the braking system in conventional vehicles.

Electric motors are powerful actuators which have a very short response time; shorter than traditional hydraulic brakes or IC engines and are more precisely controllable. Having such powerful actuators at our disposal open up lots of opportunities. Even with single motor configurations, the availability of an accurately controllable high power and torque electrical actuator allows significant control over the vehicle dynamic characteristics of the vehicle.

In recent years, due to the ever increasing electrification of drivetrains, there has also been a push towards vehicle layouts with multiple electric motors. These offer even more opportunities in terms of precision and response in control of the driveline. Additionally, increased electrification enables radically new vehicle and driveline layouts. Due to high requirements on energy efficiency, there is an equally high demand on weight reduction. This demand to reduce weight provides a strong incentive to achieve or improve existing functionalities using the electric actuators thereby eliminating or downsizing some of the existing actuators. Additionally, there is also the need to justify the increased cost. This can be done by developing new functionalities enabled by the electrified drivetrain which would otherwise have not been feasible.

There is therefore a need to identify and analyse the new opportunities provided by the electrified drivetrain. This project aims to do this.

In this project, the various new vehicle dynamic functions that are enabled by the electrification of the drivetrain are identified through brainstorming and literature survey. These functions are then analysed in detail with regards to their cost, potential benefit, actuators required, etc. Among these functions, one is chosen, developed further and validated in this project.

Apart from the new functions mentioned in this report, currently available active vehicle dynamics systems such as active roll bars, active dampers, etc. will become possible in terms of cost and size [21] due to the availability of high voltage electric supply in the car. This would not only help towards alleviating some of associated problems with electric vehicles such as worsening of handling and performance due to increased weight, but even improve them beyond those of conventional vehicles.

Although currently not possible, when electric drivetrain technology matures, it may become possible to eliminate friction brakes completely. It may also become possible to eliminate the power steering system and maybe even the mechanical steering setup completely.

1.1 Objective

The objective of this project is to identify new functionalities that can be achieved in vehicles with electrified drivetrains, select one with high potential, develop and validate it.

1.2 Limitations

To limit the scope of the project, certain constraints have been imposed.

- Single motor configurations have been ignored since they do not offer much room to develop new functionalities.
- For hybrid vehicles, only layouts with the internal combustion engine (ICE) at the front driving the front wheels are considered since this is the predominant layout.
- Functions that use the current sensor set in a well equipped car are prioritized for development.

2 Concepts

For the purposes of this project, there are three terms which are defined as follows:

- **Function:** A function is defined as a specific task that can be performed by the vehicle or the actuators which may be of benefit directly or indirectly to the user. Functions can be either customer functions which are immediately obvious to the driver or engineering functions which are not easily noticeable by the driver but can be used as part of a bigger function. Eg., friction estimation is an engineering function but friction display for the driver is a customer function.
- **Configuration:** Configuration refers to the positioning of the electric motors and the engine and the wheels they drive. Each configuration is uniquely identifiable. Eg., a vehicle layout with engine driving the front wheels and two electric motors each driving one rear wheel is a configuration.
- **Concept:** A concept is a combination of a function and a configuration. This enables accurate evaluation of the function since the capabilites and effectiveness of the actuator set towards the specific function can be evaluated. Eg., autonomous parking with a hybrid vehicle with an engine at the front driving the front wheels and two electric motors at the front each driving one front wheel is a concept.

This chapter discusses the various new functionalities or the improvements of existing functionalities that can be achieved with the electrification of the drivetrain. The various possible concepts, their requirements, feasibility, etc. will be discussed. The different drivetrain configurations will also be listed and analysed in terms of the new functionalities that can be achieved, the cost, feasibility, etc.

2.1 Functionalities

A brainstorming session was held in order to come up with new and varied ideas for functionalities. The ideas and a brief description of these along with the minimum requirements to achieve these functionalities are presented in section 2.1.1 followed by section 2.1.2 with a brief analysis of the functions and elimination of some of them.

2.1.1 Function list

Table 2.1.1: New functionalities using electric drivetrain

Function name	Function description	Min. actuator requirements
S-4WD	Switchable 4-wheel drive. Using DSLD in the middle allows regen from 4 wheels and 4-wheel drive	One motor
DYC	Direct yaw moment control using traction of the motors [4, 13, 20, 22–24, 28]. Active stability management using this allows for less stable but more responsive vehicle setups	Independently driven wheels on atleast one of the axles
DTPS	Differential Torque based Power Steering using the motor torques [25]	Independently driven wheels on the front axle
ADD	Active driveline damping using the motor torque [1]	Motor with sufficient power and torque to be able to damp drivetrain oscillations
Autonomous parking	Autonomous parking using the motors only (steering system not used) [5, 16]	Independently driven wheels on atleast one of the axles
Better slip and traction control	The much faster response time of motors allows for more accurate control of slip [14, 18, 20]	A motor atleast on the axle on which the wheel slip is to be controlled

Function name	Function description	Min. actuator requirements
WSE	Wheel state estimator. Using electric machine built-in sensors one could estimate the wheel speed and position eliminating need for separate sensors [14, 20]	Individual motors for wheels
Improved collision avoidance	Can use a combination of braking and torque distribution to brake and steer the vehicle out of harms way	Nothing new required. Addition of new motors will improve response
APC	Active pitch control can be achieved during moderate braking by distributing the torques to the front and rear appropriately	Atleast one motor on each of the axles
DTB	Dynamic front-rear torque biasing. Optimum braking and very good regen. Traction, handling and steering ability can be significantly improved especially at the limit [8–12, 15]	Atleast one motor each on the front and rear axle
ALKA	Active lane keeping assistance	Independently driven wheels on one axle
Cooperative driving	Since braking, turning and propulsion can be achieved autonomously, cooperative driving is now possible	Independently driven wheels on atleast one axle.
Regen braking	Recuperate energy while braking [2, 6, 19]	Atleast one motor
PISC	Post impact stability control [27]. Independently driven wheels allows for more possiblities regarding the control of the vehicle.	Independently driven wheels on one axle
Auto-parking brake & hill climb assist	Brakes can be actuated each time the vehicle comes to a halt. No need to brake or activate the parking brake manually. Vehicle doesn't move until driver taps the accelerator pedal	Atleast one motor
Torque vectoring	Using independently driven wheels, torque vectoring can be achieved which will improve handling and traction.	Independently driven wheels on an axle
Regeneration via road	If electric propulsion on one axle and ICE on the other, battery can be charged via road.	Motor(s) on one axle and ICE on the other
Friction estimation	With individually driven wheels, one could do "longitudinal force neutral" interventions so that some tyre contacts are temporarily excited aiding friction estimation [14, 20]	Multiple motors
Rollover prevention	Using motors to brake or provide traction to prevent rollover [3]. Improvement of existing functionality	Independently driven front wheels
Launch control	Launch control can be achieved using the electric machines	Independently driven wheels on atleast one axle
Power-slide control	Getting into and maintaining a power-slide could possibly be made easier using independently driven rear wheels	Independently driven rear wheels
DMS	Drive Mode Selector. Allows for different drive modes such as "Optimal Path", "Min tyre wear", "Min energy consumption", etc., to be selected	Atleast two motors on one axle

Function name	Function description	Min. actuator requirements
RGM	Road Grip Maximization. Distribute torque to wheels according to their capability or as required [26] to maximize wheel capacity utilization	Atleast two motors on one axle
FVC	Force Vector Control. Control the direction of tyre force. Maybe effective for path control	At least two motors on one axle
Customise "feel"	Ability to customise the steering and brake feel to "sporty" or "city" or "highway", etc.	Aleast two motors on an axle
Autonomous driving	Propulsion, braking and steering can be achieved independent of driver input. Allows for driving autonomously during some scenarios like overtaking, garages, etc	Atleast two motors on one axle
ZEM	Zero emission mode. For indoor driving, short distance driving, parking, etc.	One motor
Mobile power plant	Availability of an engine and a high voltage electrical system allows for it to be used as an emergency power source	One engine and motor and capability to recharge while stationary
Higher steering angle	In-wheel motors enable higher steering wheel angles	Two in-wheel motors at the front
Skid steering	Very low turning radius enabled by differential wheel rotational speeds [7]	Atleast two motors on one axle
Speed based ride improvement	Using wheel speed control to improve ride over wavy or rough terrain	Atleast two motors on an axle
Power boost	Provide short term power boost (even in the power limited region)	One motor
SD	Software differential. The effect of LSD, DSLD, etc can be simulated. The wheels can be locked or constrained left-right or front-rear	Atleast two motors
Yaw damping	By simulating locked differential, yaw damping can be achieved	Two motors on one axle
AWD	All wheel drive	One motor for each axle
ESC	Electronic stability control. Intervenes when vehicle is about to become unstable [18]	Independently driven wheels all round
SME	Safety margin estimation. Estimate the admissible operating region for the vehicle and keep the vehicle in that region.	One motor
Fuel efficiency improvement	By cleverly using the engine and the motors in the operating regions where they are most efficient, recharging only when the engine is at its most efficient, fuel efficiency can be improved	One motor, an engine
Brake disc cleaning	Cleaning the brake disc by using force neutral interventions	One motor on each axle
Brake condition estimation	Estimate the brake state (temperature, wear, etc) using force neutral interventions	One motor on each axle

Function name	Function description	Min. actuator requirements
Vehicle properties estimation	Since motor torque is accurately known, vehicle mass and maybe even weight distribution, drag coefficient, etc can be estimated.	One motor
Environment properties estimation	Using the motor torque required to maintain various speeds, the gradient, headwind speed, etc can be estimated	One motor
Wheel lift control	Using traction torque and braking force simultaneously, wheel lift may be possible to control	Motor driving the wheel to be controlled
Rapid brake application	Allows for rapid emergency braking. Substitute for brake pre-fill function	Motor driving wheel which needs the function
Drag free brakes	Low motor response time allows higher gaps between brake pad and disc reducing brake drag	Motor driving wheel which needs the function
Sensor assist	Using the torque, speed and distance estimation using motors, active safety functions such as platooning, overtaking, etc., can be improved	One motor
Drivability enhancement	Compensate for lack of torque response from engine using the elec. motors	Atleast one motor

2.1.2 Analysis

In the preliminary function analysis, customer functions that focus on vehicle dynamics are prioritized for development.

The regen braking and fuel efficiency improvement functions can be eliminated from further analysis since they are rather obvious functions although clearly important. The functions have been studied in detail in both academia and industry. Additionally, these are very well known and therefore not the focus of this thesis.

Torque vectoring is more of a hardware capability in the vehicle and by itself doesn't offer any advantages. Clever use of this capability is more important and such control strategies are discussed later. Therefore, torque vectoring as a functionality is not considered for further development. AWD is also a hardware capability and offers some advantages even without any form of control strategy. However, the potential for further benefits that can be obtained from good control of this capability is limited and is hence not considered for further development. On the other hand, force vector control utilizing AWD is an idea for a low level control strategy which can be used as part of higher level functions.

The large steering angle functionality is more of a hardware capability that is enabled by in-wheel electric motors. The gain in wheel steering angle is limited by the steering linkages and wheel package and not by the control of the motors. This functionality is therefore not considered for further development. ZEM or indoor driving mode, the mobile power plant and the power boost functions have very little impact on vehicle dynamics and are hence omitted from further analysis.

Rapid brake application is a substitute for brake pre-fill to enable emergency braking. This functionality is enabled on its own when electric drivetrains are available due to their short response time and no additional modifications have to be made. Drag free brakes is a CO_2 reduction option wherein brakes with low drag and higher gap between the brake pads and the discs are used since the response time of brakes are now guaranteed with the help of electric machines. It doesn't add any new vehicle dynamic functionality and is therefore not considered further.

The different types of vehicle stability control systems can be classified as a) differential braking systems, b) active steering systems and c) active torque distribution systems [17]. In [24], the authors make the case for controlling the wheel tractive forces for more effective stability enhancement than active steering. Hence active steering based manoeuvrability or stability functions will be given less priority. Additionally, since electric torque vectoring systems are generally a lot quicker than differential braking systems, torque vectoring based functions will be prioritized as well.

The ESC, yaw damping and roll-over prevention functions can be enhanced with the presence of electric machines. However, the DYC is a superior function that uses the same concepts to achieve better results. These functions can be seen as a sub-function of the DYC and are hence not chosen for further development in favour of the DYC. Similarly, the launch control function is a subset of the slip control function and is hence not considered for development.

The Auto-Parking brake (APB) and Hill Climb Assist (HCA) are existing functionalities that can be slightly enhanced with electric motors. No new functionality is added and hence the function is not considered for further development. The same is the case with Active Lane Keeping Assistance. The function already exists and no significant performance gain is forseen with electric motors.

The traction and handling improvement function through dynamic front-rear torque biasing was also not chosen for further development in favour of other higher level functions such as DYC, RGM, etc.

Some functionalities offer very little enhancement for the users while requiring significant resources or compromises. For instance, the APC and the wheel lift control systems are hard to realize as they require significant torque inputs from the motors and the brakes and are very dependent on the suspension geometry.

The co-operative driving functionality or platooning is a rather tough function to realize in such a short period. Additionally, the function largely involves processing data from various sources like video, radars, GPS, etc., and using them to plan a path. Similarly, autonomous driving, PISC and collision avoidance are functions that are too elaborate, very safety critical and cannot be realized in the short time frame.

With the speed based ride improvement function, the objective was to improve ride by controlling the wheel positions over rough terrain so as to minimize some discomfort metric (pitch or roll or vertical travel). Another possible way to improve ride is speeding up or slowing down the wheels so that longitudinal disturbances on the vehicle are minimized. However, this function is quite challenging to implement in the time period and therefore not considered for further analysis.

In the list of functions in table 2.1.1, several of them are engineering functionalities. These are no less important for their lack of user appreciation since they may be used as part of - and might well be crucial to - other high level functionalities. The safety margin estimation, vehicle and environment properties estimation, friction estimation, sensor assist, brake disc cleaning and brake condition estimation, road regen, switchable 4WD, software differential active driveline damping and wheel state estimation are all engineering functionalities and are therefore not considered for development in this project.

The remaining functions to be analysed are:

1. Direct Yaw Control (DYC)
2. Differential front wheel Torque based Power Steering (DTPS)
3. Improved Slip Control (ISC)
4. Autonomous parking (AP)
5. Power Slide Control (PSC)
6. Drive Mode Selector (DMS)
7. Road Grip Maximisation (RGM)
8. Customizable “feel” (CF)
9. Skid steering (SS)
10. Drivability enhancement (DE)

2.2 Reference Manoeuvres

In this section, the reference manoeuvres that are used to rate the various concepts in further concept evaluation sections are described. Note that the concepts are not simulated using these manoeuvres but rather engineering judgement is used to rate the concepts for their performance in these specific manoeuvres.

2.2.1 Longitudinal dynamics

To evaluate how well the available traction is utilized, the vehicle can be subjected to acceleration and deceleration tests. The vehicle can be accelerated from and decelerated to standstill over a stretch of fixed length. Different road surfaces such as split-μ, step-μ along with a normal road can be considered. This will show up any weakness in the slip control of individual wheels and how quickly it can adapt to changing conditions.

For longitudinal acceleration response time, the vehicle is accelerated from a slow speed in a high gear. The time the vehicle takes to reach a specified acceleration level is the longitudinal acceleration response time. This helps to highlight the engine's low-end power delivery.

2.2.2 Steering

The vehicle is driven at a constant speed with steadily increasing steering input. The steering torque during this manoeuvre can be used to see how well the aligning moment curve is replicated.

For signal to noise ratio of the power steering system, the same test can be run on a rough gravel track. Two other parameters of importance for the steering system is the maximum power and the maximum assist torque which can be calculated from the motor torque ratings and the steering and the suspension geometry.

2.2.3 Lateral dynamics

To test the low speed manoeuvrability of the vehicle, the vehicle can be driven at a low speed with full steering lock applied. Another test that can be done is to drive the vehicle in a tight circle of fixed radius at low speed and measure the steering torque required. The steering torque required and the turning radius achieved in the previous tests are good indicators of vehicle's low speed manoeuvrability.

For the vehicle stability, the yaw response ratio (YRR) of the vehicle can be looked at. Since the vehicles in this analysis may have torque vectoring on the front or the rear axle, for fairness, two tests can be conducted, one while accelerating and one while decelerating. The test specification can be taken from the `FMVSS126` standard. A sine with dwell steering manoeuvre is used in this test.

A simple step steer manoeuvre can be used to determine the vehicle's lateral acceleration and yaw response time. The same test can be used for determining the yaw damping performance of the vehicle as well. The test specification can be taken from the `ISO7401` standard.

The lateral acceleration gain of the vehicle can be determined by taking the lateral acceleration over the steering wheel input when the vehicle is driven with a constant speed with a constant steering angle.

For the other evaluation criteria such as cost, comfort, scalability, etc., the evaluation is done subjectively and no reference manoeuvres can be prescribed.

2.3 Concept evaluation

The concept evaluation and selection is carried out in several steps. First, the functions are evaluated for their maximum value given no restriction on the vehicle configuration. This gives us a reference as to the maximum value that each function can provide. Next, the configurations are evaluated for the maximum enabled function value that they provide per actuator cost. Lastly, the functions are evaluated once again using the best configuration as determined from the previous step. This gives an idea of the best function in real world terms and when compared with the first step, gives an idea of how much each function is crippled with the chosen configuration or how much it can be improved with a better configuration. This can be used to support a decision to adopt a configuration with more freedom in order to extract more value out of the chosen function.

2.3.1 Preliminary evaluation

In table 2.3.1, the functions listed in section 2.1.2 are evaluated based on how well they satisfy customer requirements using a comparison matrix similar to the *Pugh Matrix* method. The ratings in this matrix are based on engineering judgement. Note that cost of the function has been deliberately given a lower weight since this is a concept study and not a feasibility study to see if the function is viable. The idea here is to see if given an electric drivetrain powered vehicle, can additional functionalities be added to it that enhance the driving experience. In this case, the four motor hybrid vehicle is chosen as the configuration since this offers the maximum number of degrees of freedom thereby enabling one to extract the maximum benefit of each functionality. Choosing this configuration allows us to see the maximum potential of each of the functions in the best case scenario.

The reference function in all the following comparison matrices is a rudimentary function that works as follows:

- Under normal high speed driving, the vehicle is driven by the engine only. Partial energy recuperation is done through the front motors (if available, else the rear motors) if the battery energy reserves are low and the vehicle is driving straight.
- Under low speed city driving, the vehicle is powered by the front motors (if available, else the rear motors) as long as the battery has sufficient charge. Otherwise, the engine powers the vehicle.
- While braking, the brake forces to the wheels are distributed in the same proportion as a typical IC engine car. As far as possible, the braking is done through the e-motors, the remaining braking torque is supplied by the hydraulic brakes.
- In case of instability and the ABS, ESC or the TCS is activated, the motors are shut off completely and the hydraulic brakes and the engine take over.

Table 2.3.1: Function evaluation using comparison matrix for four motor hybrid vehicle

Criteria	Weight	Direct Yaw Control	Differential Torque Power Steering	Improved Slip Control	Autonomous Parking	Power Slide Control	Drive Mode Selector	Road Grip Maximisation	Customise feel	Skid Steering	Drivability Enhancement
Acceleration (normal)	2	0	0	++	0	0	+	++	0	0	0
Acceleration (step mu)	1	0	0	++	0	0	+	+	0	0	0
Acceleration (split mu)	1	0	0	++	0	0	+	+	0	0	0
Long. acc. resp. time	2	0	0	0	0	0	0	0	+	0	++
Str. tq. feedback	4	0	+	0	0	0	0	0	++	−	0
Low spd. maneuvr.	4	0	0	0	0	0	0	0	+	++	0
YRR (accelerating)	1	++	0	0	0	++	+	+	+	0	0
YRR (braking)	1	++	0	0	0	0	+	+	+	0	0
Yaw resp. time	2	++	0	0	0	+	+	+	+	0	0
Lat. acc. gain	1	+	−	0	0	++	+	+	−	0	0
Lat. acc. resp. time	1	+	−	0	0	0	+	+	0	0	0
Yaw damping	2	++	0	0	0	0	+	0	+	0	0
EM power req.	1	0	0	0	0	−	0	0	0	0	0
Recharge time	3	0	0	0	0	−	0	0	0	0	0
Comfort	4	0	+	0	++	++	0	0	++	++	++
Cost	8	0	+	0	−	−	0	0	0	0	0
Robustness	6	0	0	0	−−	−−	0	0	0	0	0
NVH	6	0	0	+	0	0	0	0	0	0	0
Weight	3	0	0	0	0	−	0	0	0	0	0
Space	2	0	+	0	0	−	0	0	0	0	0
Total		14	16	14	−12	−15	12	12	27	12	12

It can be seen from table 2.3.1 that the *Customise Feel* function has the best potential. One important effect that is not captured here is that if one of the functions is implemented then other functions may become less effective. The ratings in the table for each represent the scenario where the respective function and only that is implemented. This ensures that there are no conflicts and that the highest benefit of the function is extracted.

The cost criteria here refers to the cost of the additional sensors and hardware required and also the development cost to ensure the function is production ready. It does not include the cost of the required vehicle configuration itself. For instance, autonomous parking requires several sensors, more processing power and extensive testing to ensure it is safe and can detect all obstacles. The expenses arising due to these are included in the cost criteria. However, the cost comparison here is not really fair since several functions can be implemented with a significantly simpler configuration. For instance the DYC function can be implemented in a two motor front hybrid configuration. So the question now becomes whether each function should be evaluated keeping the same configuration or if a different configuration should be used for each one. If a different configuration is to be chosen, then a new question arises: what is the best configuration for each function? This is tough to answer since most functions have a minimum requirement and any configurations that offer more freedom usually result in better performance. Further, having a configuration that exceeds the minimum configuration in most cases result in being able to better implement additional functions without causing conflicts. Lastly, in a real car, multiple functions will be implemented on a single configuration and hence it is better to have a fixed configuration and analyse the functions rather than choosing a different configuration for each function.

To choose the best configuration, they are evaluated for their capabilities with respect to different functions in table 2.3.2. The rating scheme is 0-1-2 for the functions where 0 means the function cannot be implemented with the configuration, 1 means it can be implemented partially with limited functionality or performance and 2 means the function can be implemented properly. For the cost rating, the one motor-one engine hybrid vehicle is taken as the reference and the configurations are rated with respect to this configuration. All functions have equal weights. The cost criteria has a weight of 5 (values listed in the table already have the weights taken into account). Here, the cost criteria refers to the cost of the actuators, their packaging and development of the vehicle configuration. To simplify the selection process, all hybrid vehicles chosen in this project have the engine in the front driving the front wheels. Additionally, single motor fully electric vehicles have also been discounted since they offer nearly no room for new functionalities at all. Another novel configuration has also been added for consideration. This configuration uses a single motor at the rear to achieve either torque vectoring or propulsion (but not both simultaneously). As can be seen, the two motor rear hybrid configuration comes out on top. This configuration also gives a few other important advantages such as AWD capability and easier packaging as compared to the two motor front configuration. Even though the novel single motor rear configuration comes very close to the two motor rear configuration, it is at a disadvantage since it cannot do both torque vectoring and propulsion simultaneously. It also makes it harder to implement some functions. This is not captured in the analysis.

Table 2.3.2: Actuator configuration selection

Configuration	DYC	DTPS	ISC	AP	PSC	DMS	RGM	CF	SS	DE	Cost	Total
Hybrids												
f:2M	1	2	1	1	0	1	0	2	1	1	-5	5
r:2M	1	0	1	1	2	1	1	1	2	1	-5	6
f:1M,r:1M	0	0	2	0	1	0	1	1	0	1	-5	1
f:1M,r:2M	1	0	2	1	2	1	2	1	2	1	-10	3
f:2M,r:1M	1	2	2	1	1	1	2	2	1	1	-10	4
f:2M,r:2M	2	2	2	2	2	2	2	2	2	1	-15	4
r:1M,sw	1	0	1	0	1	1	1	1	1	1	-2.5	5.5
Pure electric												
f:2M	1	2	1	1	0	1	0	2	1	2	-10	1
r:2M	1	0	1	1	2	1	1	1	2	2	-10	2
f:1M,r:1M	0	0	2	0	1	0	1	1	0	2	-10	-3
f:1M,r:2M	1	0	2	1	2	1	2	1	2	2	-15	-1
f:2M,r:1M	1	2	2	1	1	1	2	2	1	2	-15	0
f:2M,r:2M	2	2	2	2	2	2	2	2	2	2	-20	0

In table 2.3.3, the concepts are evaluated once again for the two motor rear hybrid configuration. Note that the *Differential Torque based Power Steering* system is omitted from this analysis since it cannot be achieved with this configuration. As can be seen, the *Customise Feel* function still has the highest potential. It is also easy to see that it is no longer as valuable as it was with the four motor hybrid configuration. This is because without the motors at the front, the capability to customise the steering feel is lost.

Table 2.3.3: Function evaluation using *Pugh Matrix* for rear two motor hybrid

Criteria	Weight	Direct Yaw Control	Improved Slip Control	Autonomous Parking	Power Slide Control	Drive Mode Selector	Road Grip Maximisation	Customise feel	Skid Steering	Drivability Enhancement
Acceleration (normal)	2	0	+	0	0	+	+	+	0	0
Acceleration (step mu)	1	0	+	0	0	+	+	0	0	0
Acceleration (split mu)	1	0	+	0	0	+	+	0	0	0
Long. acc. resp. time	2	0	0	0	0	0	0	+	0	++
Str. tq. feedback	4	?	0	0	0	0	0	0	−−	0
Low spd maneuvr	4	0	0	0	0	0	0	0	++	0
YRR (accelerating)	1	++	0	0	++	+	+	+	0	0
YRR (braking)	1	++	0	0	0	+	+	+	0	0
Yaw resp. time	2	++	0	0	+	+	+	+	0	0
Lat. acc. gain	1	+	0	0	++	+	+	0	0	0
Lat. acc. resp. time	1	+	0	0	0	+	+	+	0	0
Yaw damping	2	++	0	0	0	+	0	+	0	0
EM power req.	1	0	0	0	−	0	0	0	0	0
Recharge time	3	0	0	0	−	0	0	0	0	0
Comfort	4	0	0	++	++	0	0	+	++	++
Cost	8	0	0	−	−	0	0	0	0	0
Robustness	6	0	0	−−	−−	0	0	0	0	0
NVH	6	0	+	0	0	0	0	0	0	0
Weight	3	0	0	0	−	0	0	0	0	0
Space	2	0	0	0	−	0	0	0	0	0
Total		14	10	−16	−15	12	10	15	8	12

To ensure that the best functions are selected, the top four functions from 2.3.1 - *Direct Yaw Control* (DYC), *Differential Torque based Power Steering* (DTPS), *Improved Slip Control* (ISC) and the *Customise Feel* (ISC) - are analysed once again in detail. The aim of this is to capture other characteristics, advantages and disadvantages that have not been captured in the comparison matrices.

2.3.2 Detailed evaluation

2.3.2.1 Direct Yaw Control (DYC)

One limited kind of DYC that can be achieved during acceleration or braking is by varying the ratio of torques being distributed between the front and rear axle. In this setup, sending drive or braking torque to the appropriate axle is used to control the lateral force capacity of that axle and therefore control the yaw rate of the vehicle. As mentioned, this method is limiting since, to affect the lateral capacity of an axle, the vehicle needs to be accelerating or decelerating and the tyres already need to be near their limit. This brings down the number of situations where this method can be used and it also results in large vehicle side slip angles to be generated. So even though, the yaw rate may be controlled, the vehicle will be offtracking significantly and hence is unstable anyway. Hence this method of controlling yaw is not considered in this project.

A more common version of this function requires torque vectoring capability to apply a net yaw moment on the vehicle. This torque vectoring capability is used to provide unequal torques between the left and right wheels to generate a turning moment which in turn affects the yaw rate. The torque vectoring system is likely to be more effective on the rear axle than on the front axle on a vehicle with 50-50 front-rear weight distribution. This is because, since the rear axle is unsteered, all the torque difference is used to create a turning moment. Whereas on the front axle, only the *cosine* component of the torque difference is used to create a yaw moment. However, since the front wheels are steered, the *sine* component of the net drive torque on the front wheels can be used to create the yaw moment as well. The problem with this is that to counter the *cosine* component of the driving torque on the front wheels, the rear wheels have to be braked and this reduces their lateral force capacity leading to higher sideslip angles. Note also that the weight distribution of the vehicle places some limitations on how much torque vectoring can be done on each axle. For example, vehicles typically have a weight distribution with more load on the front and this means more torque vectoring can be done on the front axle. Overall, taking all factors into account, with the torque vectoring system on the front axle, more unnecessary tractive work is performed which reduces the overall effectiveness of the DYC. Further, a torque vectoring system on the front axle will affect the steering wheel feel as the unequal front wheel torques will typically exert a net aligning moment on the steering system.

One disadvantage of implementing torque vectoring on only one axle is that while torque vectoring is being done, other factors like steering feel, wheel slip, etc may be adversely affected. It may not be possible to resolve conflicts between the requirements of different functions and hence it may not be possible to implement different other functions.

A better scenario is when the torque vectoring system is implemented on both the front and rear axles. This allows the conflicts between different functions to be better resolved. For example, in the case of DYC, torque vectoring can be done on the rear axle while torque vectoring on the front axle will give the required steering feel. Additionally, if the tyre forces at the rear axle saturate, torque vectoring can now be done on the front axle leading to better yaw performance. Overall, even though torque vectoring on one axle is sufficient, the additional degrees of freedom offered by the two axle torque vectoring system can be effectively utilised to improve performance and enable other functions to be implemented.

2.3.2.2 Differential Torque based Power Steering (DTPS)

This function needs torque vectoring capability at the front axle. The idea here is to generate differential torques at the front wheels which will then cause a torque to be applied on the steering system due to the offset of the forces from the kingpin axis. It is important to note that the relationship between steering moment and the differential wheel torques are different depending on whether the torques are generated by in-wheel motors or in-board motors.

One issue with this function is that it influences quite a lot of other functions. Since this function has to be active all the time, the influence is even greater. The differential torques cause a net moment to be applied on the vehicle chassis and this can adversely impact the lateral dynamics of the car. The functions that could be adversely impacted include DYC, DMS, RGM, SS and SD. Given a torque vectoring system on only the front axle, the afore mentioned functions cannot be implemented alongside the power steering system. However, given torque vectoring system on both axles, they can be implemented with some performance penalty. This is because, the rear axle will have to compensate the front axle inputs and also apply additional inputs to satisfy the second function.

An alternative implementation of this system is to just allow it assist the traditional power steering system. This way the power steering system can be downsized and the differential torque based power steering kicks in only when the normal power steering system can't cope with the demands. For instance, during rapid lane change manoeuvres (power limited) and kerb push off (torque limited), the DTPS system can assist the power steering system. In the kerb push off case, since the vehicle is stationary, no other function is affected. On the other hand, applying the moment during rapid lane change will improve the yaw response of the vehicle. However, now the possibility to tune steering feel as required using the DTPS is virtually non-existent and the cost benefits are also significantly lower since the hydraulic power steering system is retained.

One big downside is the difficulty in getting the correct steering feel using this system. The correct feedback torque required from the steering wheel during various scenarios is hard to define and the correct amount of isolation from road disturbances while retaining steering feel might be hard to achieve. This is because the steering torque generated by the motors depend on the kingpin offset, wheel radius, the castor and camber angle and the kingpin inclination. These parameters can change as the steering wheel is turned or as the wheel moves up and down, etc and hence the steering torque assist generated by the motors vary and it will be hard to get the steering feel correct.

2.3.2.3 Improved Slip Control (ISC)

This function needs a motor to power the axle or the wheels on which the ISC function is to be implemented. The advantage of using the electric motor to do this slip control is that the motors have a much shorter response time and are better controllable and therefore can perform much better slip control compared to the traditional hydraulic brakes. With one motor driving the axle, a *select low* slip control strategy can be implemented, i.e., the driving or braking torque is limited by the capacity of the wheel with lesser traction. For instance, during split-μ scenarios, the braking torque for both wheels on an axle will be limited by the braking force that can be applied on the wheel with lower friction. One advantage of this strategy is that since equal braking forces are applied on the left and right wheels, no moment is applied on the vehicle and hence it will tend to go straight without the steering being pulled to one side. The disadvantage is that the higher traction capability of the wheel on the high-μ surface cannot be exploited. If necessary, the hydraulic brakes can be used to take advantage of the wheel with high μ as well, but this will not be as effective since the hydraulic brakes respond slower. If the wheels are independently driven, the individual wheel slips can be controlled and can be made to take advantage of split-μ scenarios.

During hard acceleration, since the electric motors will be providing assist, when slip does occur, the motor torques can be modulated to control slip while the engine torque can be kept constant or taken down slowly if required. During braking, part of the braking (or fully if possible) can be done by the electric motors and hence when the wheel slips too much, the regenerative braking torque can be modulated rapidly while the hydraulic brakes can be kept constant.

This slip control can also be adopted to achieve rapid acceleration from standstill (launch control like in sports cars). The slip can be held between a predetermined optimum level for best acceleration as long as the throttle request is enough to cause the wheels to surpass the specified slip level.

2.3.2.4 Customise Feel (CF)

This function needs atleast one torque vectoring system on one axle. If the torque vectoring system is at the front, it can be used to customise the steering feel or tune the lateral dynamics of the vehicle but not both. If the torque vectoring system is at the rear axle, then steering feel customization cannot be achieved and instead the lateral dynamics of the vehicle can be tuned by making it more responsive or damping the vehicle yaw rate depending on the driver's preferences. However, it needs to be noted that while changing the lateral dynamics, the steering feel of the vehicle will most likely be affected. But this cannot be used to tune the steering feel since this effect will be minor compared to the change in lateral dynamics. Additionally, if it can also achieve propulsion, then the motor can be used to improve the throttle response by providing additional torque and compensate for the engine's response time. It can also act as a driveline damper for the engine at low speeds in comfort mode.

If the torque vectoring system is available on both axles, then the front torque vectoring system can be used to customise steering feel while the rear torque vectoring system can be used to customise the lateral dynamics of the car. Since the steering feel customization only involves providing some differential torque to adjust steering feel and not replace the steering system, the impact on lateral dynamics is minimal.

One important advantage with this system is that since the vehicle feel can be customised using the motors, the basic vehicle setup can be set more neutral and the active systems can be used to make it more stable or "safe" under normal conditions. This allows inherently better handling with the same level of safety as a traditional IC engine car using the motors. In a market where hybrid and electric cars are seen as "boring", having a driver focused car will help improve customer perception and make them more favourable towards hybrids and electric cars.

This function is a macro-function that includes - or atleast uses concepts from - *Direct Yaw Control*, *Differential Torque based Power Steering* and *Drivability Enhancement*. The DYC function is used to tune the lateral dynamics of the vehicle, concepts from DTPS to customise steering feel and DE to enhance the longitudinal dynamics and to adjust throttle sensitivity based on driver requirements. Appropriate combinations of these three factors can make the vehicle feel more sporty or stable.

2.3.3 Final selection

The four functions chosen are evaluated once again using the comparison matrix. Even though the rear two motor configuration was seen to be the best, the four motor configuration is chosen for further function development and analysis. This is because, this allows more design freedom and opportunities to enhance the control. Further, the DTPS (Differential Torque based Power Steering) cannot be implemented with the rear two motor configuration. If a different configuration is chosen for the final vehicle prototype, the control can be easily modified to work for the new configuration by simply disabling some of its subfunctions. The controller performance will be reduced, but it will still work nevertheless.

Table 2.3.4: Final round of concept evaluation using *Pugh Matrix* for four motor hybrid

Criteria	Weight	Direct Yaw Control	Differential Torque Power Steering	Improved Slip Control	Customise feel
Acceleration (normal)	2	0	0	++	+
Acceleration (step mu)	1	0	0	++	0
Acceleration (split mu)	1	0	0	++	0
Long. acc. resp. time	2	0	0	0	++
Aligning mom. curve	2	0	++	0	+
Signal to noise ratio	1	0	+	0	+
Max str. assist tq.	1	0	+	0	+
Max str. assist power	1	0	+	0	+
Min turning radius	2	0	+	0	+
Str. tq. req. for tight turn	2	0	++	0	+
YRR (accelerating)	1	++	−	0	+
YRR (braking)	1	++	−	0	+
Yaw damping	2	++	−	0	+
Yaw resp. time	2	++	+	0	+
Lat. acc. resp. time	1	+	+	0	+
Lat. acc. gain	1	+	0	0	0
Scalability (2 motor front)	4	++	++	+	+
Scalability (2 motor rear)	4	++	0	+	+
Synergy with other func.	4	+	−	0	++
Comfort/Desired feature	4	0	+	0	++
Cost	8	0	+	0	0
Robustness	6	0	0	0	−
NVH	6	0	0	+	0
Total		34	28	22	40

As can be seen from table 2.3.4, the *Customise Feel* function once again comes out on top and is chosen as the function for further development in this project.

2.4 Chosen function

In this section the scope and the limitations of the chosen functions are described. An outline of the objectives and the method of operation for the function is also described. The reference manoeuvres which will be used to evaluate the funcion is specified.

The scope of the *Customise Feel* function in this project is limited to the steering feel and the lateral dynamics. The longitudinal dynamics component of the function is ignored. The torque vectoring capability on the front axle will be used to tune the steering feel. Due to time limitations and the subjective nature of steering feel, its tuning is limited to just providing assist to the steering system. In other words, it acts as a power steering system. It is assumed that the vehicle is not equipped with a traditional power steering system. The torque vectoring capability at the rear axle is used to improve the transient lateral dynamics of the car. The objective is to reduce the yaw response time while at the same time reducing the yaw overshoot of the vehicle during a rapid steering manoeuvre. The torque vectoring capability on the rear axle will also be used to ensure that the torque vectoring done on the front axle with the aim of reducing steering effort does not affect the yaw dynamics of the car. Note also that the objective of the controller is not to alter the steady state lateral dynamics of the vehicle but instead to alter only the transient dynamics.

During the design and evaluation of the function, the vehicle will be tested using the step steer and the sine wave steering manoeuvres from the `ISO 7401` standard. In brief, the `ISO` step steer manoeuvre is defined as:

- The steering amplitude is chosen such that the steady state lateral acceleration for the steering amplitude and the chosen vehicle speed combination is $4\ m/s^2$.
- While driving the vehicle straight ahead at the chosen initial velocity, the predetermined step steer input is applied to the steering wheel such that the time period between 10% and 90% of the steering input is less than $0.15\ s$.

The sine wave steering input is specified as follows:

- The steering amplitude is chosen in the same manner as for the step steer.
- A single sinusoidal wave steering input is made at a frequency of $0.5\ Hz$.
- An additional test is also made with the same speed and steering angle but with $1\ Hz$ frequency instead.

Figure 2.4.1 shows the step steer and the sine wave steering inputs that are used in the tests.

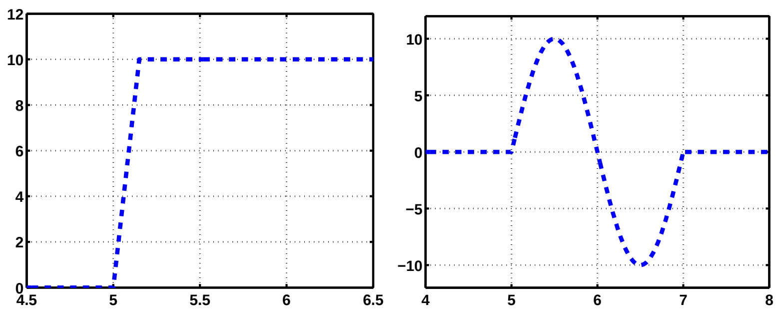

(a) *Step steer* (b) *Sine wave steer*

Figure 2.4.1: *Reference manoeuvres*

For the steering assist part of the function, the vehicle will be tested at constant speed with a ramp steer input. The aligning moment vs the front axle slip angle curve will be of interest here.

For purposes of validation the same tests as above will be performed with different specifications as well, i.e., with different amplitudes, frequencies, ramp rates, etc. Additionally, the vehicle will be tested with a sine with dwell steering manoeuvre to ensure that the controller does not worsen stability in extreme situations.

Both model based and empirical approaches will be used to design the controller. The empirical approach will be used in combination with optimisation to achieve good controller performance. However, while this may assure good performance, it may be difficult to use this controller as such emperical controllers will be tuned for a specific case and may be difficult or infeasible to adapt to other conditions. To that end, keeping in mind the performance achievable with such a system, a model based controller is also designed. These controllers are likely to have slightly worse performance, but do not require significant re-tuning for different scenarios.

3 Function Development

This chapter details the process adopted in developing the function, the issues faced, the controller performance and the final design of the controllers.

3.1 Yaw response controller

The yaw response controller needs to be able to respond very quickly to steering inputs if it has to be able to effectively alter the transient yaw dynamics of the vehicle. Additionally, the controller also needs to be very robust as a false intervention could potentially cause the vehicle to become unstable and cause a crash. In order for these two requirements to be satisfied, a feed-forward controller has been chosen. This also reduces the risk that the controller alters the steady state dynamics of the vehicle.

In figure 3.1.1, the ideal and actual yaw rate of the vehicle at 150 km/h with a step steer input is shown. The figure also shows the regions where the yaw response needs to be improved and where it needs to be damped. The ideal yaw rate is assumed to be the steady state yaw rate as predicted by the linear model-matched vehicle model for the steering input.

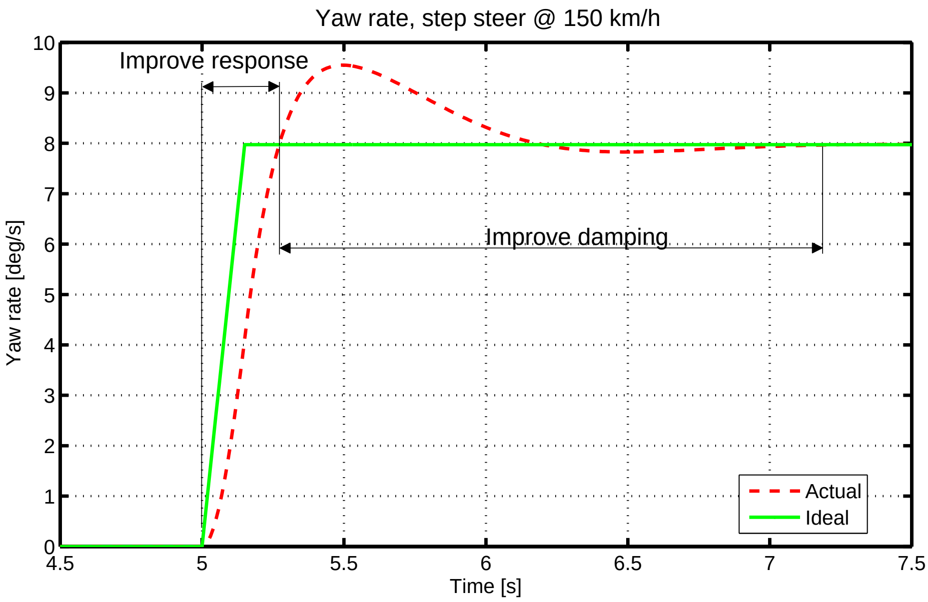

Figure 3.1.1: *Actual and Ideal yaw rate for a vehicle at 150 km/h and step steer input*

The area where the yaw response has to be improved roughly corresponds to the region where the steering angle is increasing. This area can be identified by taking the derivative of the steering angle and this can be used as an input to the controller. A non zero derivative of the steering angle indicates that the yaw response has to be improved. However, to ensure that the derivative is robust in the presence of noise, it is modified into a derivative of the first order filter.

For the region where the yaw overshoot occurs, taking the derivative of a second order filter of the steering angle might be of help. A second order filter has a frequency component and can be written as in equation 3.1.1 where ω_0 is the natural frequency and ζ is the damping factor.

$$y = \frac{\omega_0^2}{s^2 + 2\omega_0\zeta s + \omega_0^2} x \tag{3.1.1}$$

This frequency component in the filter helps in recreating the oscillating overshoot region of the yaw response curve. Figure 3.1.2 shows the vehicle for a step steer manoeuvre at 150 km/h along with the signals generated using the derivatives of the first and second order filters of the steering angle as mentioned above. The derivative of the first order filter is used for yaw response and the derivative of the second order filter is used for yaw damping. Note that these two signals are scaled to be visible clearly and do not represent the actual magnitudes or the sign in the case of the second order filter.

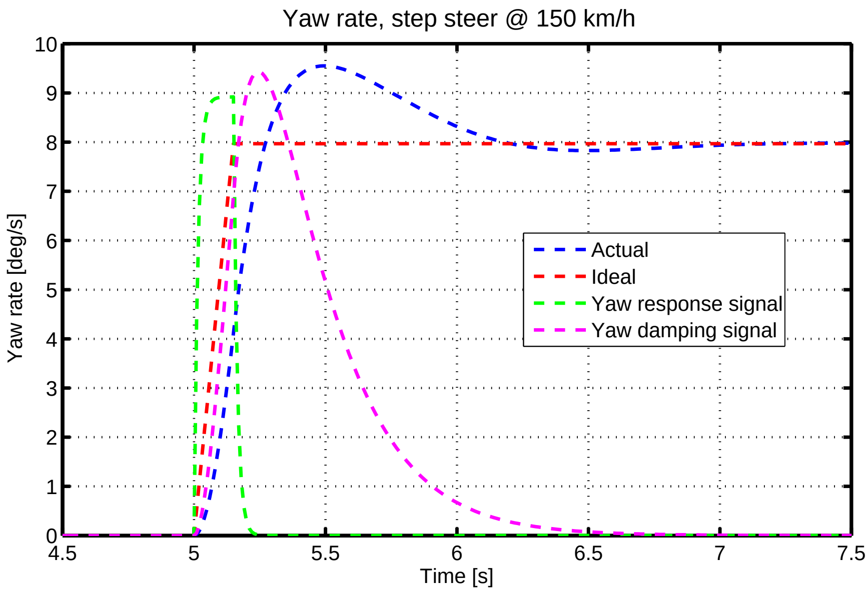

Figure 3.1.2: *Step steer at 150 km/h showing the signals used for yaw response and yaw damping control*

Using a combination of the first and the second order filters it would be possible to reconstruct the behaviour of the vehicle for a certain scenario. Therefore taking a suitable combination of the derivatives of the two aforementioned filters, suitable response improvement and damping of the vehicle can be done. A controller designed based on this idea is shown in figure 3.1.3. The parameters c_i here are tunable and need to be optimized for different scenarios. Note that a limit of 600 Nm of torque has been imposed on the total torque difference that can be requested by both the yaw response and the steering torque controllers put together.

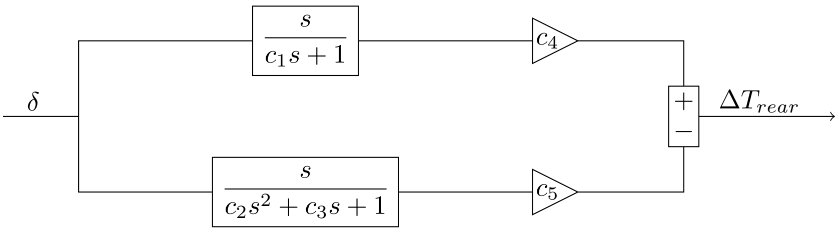

Figure 3.1.3: *Schematic of the empirical yaw response controller*

The tuning of the parameters is done using optimisation. `Matlab`'s built-in *Genetic Algorithm* (GA) function was used for the optimisation. Other algorithms including *Swarm Optimisation* and an own version of the genetic algorithm were tried. However, `Matlab`'s version was seen to be faster overall even though the other algorithms were slightly better in terms of consistently finding the optima.

In initial optimisation attempts, the fully detailed two track model was used. However, it was seen that the optimisation runs took too long and the runs required more iterations to converge to a solution. Hence, it was chosen to use a single track model for the optimisation process.

Before the linear bicycle model was used for optimisation, it is first matched to the two track model using optimisation. The same step steer manoeuvre as defined by the `ISO 7401` standard is used for the optimisation as well as model-matching. For model matching, the objective function is taken as the sum of the areas between the yaw rate vs. time and lateral acceleration vs. time curves of the single track and the two track model. The two areas are weighted so as to be able to tune the matching between the two models. The objective function can be written as shown in equation 3.1.2, where, t is the time at the end of the simulation, k is a constant factor to ensure the magnitude of the objective function is reasonable and w is the weighting factor which can be used to prioritize yaw or lateral acceleration match over the other. The parameter w lies in the range $(0, 1)$.

Only one parameter is tuned during the model matching, which is the ratio of the front to rear tyre stiffnesses.

$$J(x) = k(w \int_0^t |r_{act} - r_{ideal}|\mathrm{d}t + (1-w) \int_0^t |a_{y,act} - a_{y,ideal}|\mathrm{d}t) \tag{3.1.2}$$

The results of the model matching is shown in figure D.1.2. As can be seen, the linear model matches the two track model very well in all cases. The only small deviation is in the yaw overshoot in the step steer case at high speed and this is because there is now a significant amount of torque from the engine driving the front wheels to keep it at constant speed. This torque eats away the front axle's lateral capacity. This, in addition to the fact that the two track vehicle has non-linear dynamic effects from roll and pitch cause the deviation in the yaw overshoot. But more importantly, the steady state yaw rate is well matched in all cases.

Once the model matching is done, the single track model with the tuned tyre stiffnesses is used for the controller optimisation. This optimisation is significantly more time consuming since five different parameters are optimised now. Here, the objective function is split into two parts: the first part being the area between the actual and the ideal yaw rate curves from the start of the steering manoeuvre till the time the actual yaw rate hits the steady state yaw rate ("yaw response" part), and the second part being the area between the actual and ideal yaw rate curves from the time the actual yaw rate hits the steady state yaw rate till five seconds after the start of the steering manoeuvre ("yaw damping" part). These two parts of the objective function are weighted depending on the vehicle speed and the required dynamic characteristics. Mathematically, the objective function can be written as shown in equation 3.1.3 where, x is the set of design variables, k is just a constant factor to ensure that the magnitude of the objective function does not become too small for the GA, w is the relative weighting factor and is in the range $(0, 1)$, T_s indicates the time when the steering manoeuvre is started, T_{ss} is the time when the actual yaw rate hits the steady state yaw rate and T_e is 5 seconds after the start of the steering manoeuvre.

$$J(x) = k(w \int_{T_s}^{T_{ss}} |r_{act} - r_{ideal}|\mathrm{d}t + (1-w) \int_{T_{ss}}^{T_e} |r_{act} - r_{ideal}|\mathrm{d}t) \tag{3.1.3}$$

The optimisation is run for three different speeds: 50, 100 and 150 km/h. The steering angle is chosen such that the steady state lateral acceleration level in each case is 4 m/s^2. The weighting factor w is altered for different speeds depending on the yaw response and damping requirements.

The optimisation was intially done for both a step steer and sine wave steering input. In case of the sine wave steering input, the objective function changed to simply the area between the actual and ideal yaw rates during a 5 second period after the start of the steering manoeuvre as shown in equation 3.1.4. However, it was seen that the solution from the optimisation done for the step steer manoeuvre performed just as well and hence the controller was not further optimised for the sine wave steering input.

$$J(x) = k(\int_{T_s}^{T_e} |r_{act} - r_{ideal}|\mathrm{d}t) \tag{3.1.4}$$

While optimising, it was noticed that successive optimisation runs did not always generate the same solution even though their performance was roughly the same. This indicates that there are multiple global optima instead of a single optimum. Additionally, it is not guaranteed that the same global optima is being determined each time the optimisation is done. This makes it difficult to do gain scheduling to interpolate the control parameters for different speeds. Hence this control algorithm may be difficult to implement in a vehicle. However, it is still worth investigating since this control method uses optimisation to determine the best possible solution and hence gives an idea of the maximum benefit that might be achieved using torque vectoring in terms of transient yaw dynamics.

Several optima were determined and recorded by running multiple optimisation runs. Other validation tests were run using these settings and the best among the optima was chosen as the preferred controller settings.

3.2 Steering torque controller

As mentioned before, while the original objective of this system is to adjust or tune steering feel, due to time limitations and the subjective nature of steering feel, the objective was modified to just providing torque assist to the steering system which is proportional to the self aligning torque at the front wheels.

This steering torque controller is just a proof of concept that the motors can be successfully used to assist the steering system or even replace the power steering system entirely. The aim of this controller is to reduce the required steering torque by a constant fraction of the normally required steering torque.

The schematic of the steering torque controller is shown in figure 3.2.1.

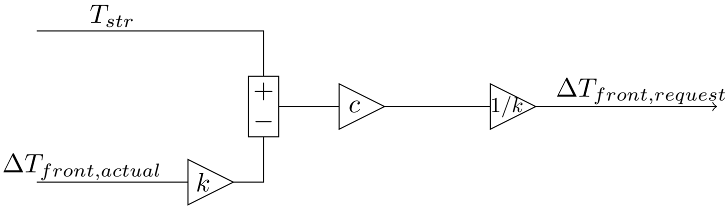

Figure 3.2.1: *Schematic of the steering torque controller*

The controller uses the signal from the torque sensor on the steering column (T_{str}). This torque is the sum of the steering torque due to the tyre forces and the steering assist from the torque vectoring system. The controller also has access to the torque difference currently being supplied to the front wheels ($T_{front,actual}$). The controller uses this to determine the current assist being provided which in turn is used along with the steering torque signal to detemine the actual torque felt in the steering column due to the tyre forces alone, i.e., without the influence of steering assist.

Once the actual steering torque is known, this torque is then multiplied by the contant (c) to determine the torque assist that needs to be supplied. This required torque assist is then translated into the wheel torque difference ($T_{front,request}$) which is a function of the wheel and steering geometry.

4 Results and discussions

In this section, the results of the simulation using the various controllers and tunings are presented and analysed. In section 4.1, the results corresponding to the yaw response controller alone (steering torque controller switched off) are presented while in section 4.2, the results of the steering torque controller in combination with the yaw response controller are presented.

4.1 Yaw response controller

Figure 4.1.1 shows the lateral dynamics and the torque vectoring done at 50 km/h during the step steer manoeuvre.

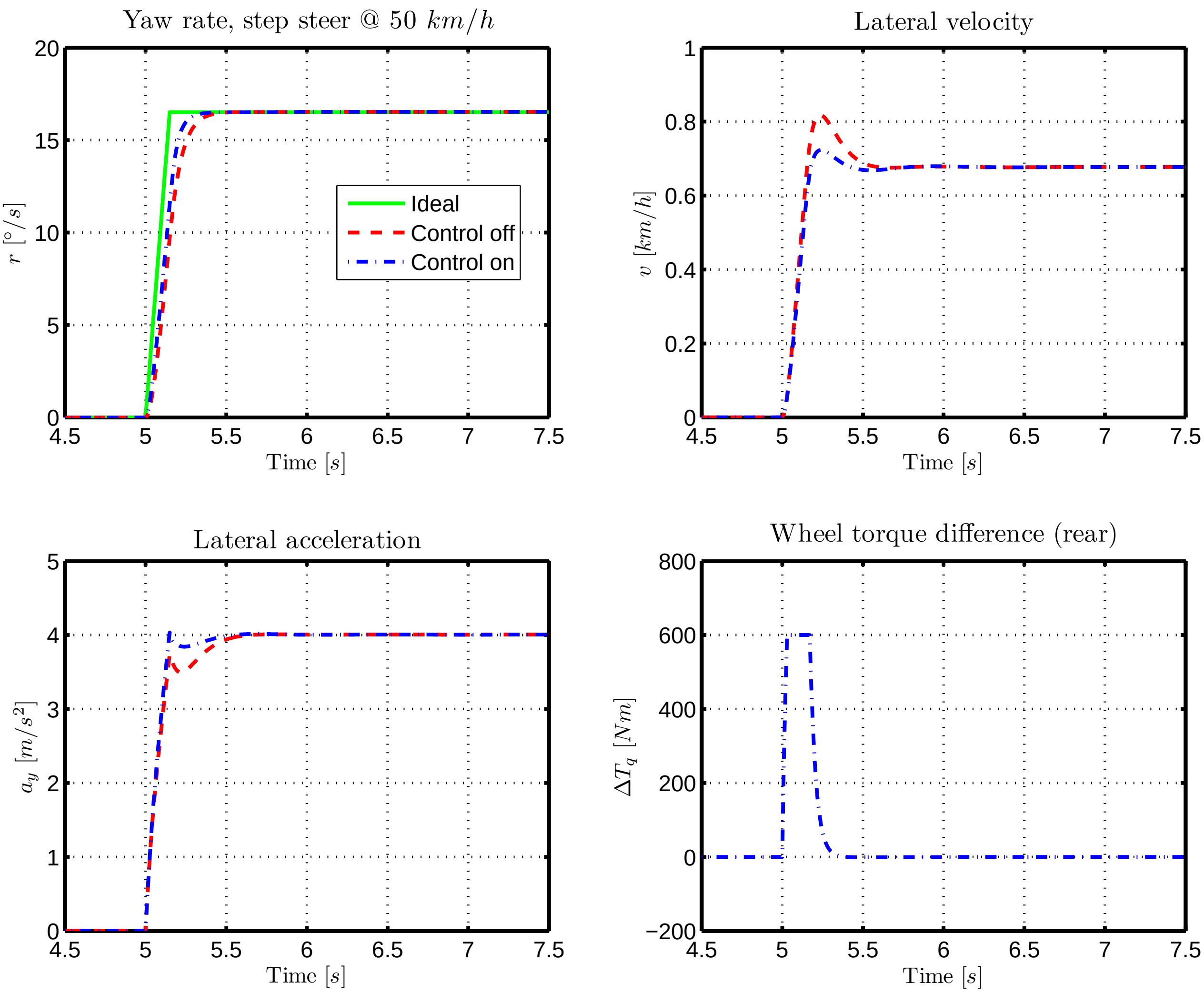

Figure 4.1.1: *Vehicle performance at 50 km/h with empirical controller*

Significant improvement can be seen in the yaw response of the vehicle. However, it can be seen in the torque vectoring plot that the torque limit of 600 Nm is hit for the majority of the intervention. This indicates that better response can be achieved with more torque. Note that since these manoeuvres are specified so as to achieve 4 m/s^2 of lateral acceleration, at low speeds, high yaw rates and therefore high yaw accelerations are involved. This means the torque vectoring required at low speeds to achieve the same level of yaw response is higher than at high speeds. The torque vectoring also reduces the lateral velocity overshoot.

One possible cause for concern is the lateral acceleration, which in the presence of torque vectoring has a small peak that is higher than the steady state lateral acceleration. This could cause the vehicle to become unstable on low μ surfaces. Since this overshoot is caused by the torque vectoring to improve yaw response, the parameters c_1 and c_4 (which control the yaw response part of the controller) are manually tweaked to yield a slightly modified response where the lateral acceleration peak is eliminated as shown in figure D.1.3. This however comes at a slight cost of the yaw response.

Figure 4.1.2 shows the vehicle response at 100 km/h.

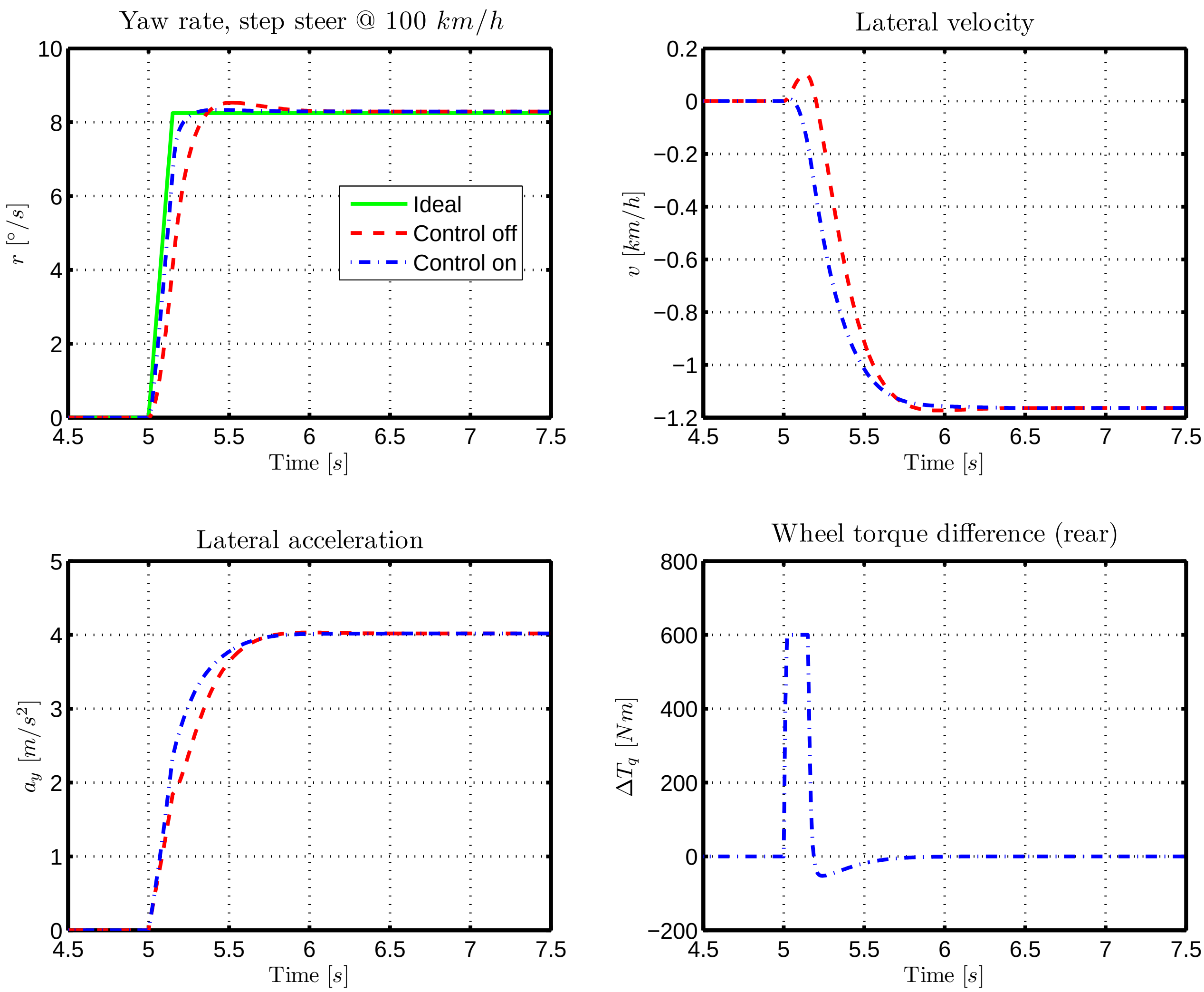

Figure 4.1.2: *Vehicle performance at 100 km/h with empirical controller*

It can be seen that now, the yaw response is improved dramatically with almost no yaw overshoot. The torque profile shows a small negative torque region which indicates that the vehicle has a tendency to oversteer which is actively being counteracted by the torque vectoring system.

The lateral velocity and the lateral acceleration profiles also show improvement in terms of smoothness. The lateral velocity profile in particular does not show the reversal of direction which is seen in the passive vehicle. It is yet unclear how this will be perceived by the driver.

Figure 4.1.3 shows the vehicle response at 150 km/h during a step steer steering manoeuvre.

It is seen that the yaw response of the vehicle in the presence of the torque vectoring at such high speed is close to ideal. There is a small overshoot of the yaw rate. This is however very low compared to the passive vehicle. The torque vectoring profile shows a significant amount of negative torque being applied to stabilise the vehicle.

It can also be seen that the lateral acceleration and the lateral velocity profiles show a behaviour where they reach the steady state conditions gradually. Once again it is unclear as to whether this is favourable or not in terms of "feel". In terms of stability however, it can be seen that the passive vehicle is less stable since there

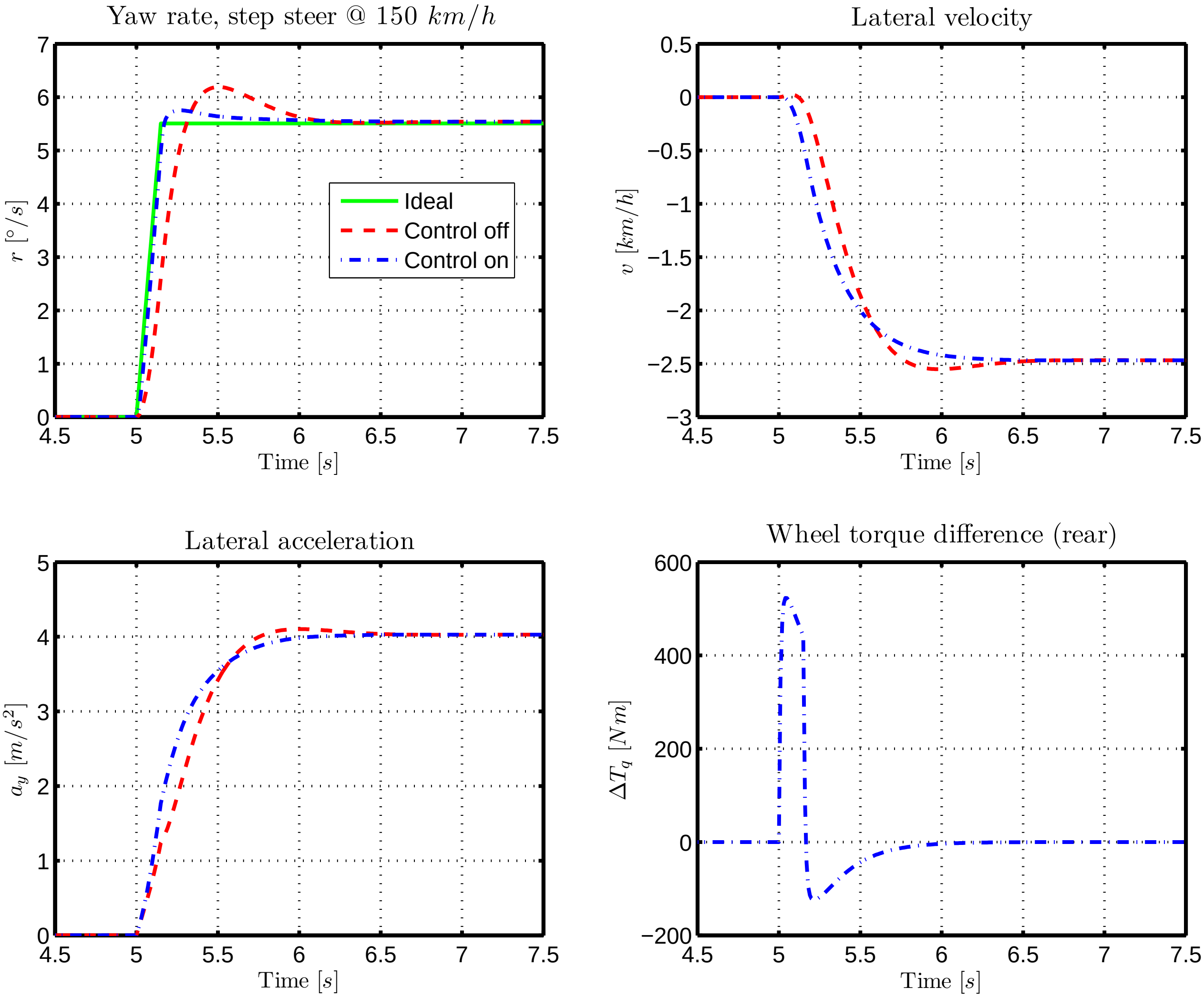

Figure 4.1.3: *Vehicle performance at 150 km/h with empirical controller*

is a small overshoot in the lateral acceleration which is eliminated in the active vehicle. The lateral velocity profile - which grows faster and reduces the overshoot - indicates a smoother turn-in response.

Tests have also been done using the sine wave steering manouevre. Note that all the sine wave steering manoeuvres are done with the controllers tuned for the step steer case (in case of empirical controller). The controller has been tuned for the speed but not specifically for the manoeuvre.

Figure D.1.4 shows the vehicle performance at 50 km/h during a sine wave steering manoeuvre. The yaw response is significantly better in this case compared to the step steer manoeuvre. The yaw response time is approximately halved without any adverse effect. The vehicle is also much quicker to get back to zero yaw rate after the end of the steering manoeuvre. Significant amount of torque vectoring is done to cause this improvement, however, unlike in the case of the step steer manoeuvre, the torque limit is not reached. This indicates that in more realisitic driving scenarios, the torque vectoring limit of 600 Nm is unlikely to be hamper the performance.

Figure D.1.5 shows the vehicle lateral dynamics at 100 km/h. Even better yaw response can be seen in this case. The yaw response is almost immediate and the torque vectoring done to achieve this is less than in the 50 km/h scenario. It can also be seen that the controller does some torque vectoring at the end of the steering manoeuvre to stabilize the vehicle.

The lateral dynamics of the vehicle at 150 km/h is shown in figure D.1.6. Not only is the yaw response significantly improved, it can also be seen that the yaw overshoot both during and after the steering manoeuvre are either eliminated or significantly reduced. The torque vectoring plot shows that a significant amount of torque vectoring is done after the end of the manoeuvre to eliminate the yaw overshoot that occurs in the passive vehicle.

It is interesting to note that the highest gain in yaw performance is achieved at high speed and is achieved at the least cost. It is only at high speed that the yaw performance becomes important. Not only is the yaw response improved at high speed, but also the safety and the feel of the vehicle is improved as the yaw overshoot that is seen in the passive vehicle is almost eliminated.

Figure D.1.1 shows the vehicle yaw performance when non ideal motors are used. Until now, the motors were assumed to be ideal, i.e., the motor delivers the requested torque instantaneously. While motors do respond a lot quicker than traditional hydraulic brakes, these are located inboard while the brakes act on the wheels directly. The motor torque on the other hand has to be transferred through maybe a gearbox, driveshafts, CV joints, etc. All these have stiffness which cause a small delay in the transfer of torque to the wheels. Additionally, there might be delay in the various sensors whose signals are used by the controller and delay in the CAN network, etc which add up to effectively cause a delay in the motor torque supply. A motor delay of 50 ms is tested with the controller.

As can be seen in figure D.1.1a, a small overshoot in the yaw rate is seen. This overshoot increases at higher speed as seen in figure D.1.1b and at 150 km/h it gets even higher (figure D.1.1c).

If the motor response time is known, it can be taken into account while optimising the controller parameters. This was done for the step manoeuvre at 150 km/h and the result of this optimisation is shown in figure D.1.1d. As can be seen, while the controller performance is not as good as the case of the ideal motor, it is still far better than the passive vehicle and the previous controller. This shows that the empirical controller can take into account such new and unexpected effects by simply re-optimising the controller parameters.

4.2 Steering torque controller

The lateral dynamics, the torque vectoring and the steering torques during a ramp steer manoeuvre are shown in figure 4.2.1. Four vehicle setups are simulated. For reference, the passive vehicle and the vehicle with the previously described yaw controller (Direct Yaw Control, DYC) are also simulated and shown. The steering torque controller (Power steering, PS) only and in combination with the DYC are simulated and their performance analysed.

As can be seen, the yaw rate of the vehicle in all four cases are quite similar. The DYC is not intended to change the steady state lateral dynamics and since the ramp steer is rather slow ($3°/s$) it does not alter the vehicle behaviour in this case. The vehicle setups with the PS do show a small deviation in the peak yaw rate. This is because, the PS controller applies a significant amount of torque (the torque limit is hit) to achieve the power steering. And since the lateral dynamics of the vehicle should not be affected, an equal and opposite torque is applied on the rear axle as well. This has the side-effect of reducing the lateral capacity on both the front and rear axles and hence the peak yaw rate and the peak lateral acceleration are slightly lower when the

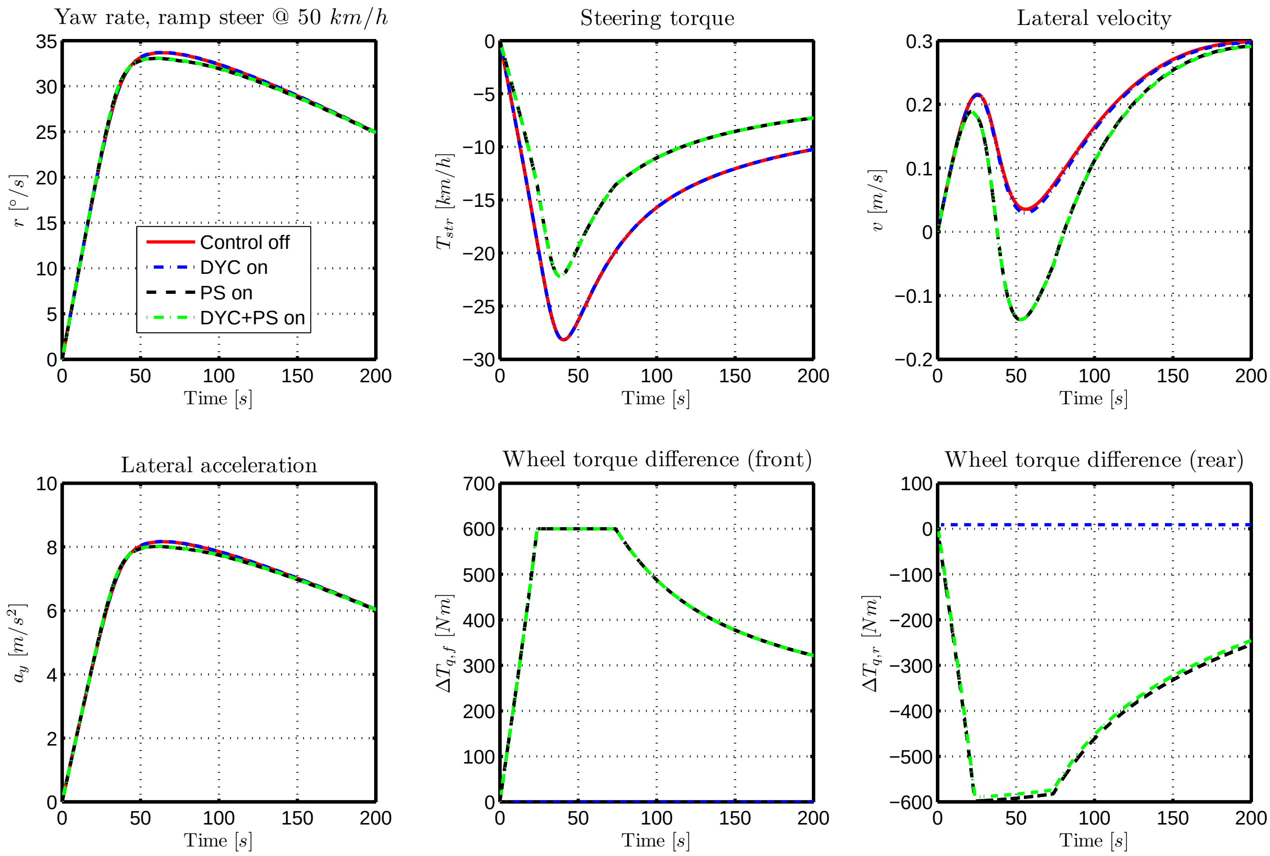

Figure 4.2.1: *Steering torque assist and lateral dynamics at 50 km/h with ramp steer*

PS controller is on.

Another consequence of this is that the lateral velocity profile which is significantly different from the passive vehicle or the vehicle with just the DYC on. Once again, since the lateral capacity of the tyres is reduced, the side slip angles of the wheels have to be higher to achieve the same level of lateral force and hence the vehicle lateral velocity is lower. This also causes a change in the body sideslip angle of the vehicle as well.

The steering torque profile shows, as expected, a 30% drop in steering torque. The shape of the steering torque curve from the passive vehicle is replicated well with the power steering controller. Some variation is seen in the shape near the region where peak yaw rate is achieved. This can be explained by looking at the torque vectoring profile on the front axle. Since the peak torque limit is hit in this region, the full amount of steering torque assist is not supplied and hence a small variation in the shape is seen.

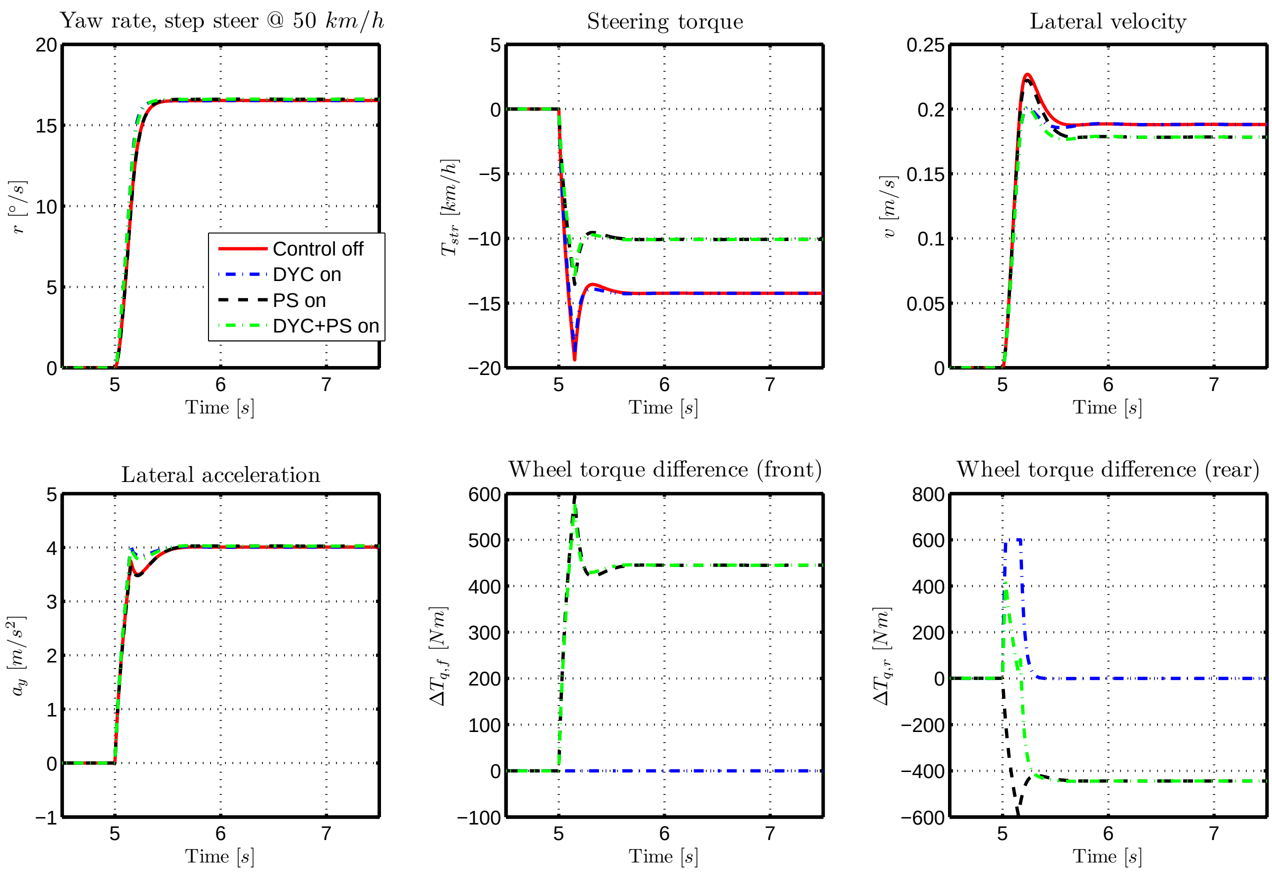

Figure 4.2.2: *Steering torque assist and lateral dynamics at* 50 km/h *with step steer*

The PS controller performance in the case of step steer at 50 km/h is shown in figure 4.2.2. When the PS controller alone is on, it can be seen that the yaw response remains the same while the steering torque requirement goes down by 30%. It can also be seen that the DYC and the PS controllers are independent in terms of their performance, i.e., one does not affect the performance of the other. This makes their design easier since they can be designed independently and used separately or simultaneously. It can be seen that the torque limit is hit on the front axle briefly. This indicates that it might be difficult to replace the traditional power steering system at low speeds with the current torque vectoring based steering assist system. It can however, still be used to downsize the traditional power steering system and assist the same when required.

Figure D.1.10 shows the PS controller performance for the vehicle at 100 km/h with the step steer manoeuvre. Once again, similar performance can be seen with the PS reducing the steering effort and the DYC improving the yaw response. Lower lateral slip velocities and lower steering torques can be seen in the scenarios when the PS system is switched on. The torque limit is no longer hit on the front axle. A small difference can be seen in the steady state values of the yaw rate and the lateral acceleration when the PS system is on. A possible reason is that the front axle's lateral capacity is significantly reduced by the drive torque from the engine in addition to the torque vectoring. The engine provides a drive torque to the front axle to maintain the vehicle speed.

Sufficient drive torque is provided so as to counter-act the aerodynamic drag and the rolling resistance. Since the aerodynamic drag is significant at high speeds, more drive torque is required (approx 147 Nm at 100 km/h) to maintain the speed and hence the front axle's lateral capacity is reduced when the torque vectoring is done as well.

Note than when both the controllers are on simultaneously, the torque requests on the rear axle add up. Care needs to be taken to ensure that the rear axle's lateral capacity is not saturated. This is not very likely to happen since the DYC only acts during transient and not during steady state. Since these controllers are only tuned for the linear region, if they are used in such situations or in low-μ scenarios or in the non-linear region, the controller is still expected to improve the vehicle dynamics although its performance may drop.

4.3 Validation

The controller is valiated in this section. Only the yaw controller is validated here as it has been tuned for only specific scenarios and their performance in other scenarios is suspect. The steering torque assist controller is more straight-forward and has worked well in several scenarios even though it has not been designed or tuned with any one manoeuvre in mind.

The validation has been done by testing the controller under various test conditions, like different frequencies for the sine wave, different amplitudes of steering and a sine sweep to determine the frequency response and the phase shift of the yaw response. The validation tests for the specific manoeuvres have been performed at 150 km/h since this is a tougher scenario for the controller.

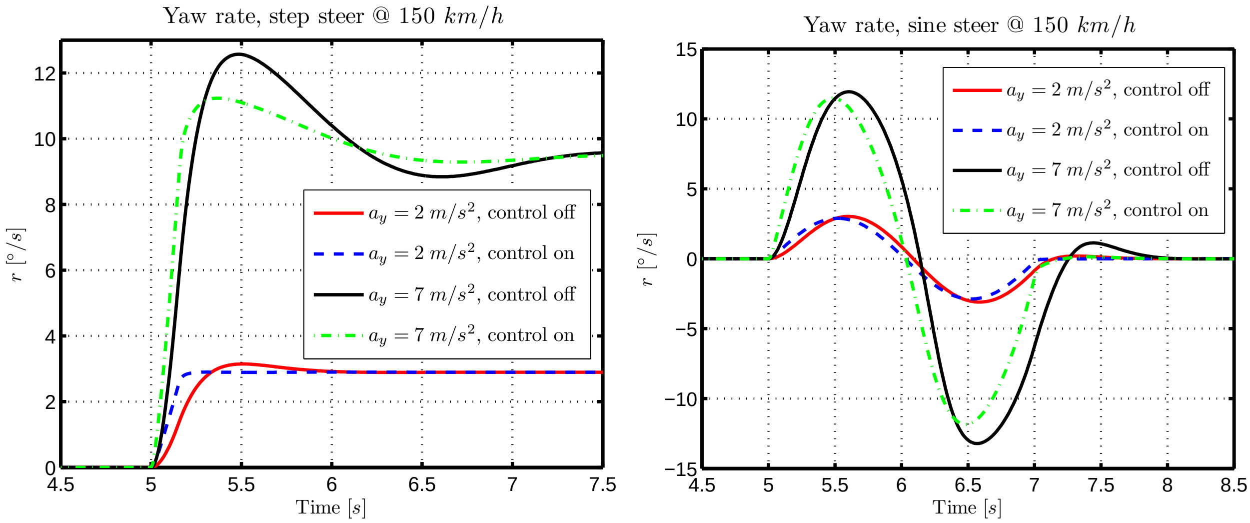

(c) *Step steer*

(d) *Sine wave*

Figure 4.3.1: *Validation of the yaw controller at* 150 km/h *for different steering amplitudes*

Figure 4.3.1 shows the validation runs using the step and sine wave steering manoeuvre. The steering amplitudes were chosen so as to have a steady state lateral acceleration of approximately 2 m/s^2 and 7 m/s^2. As can be seen, the vehicle with the controller performs better irrespective of the manoeuvre or the steering amplitude. In the step steer manoeuvre at 7 m/s^2, the improvement in the yaw response is not as good as it could have been. However, it is important to keep in mind that the controller is now operating well within the non-linear region of the tyres and hence the performance drop is understandable.

The controller performance under different frequencies of sine wave input was also tested. This is shown in figure D.1.11. It can be seen clearly that the controller performs well at both 0.25 and 1 Hz. The yaw response is improved and the overshoot at the end of the manoeuvre is reduced as well.

Interpolation of the control parameters was tried using `Matlab`'s `interp1` function. The results from this validation test are shown in figure D.1.12. Cubic and spline based interpolation worked well for speeds between 50 and 150 km/h, but did not work well when extrapolation was required. Hence a simple linear interpolation-extrapolation method was used. Even though such a rudimentary method was used, the controller performance even with these parameters is seen to be quite good.

Additionally, the controller was also tested for robustness against changes or variations in environment and vehicle properties. Figure D.1.7 shows the controller performance when the friction coefficient is 0.6 and 0.8 instead of 1 for which the controller is tuned. While it is seen that the controller performance significantly worsens, it can also be seen that the controller always improves performance as compared to the passive case. It should also be noted that due to the lower friction, the controller is now operating in the non-linear region.

Figure D.1.8 and D.1.9 show the yaw velocity when the vehicle is tested with the step steer manoeuvre at 150 km/h with different tyre stiffnesses and different weight distributions respectively. Once again, it can be seen that while the controller performance worsens, it still manages to improve the vehicle performance as compared to the passive case.

From the figures, it appears that the controller is far more sensitive to variations in environmental and vehicle parameters than any changes in driver input.

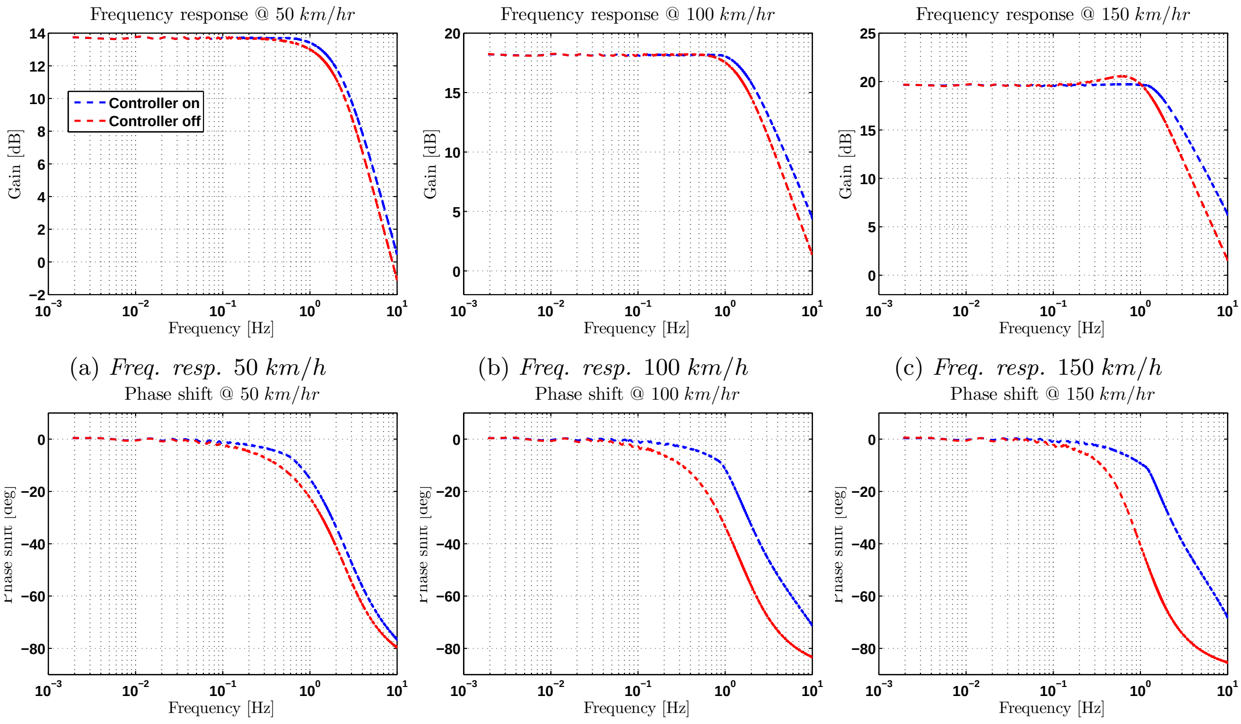

(a) *Freq. resp.* 50 km/h (b) *Freq. resp.* 100 km/h (c) *Freq. resp.* 150 km/h

(d) *Phase shift* 50 km/h (e) *Phase shift* 100 km/h (f) *Phase shift* 150 km/h

Figure 4.3.2: *Frequency response and phase shift at* 4 m/s^2

Figures 4.3.2 and D.1.13 show the frequency response and the phase shift of the passive vehicle and the vehicle with the yaw controller at 4 m/s^2 and 7 m/s^2 of lateral acceleration. The controller is evaluated for the three speeds for which it has been tuned. As it can be seen, the controller improves the phase shift in all cases and increases the frequency bandwidth of the vehicle as well. Only at 100 km/h and 7 m/s^2 is the controller's contribution to the bandwidth not clear. Additionally, it also reduces the vehicle yaw rate's tendency to resonate with certain frequencies of steering inputs.

Since the target of the controller was mainly to decrease the reponse time of the vehicle (equivalent to reducing phase shift), the improvement in bandwidth is not consistent. However, it can be seen that almost always it improves the bandwidth and reduces the resonant peak. It also unfailingly reduces the phase shift of the vehicle's yaw response.

The controller performance during a sine with dwell steering manoeuvre at 150 km/h with 30° steering angle is shown in figure D.1.14. As can be seen, the controller improves the yaw response and performance of the vehicle significantly despite the fact that it is operating in the non-linear region now (7 m/s^2). The controller improves the yaw response, the overshoot and the YRR of the vehicle significantly. The torque vectoring plot shows a significant amount of torque vectoring being done and the torque supplied changing rapidly. As a result, in this case, any response time for the motor might make a significant difference in the performance of the vehicle.

Note that the steering profile plot in the two sine with dwell plots have been provided to get a reference for the time scale. These steering profile plots are not to scale.

Figure D.1.15 shows the vehicle performance once again for a sine with dwell manoeuvre at 150 km/h but at 45° steering angle instead. The controller improves the yaw response and the decreases the overshoot and the YRR of the vehicle. However, at around 6 s, the controller does some unwanted intervention causing the vehicle yaw rate to fluctuate. This may be received badly by the driver since it is very counter-intuitive that the yaw rate increases and decreases even when the steering wheel is kept in the straight ahead position. But it is important to note that now the controller is operating close to the limit (8 m/s^2). Hence, while the "feel" may be bad, the controller unarguably makes the vehicle safer in these conditions.

The controller was finally also tested for robustness against noise in the steering wheel angle signal. First, the typical noise in a steering wheel angle signal had to be studied. It was seen that on average, a noise of magnitude 0.025° and of frequencies upto 100 Hz could be expected in the steering wheel angle signal. For the simulation, *Gaussian White noise* of 0.1° (4 times as much as the average) and 100 Hz frequency was generated which was added only to the steering wheel angle signal going to the controller. The steering wheel angle signal with the noise and the noise alone are shown in figure D.1.16. Simulations showed that the effect of the noise was greater at higher speeds. The simulation results of the controller at 150 km/h with steering angle noise are shown in figure D.1.17. It can be seen that the noise caused no noticeable change in the vehicle's performance. All the vehicle states (yaw rate, lateral acceleration and lateral velocity) show the same trend as the case without any noise. The only difference was that, in the presence of noise, significant torque vectoring oscillations are seen even during steady state. One possible reason for this could be the low values of the filter parameters which, while making the controller more responsive, also make it more sensitive to noise. With the default controller, during optimisation, a lower bound of 0.01 was set on the controller filter parameters. This low value causes the increased sensitivity to noise.

Two possible solutions to this issue are investigated. In the first solution, the controller is re-optimised with the lower bounds for the controller filter parameters raised to 0.03. The performance of the original controller and this new controller are shown in figure D.1.18. As can be seen, the vehicle performance is slightly worsened, but the oscillations in the torque vectoring are significantly reduced.

In the second solution, a dead-band filter is implemented on the steering wheel angle signal going to the controller. The results of the simulation with this controller are shown in figure D.1.19. Note that the controller parameters are the same in this case. It can be seen that the torque vectoring oscillations seen during steady state are completely eliminated. The torque vectoring performance during transients are similar to the case without the filter. If necessary, the two solutions can be combined to produce a controller that has no torque vectoring oscillations at steady state and lower torque vectoring oscillations during transients at the cost of slightly lowered performance as seen in figure D.1.20.

5 Conclusions

The concept selection process showed that there are a large number of useful functions that can be achieved with electrified drivetrains. During the brainstorming session, 46 new functions were identified. A large proportion $(60 - 70\%)$ of these functions can be implemented - in some cases with reduced performance or functionality - on a two motor hybrid configuration. The functions affected not only vehicle dynamics but also comfort, cost, weight reduction, safety and performance. There were also engineering functions which are not directly noticable by the driver but can be used as part of other bigger functions to enable or enhance them.

While having four independently driven wheels is the best from the point of view of function implementation, it was seen that having just two independently driven wheels on one axle enabled lots of new functions. Such a layout (with torque vectoring capability) is especially intriguing from the vehicle dynamics and active safety point of view as it enables autonomous driving (to some extent) and effective and quick control of vehicle motion. Specifically, the hybrid layout with the engine at the front driving the front wheels and two electric motors at the rear with each driving one of rear wheels was seen to be the best layout from a cost-benefit perspective.

The simulation results of the function in various manoeuvres show that torque vectoring on the rear axle can be effectively used to improve the yaw response of the vehicle. A yaw response time reduction of between 30% to 60% and a yaw overshoot reduction of between 15% to 80% were recorded in the step steer manoeuvre at different speeds. The torque vectoring done to improve yaw response does modify the steering torque slightly during transient cornering but is not expected to be significant enough to be a cause for concern.

Torque vectoring on the front axle was seen to be an effective way to achieve power steering. When used in conjuction with torque vectoring on the rear axle, it can be used to reduce steering torque required without significantly altering the vehicle's lateral dynamics and can even be used to improve it. It was also seen during the controller design that when the steering assist requirement was increased along with the lateral acceleration level, the inner rear wheel had a tendency to spin. This indicates that there is a limit to the amount of steering assist that can be provided. But this limit is less of an issue at lower speeds when there is less lateral acceleration and therefore less load transfer. And since it is at low speeds that power steering is really required, the limit on the steering assist becomes even less significant.

The empirical yaw response controller was seen to be very effective, robust and flexible. Preliminary tests indicated that the empirical controllers closely matched the performance of model based controllers without displaying any weakness. Incorporating the effects of new, previously unaccounted for disturbances is just a matter of replacing the five controller parameters with new ones as was seen when accounting for the motor response time. The controller itself does not need to be modified. This would not be possible with a model based controller and would require a model/approximation of the new disturbance or influence.

The effectiveness of the torque vectoring system in controlling the yaw response as seen from the simulations validates the hypothesis that the wheel traction forces can be used to effectively control vehicle motion as opposed to using the road wheel angle of the steered wheels. This opens up radical new possiblities to use this system to enhance or enable new active safety systems which use this capability to avoid dangerous situations, override the user in case of user error and keep or even drive the vehicle away from harm.

6 Future work

There are several avenues for future work:

- The current version of steering torque controller is quite rudimentary and is either switched on or off. There is no speed dependency or lateral acceleration dependence. The steering torque controller can be tuned to take these into account so that it provides more assist at low speeds and less assist at higher levels of lateral acceleration to retain steering feel. Alternatively it can be used to assist the normal power steering system only when the required assist goes above a certain threshold. Yet another possible mode of operation for the steering torque controller which might be worth investigating is to nullify the impact of the yaw response controller on the steering torque.
- It has already been shown that leveraging the wheel traction forces to control vehicle yaw response is very effective. It might also be possible to extend this idea and control the vehicle motion as a whole (taking into account vehicle lateral acceleration, lateral velocity, path, etc.) using the torque vectoring system. This could be of huge benefit in enabling new or improving existing active safety functions and this needs to be investigated.
- The possibility of eliminating the traditional power steering system in a small city car can be investigated. In a small city car, where the steering torque assist required is not as high and where due to low speeds, the impact on yaw dynamics is not that important, it might be possible to use the motors alone to provide steering assist. For this study, low speed scenarios with tyre-road friction (due to scrubbing) being more dominant will need to be considered.
- The controller can be extended to work in the non-linear region and limit-friction conditions as well. In these cases, it will also be required to work in coordination with the brakes (which will be used by the ABS, ESC, etc).
- A model based approach to the yaw response controller can be investigated. A preliminary investigation into two possible approaches to this have already been investigated and are detailed in sections C.1 and C.2 in the appendix. This approach would eliminate any requirement to optimise the controller parameters to various manoeuvres and configurations. Instead, with a sufficently detailed model, most of the effects can be captured in the model and the required parameters can be updated as and when required without any requirement for costly optimisation.

References

[1] **N. Amann**, **J. Bocker**, and **F. Prenner**. "Active damping of drive train oscillations for an electrically driven vehicle". In: *Mechatronics, IEEE/ASME Transactions on* 9.4 (Dec. 2004), pp. 697 –700. ISSN: 1083-4435. DOI: 10.1109/TMECH.2004.839036.

[2] **M. Boerboom**. "Electric Vehicle Blended Braking". MA thesis. Chalmers University of Technology, 2012.

[3] **J. Kang**, **J. Yoo**, and **K. Yi**. "Driving Control Algorithm for Maneuverability, Lateral Stability, and Rollover Prevention of 4WD Electric Vehicles With Independently Driven Front and Rear Wheels". In: *Vehicular Technology, IEEE Transactions on* 60.7 (Sept. 2011), pp. 2987 –3001. ISSN: 0018-9545. DOI: 10.1109/TVT.2011.2155105.

[4] **I. Karogal** and **B. Ayalew**. "Independent Torque Distribution Strategies for Vehicle Stability Control". In: (Apr. 2009). DOI: 10.4271/2009-01-0456. URL: http://dx.doi.org/10.4271/2009-01-0456.

[5] **K. Kondak** and **G. Hommel**. "Computation of time optimal movements for autonomous parking of non-holonomic mobile platforms". In: *Robotics and Automation, 2001. Proceedings 2001 ICRA. IEEE International Conference on.* Vol. 3. 2001, 2698 –2703 vol.3. DOI: 10.1109/ROBOT.2001.933030.

[6] **H. Lai** and **D. Madås**. "Test Vehicle for Regenerative Braking Emulation". MA thesis. Chalmers University of Technology, 2011.

[7] **W Li**, **T. Potter**, and **R. Jones**. "Steering of 4WD Vehicles with Independent Wheel Torque Control". In: *Vehicle System Dynamics* 29.sup1 (1998), pp. 205–218. DOI: 10.1080/00423119808969560. eprint: http://www.tandfonline.com/doi/pdf/10.1080/00423119808969560. URL: http://www.tandfonline.com/doi/abs/10.1080/00423119808969560.

[8] **N. Mutoh** and **A. Higashikubo**. "Electric vehicle system independently driving front and rear wheels". In: *IECON 02 [Industrial Electronics Society, IEEE 2002 28th Annual Conference of the].* Vol. 2. Nov. 2002, 1386 –1391 vol.2. DOI: 10.1109/IECON.2002.1185480.

[9] **N. Mutoh**, **T. Kazama**, and **K. Takita**. "Driving characteristics of an electric vehicle system with independently driven front and rear wheels". In: *Industrial Electronics, IEEE Transactions on* 53.3 (June 2006), pp. 803 –813. ISSN: 0278-0046. DOI: 10.1109/TIE.2006.874271.

[10] **N. Mutoh**, **K. Suzuki**, and **K. Kawaguchi**. "Front and rear wheel independent drive type electric vehicle (FRID EV) providing efficient running performance on various road surfaces". In: *Vehicle Power and Propulsion Conference (VPPC), 2011 IEEE.* Sept. 2011, pp. 1 –6. DOI: 10.1109/VPPC.2011.6043250.

[11] **N. Mutoh** and **T. Takayanagi**. "Cornering performance of front and rear wheel independent drive type electric vehicles (FRID EVs) under severe road conditions". In: *Intelligent Transportation Systems (ITSC), 2011 14th International IEEE Conference on.* Oct. 2011, pp. 101 –106. DOI: 10.1109/ITSC.2011.6082965.

[12] **N. Mutoh** et al. "Braking control method for front-and-rear-wheel-independent-drive-type electric vehicles (FRID EVs) on low-friction-coefficient roads". In: *Vehicle Power and Propulsion Conference (VPPC), 2010 IEEE.* Sept. 2010, pp. 1 –6. DOI: 10.1109/VPPC.2010.5729108.

[13] **A. H. Niasar** et al. "Control of Independent Rear Wheel Drives for Electric and Hybrid Vehicles Using One Neuro-Fuzzy Controller". In: (Mar. 2003). DOI: 10.4271/2003-01-0107. URL: http://dx.doi.org/10.4271/2003-01-0107.

[14] **K. Ohishi** et al. "Anti-slip control of electric motor coach based on disturbance observer". In: *Advanced Motion Control, 1998. AMC '98-Coimbra., 1998 5th International Workshop on.* June 1998, pp. 580 –585. DOI: 10.1109/AMC.1998.743601.

[15] **R. P. Osborn** and **T. Shim**. "Independent control of all-wheel-drive torque distribution". In: *Vehicle System Dynamics* 44.7 (2006), pp. 529–546. DOI: 10.1080/00423110500485731. eprint: http://www.tandfonline.com/doi/pdf/10.1080/00423110500485731. URL: http://www.tandfonline.com/doi/abs/10.1080/00423110500485731.

[16] **I. E. Paromtchik** et al. "Motion Control for Autonomous Car Maneuvering". In: *Proceedings of the Fifth International Conference on Control, Automation, Robotics and Vision, Singapore.* 1998, pp. 136–140.

[17] **R. Rajamani**. *Vehicle dynamics and control.* Mechanical engineering series. Springer Science, 2006. ISBN: 9780387263960. URL: http://books.google.se/books?id=NOcVzjChUccC.

[18] **M. Ringdorfer** and **M. Horn**. "Development of a wheel slip actuator controller for electric vehicles using energy recuperation and hydraulic brake control". In: *Control Applications (CCA), 2011 IEEE International Conference on.* Sept. 2011, pp. 313 –318. DOI: 10.1109/CCA.2011.6044472.

[19] **S. Rydberg**. *Comparison of Vehicle Dynamics for Different Electric Propulsion Configurations of a Passenger Car*. Tech. rep. Chalmers University of Technology, 2011.

[20] **S. Sakai**, **H. Sado**, and **Y. Hori**. "Motion control in an electric vehicle with four independently driven in-wheel motors". In: *Mechatronics, IEEE/ASME Transactions on* 4.1 (Mar. 1999), pp. 9 –16. ISSN: 1083-4435. DOI: 10.1109/3516.752079.

[21] **J. Scoltock**. "City Spark". In: *Automotive Engineer* (Dec. 2011), pp. 34–35.

[22] **M. Shino** and **M. Nagai**. "Independent wheel torque control of small-scale electric vehicle for handling and stability improvement". In: *JSAE Review* 24.4 (2003), pp. 449 –456. ISSN: 0389-4304. DOI: 10.1016/S0389-4304(03)00080-8. URL: http://www.sciencedirect.com/science/article/pii/S0389430403000808.

[23] **J. H. Sill** and **B. Ayalew**. "Saturation Balancing Control for Enhancing Dynamic Stability of Vehicles with Independent Wheel Drives". In: (Apr. 2011). DOI: 10.4271/2011-01-0982. URL: http://dx.doi.org/10.4271/2011-01-0982.

[24] **F. Tahami**, **R. Kazemi**, and **S. Farhanghi**. "A novel driver assist stability system for all-wheel-drive electric vehicles". In: *Vehicular Technology, IEEE Transactions on* 52.3 (May 2003), pp. 683 –692. ISSN: 0018-9545. DOI: 10.1109/TVT.2003.811087.

[25] **Q. Wang**, **J. Wang**, and **L. Jin**. "Driver-vehicle closed-loop simulation of differential drive assist steering control system for motorized-wheel electric vehicle". In: *Vehicle Power and Propulsion Conference, 2009. VPPC '09. IEEE*. Sept. 2009, pp. 564 –571. DOI: 10.1109/VPPC.2009.5289799.

[26] **J. Yamakawa** and **K. Watanabe**. "A method of optimal wheel torque determination for independent wheel drive vehicles". In: *Journal of Terramechanics* 43.3 (2006). 7th Asia-Pacific Conference of the International Society of Terrain Vehicle-Systems (ISTVS), pp. 269 –285. ISSN: 0022-4898. DOI: 10.1016/j.jterra.2005.05.004. URL: http://www.sciencedirect.com/science/article/pii/S0022489805000492.

[27] **D. Yang**. *Post impact vehicle path control in multiple event accidents*. Technical report (Department of Applied Mechanics, Chalmers University of Technology, Göteborg, Sweden). Chalmers University of Technology, 2011. URL: http://books.google.se/books?id=p2pCAwEACAAJ.

[28] **S. Zhang**, **T. Zhang**, and **S. Zhou**. "Vehicle Stability Control Strategy Based on Active Torque Distribution and Differential Braking". In: *Measuring Technology and Mechatronics Automation, 2009. ICMTMA '09. International Conference on*. Vol. 1. Apr. 2009, pp. 922 –925. DOI: 10.1109/ICMTMA.2009.380.

A Data

A.1 Optimised control parameters

Table A.1.1: Tuned control parameters

Speed $[km/h]$	c_1	c_2	c_3	c_4	c_5	Comment
50	0.0364	0.0126	0.5373	0.2697	0.0019	
100	0.0134	0.0162	0.2499	0.6355	0.1084	
150	0.0100	0.0140	0.2725	0.7954	0.4583	
50	0.0500	0.0126	0.5373	0.1300	0.0019	Reduced a_y overshoot
150	0.0100	0.0101	0.2191	0.5911	0.5141	Compensated for motor delay
150	0.0300	0.0300	0.2893	0.6477	0.4284	Robust against noise in steering wheel angle signal

A.2 Vehicle data

```
% ========================================================================
% vehicle_parameters
% - - - - - - - - - -
%
% Description:  File defining vehicle parameters.
% ========================================================================


% == Enviromental Parameters
g           = 9.81;         % Gravitational Constant [m/s^2]
rhoair      = 1.204;        % Density of Air [kg/m^3]

% == Vehicle Parameters
m           = 1675;         % Vehicle Mass [kg]
Izz         = 2617;         % Yaw Moment of Inertia [kg m^2]
Iw          = 1;            % Wheel Moment of Inertia [kg m^2]

l           = 2.675;        % Wheel Base [m] (Required by VSE)
a           = 0.4*l;        % Distance from CoG to Front Axle [m]
b           = 0.6*l;        % Distance from COG to Rear Axle [m]

s1          = 1.517/2;      % Half Track Width Front [m]
s2          = 1.505/2;      % Half Track Width Rear [m]
Rw          = 0.316;        % Tyre Radius [m]
nst         = 15.9;         % Steering Ratio [-] (Required by VSE)
AF          = 2.17;         % Frontal Area [m^2]
CD          = 0.3;          % Drag Coefficient [-]
fr          = 0.01;         % Coefficient of rolling resistance [-]

% == Tyre data
mu0         = 1;            % Friction Coefficient [-]
mu1         = 6e-5;         % Friction [N^-1]
c0=[21.3; 21.3; 21.3; 21.3];% Lateral Stiffnes Parameter 1 [-/rad]
c1          = 1.11E-4;      % Lateral Stiffnes Parameter 2 [N^-1]
FzStatic=m*g/l*[b;b;a;a]/2; % Vertical Load at each Wheel
                            % [front;front;rear;rear]

Ca_f_ref    = 2*94.17e3;    % Linear front axle stiffness [N/rad]
```

```
Ca_r_ref    = 2*75.54e3;    % Linear rear axle stiffness [N/rad]

h0r         = 0.43;         % Height of CoG above Roll Axis [m]
h1r         = 0.045;        % Front Roll Center Height [m]
h2r         = 0.10;         % Rear Roll Center Height [m]

h0p         = 0.43;         % Height of CoG above Pitch Axis [m]
h1p         = 0.045;        % Front Pitch Center Height [m]
h2p         = 0.10;         % Rear Pitch Center Height [m]

Ixxs        = 800;          % Roll Moment of Inertia [kg m^2]
Iyys        = 2700;         % Pitch Moment of Inertia [kg m^2]
mun         = 200;          % Unsprung mass [kg]
ms          = m - mun;      % Sprung mass [kg]

kPhi        = 7e4;          % Roll stiffness [N/rad]
cPhi        = 8000;         % Roll damping [N s/rad]
kLambda     = 0.51;         % Ratio of front-rear roll stiffness [-]
cLambda     = 0.56;         % Ratio of front-rear roll damping [-]
kTheta      = 1e5;          % Pitch stiffness [N/rad]
cTheta      = 1e4;          % Pitch damping [N/rad]

kPO         = 0.050;        % Kingpin Offset Wheel Center [m]
sR          = 0.010;        % Scrub radius [m]
kPI         = 12*pi/180;    % Kingpin inclination [rad]
castor      = 4*pi/180;     % Castor angle [rad]
```

B Vehicle and simulation model

In this chapter, the vehicle and the simulation model built for the optimisation and the analysis of lateral dynamics are discussed.

B.1 Single track linear vehicle model

A single track linear vehicle model was made for optimisation purposes. To ensure accuracy, this model is first matched to the two track model using optimisation and then used.

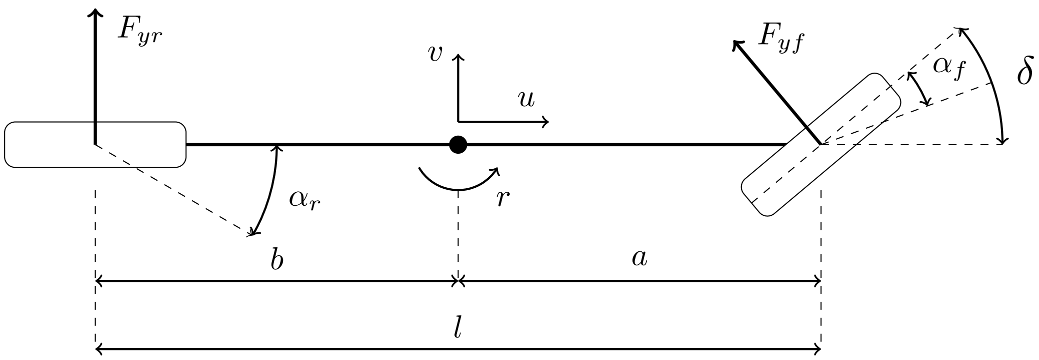

Figure B.1.1: *Single track vehicle model*

In figure B.1.1, the single track vehicle model is shown. Since only the lateral dynamics are of interest, it is a two degree of freedom vehicle model (v, r). The tyres are assumed to be linear without any load-based non-linearity effects. Consequently, load transfer is not modelled either.

The equations of motion for the lateral acceleration and the yaw acceleration can be written as shown in equation (B.1.1). Here, C_f and C_r are the tyre lateral stiffness and are constant. ΔT is the total difference in the torques of the wheels requested by the controllers.

$$\begin{bmatrix} \dot{v} \\ \dot{r} \end{bmatrix} = - \begin{bmatrix} \dfrac{C_f + C_r}{mu} & \dfrac{C_f a - C_r b}{mu} + u \\ \dfrac{C_f a - C_r b}{I_{zz} u} & \dfrac{C_f a^2 + C_r b^2}{I_{zz} u} \end{bmatrix} \begin{bmatrix} v \\ r \end{bmatrix} + \begin{bmatrix} \dfrac{C_f}{m} & 0 \\ \dfrac{C_f a}{I_{zz}} & \dfrac{s_2}{R_w I_{zz}} \end{bmatrix} \begin{bmatrix} \delta \\ \Delta T \end{bmatrix} \tag{B.1.1}$$

B.2 Two track non-linear vehicle model

Figure B.2.1 shows the schematic of the two track vehicle model. This vehicle model has 9 degrees of freedom (4 wheel degress of freedom, pitch, roll, yaw, lateral and longitudinal). This model is used to simulate the actual vehicle response and is used to validate the optimal solutions obtained from the single track models.

Initial versions of the vehicle model also included an extra degree of freedom. The longitudinal displacement of the sprung mass with respect to the unsprung mass was taken into consideration. However, it became clear after a few simulations, that this had negligible impact on the simulation result and hence was removed from newer versions of the model.

Initially, the model was made in `Simulink` and was used for optimisation. However, it was seen that `Simulink` models were significantly slower compared to native `Matlab` script based models. The models were hence converted into `Matlab` script based models.

Even though the model has equations to take into account the degree of freedom in the longitudinal direction, this acceleration was forcibly set to zero since all the simulations being considered in this project are for the purpose of investigating lateral dynamics and are at constant speed.

The model uses the *Magic formula* tyre model with combined slip implemented. The tyre model can be described using the formula shown in B.2.1. Here, μ_0 is the tyre-road friction coefficient, c_0 is the normalized tyre stiffness coefficient and μ_1 and c_1 are the non-linear load dependence parameters for friction and tyre

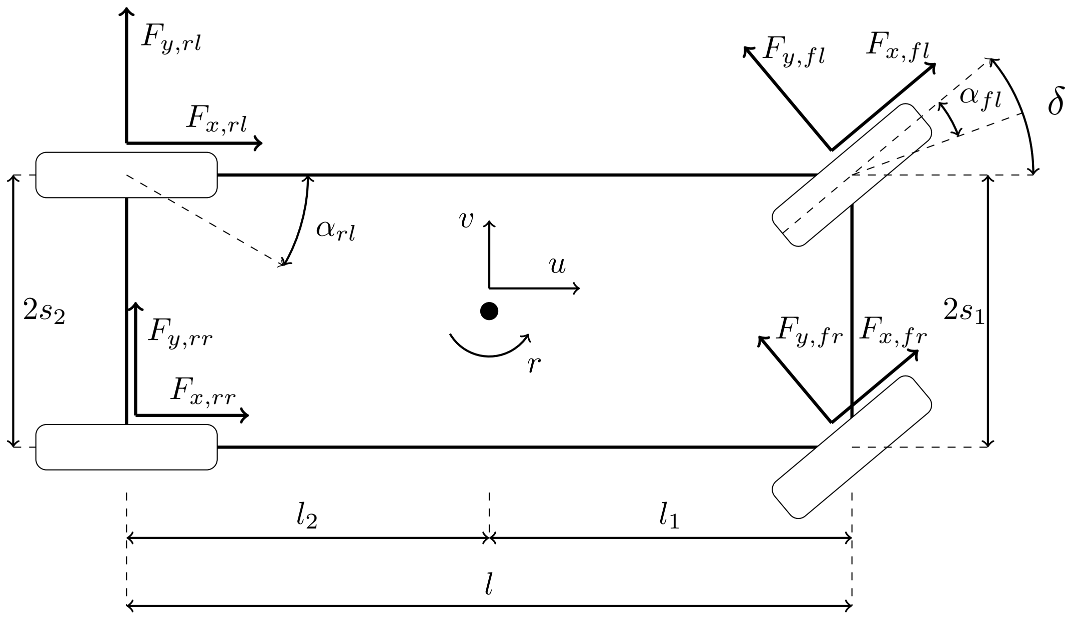

Figure B.2.1: *Two track vehicle model*

normalized stiffness. C is a tyre parameter for the *Magic formula*.

$$F(\sigma) = \mu F_z \sin(C \arctan(B\sigma - E(B\sigma - \arctan(B\sigma)))) \tag{B.2.1}$$

where,

$$\begin{aligned} B &= c/(\mu C) \\ c &= c_0(1 - c_1(F_z - F_{z0})) \\ \mu &= \mu_0(1 - \mu_1(F_z - F_{z0})) \end{aligned}$$

The tyre slip equations are shown in equation (B.2.2), where $v_{x,i}$ and $v_{y,i}$ are the wheel longitudinal and lateral velocities in the wheel plane coordinate system.

$$\begin{aligned} \alpha_i &= \delta_i - \arctan\left(\frac{v_{y,i}}{|v_{x,i}|}\right) & \kappa_i &= \frac{\omega_i R_w - v_{x,i}}{\max(|\omega_i R_w, v_{x,i}|)} \\ \sigma_{x,i} &= \frac{\kappa_i}{1 + |\kappa_i|} & \sigma_{y,i} &= \frac{\tan\alpha_i}{1 + |\kappa_i|} \\ \sigma_i &= \sqrt{\sigma_{x,i}^2 + \sigma_{y,i}^2} \end{aligned} \tag{B.2.2}$$

In equation (B.2.1), it can be seen that the friction and tyre normalized stiffness depend on the normal force on the tyre. To capture this non-linearity effect, the load transfer needs to be modelled accurately. Hence the roll and pitch dynamics of the vehicle are taken into account. Figures B.2.2 and B.2.3 show the free body diagram of the sprung and unsprung mass during roll. Here, ϕ represents the roll angle, h' the height of the center of gravity over the roll axis, h_i represents the respective roll center height, l_i the distance of the respective axle from the center of gravity and s_i represents the respective half track width. The equations for load transfer during roll can be written based on these figures as shown in equations (B.2.3).

$$\begin{aligned} \ddot{\phi} &= (m_s a_y h_{0,r} - c_\phi \dot{\phi} - (k_\phi - m_s g h_{0,r})\phi)/(I_{xx} + m_s h_{0,r}^2) \\ \Delta F_{z,i,r} &= \frac{1}{2s_i}\left(m a_y h_{i,r}(l - l_i)/l + k_{\phi,i}\phi + c_{\phi,i}\dot{\phi}\right) \end{aligned} \tag{B.2.3}$$

Similarly, the equations for load transfer during pitch can be written as shown in equations (B.2.4). Note that the acceleration that influences pitch is not the full longitudinal acceleration of the vehicle but instead the

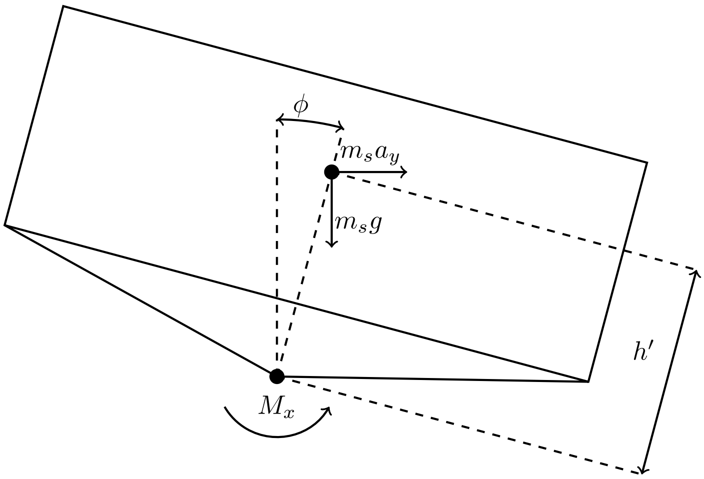

Figure B.2.2: *Free body diagram of sprung mass undergoing roll*

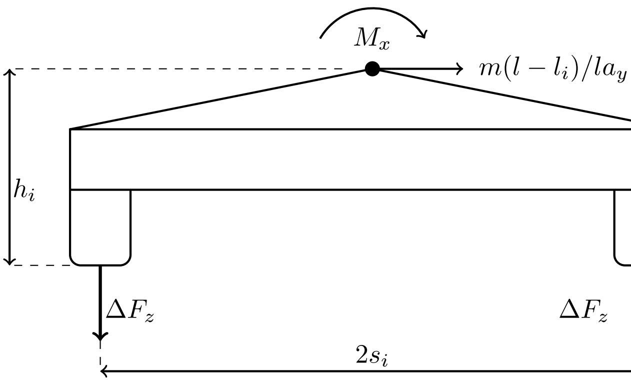

Figure B.2.3: *Free body diagram of unsprung mass*

longitudinal acceleration of the vehicle caused due to all forces except the aerodynamic drag. This is because, the aerodynamic drag force acts close to in-line with the center of gravity of the vehicle and consequently doesn't contribute significantly to the pitch moment of the vehicle. This acceleration is represented as $a_{x,p}$ in the equations.

$$\ddot{\theta} = (m_s a_{x,p} h_{0,p} - c_\theta \dot{\theta} - (k_\theta - m_s g h_{0,p})\theta)/(I_{yy} + m_s h_{0,p}^2)$$
$$\Delta F_{z,i,p} = \frac{1}{2l}\left(m a_{x,p} h_{1,p}(l - l_1)/l + m a_{x,p} h_{2,p}(l - l_2)/l - k_\theta \theta - c_\theta \dot{\theta}\right) \tag{B.2.4}$$

A highly simplified powertrain model is used in the simulation. The engine drives the front wheels and delivers any requested constant torque equally to the front two wheels. The electric powertrain can only deliver torque vectoring, i.e., they can only provide equal and opposite torques to the wheels of each axle. A first order filter has been added to the torques delivered by the motors. This was done in order to investigate the effect of motor response time on the yaw dynamics. However, in normal simulations and optimisation, the motor is assumed to be ideal. The time constant in these cases for the filters is set to 10^{-8} s which is negligible.

A simple brake model is also included in the model although it is not required for any of the manoeuvre used in the simulations. The brake is modelled as shown in equation (B.2.5). The tanh function is used to take into account the direction of wheel rotation when detemining the direction of braking force. The factor of 10 is used simply to ensure that the tanh function is steep enough near zero wheel speed to ensure a good degree of accuracy.

$$T_{B,i} = F_{B,dmd} R_w \tanh(10\omega_i) \tag{B.2.5}$$

Using the equations set up until now, the force balance equation in the longitudinal direction can be written as:

$$
\begin{aligned}
\Sigma F_x &= m a_x = m(\dot{u} - vr) \\
\Sigma_{i=1}^{4}(F_{x,i}\cos\delta_i - F_{y,i}\sin\delta_i) &= m(\dot{u} - vr)
\end{aligned}
\tag{B.2.6}
$$

In the lateral direction, the force balance equation can be written as:

$$
\begin{aligned}
\Sigma F_y &= m a_y = m(\dot{v} + ur) \\
\Sigma_{i=1}^{4}(F_{y,i}\cos\delta_i + F_{x,i}\sin\delta_i) &= m(\dot{v} + ur)
\end{aligned}
\tag{B.2.7}
$$

The moment balance equation about the $\mathcal{Z}$ axis can be written as:

$$
\begin{aligned}
\Sigma M_z &= I_{zz}\dot{r} \\
\Sigma_{i=1}^{4}\left((F_{y,i}\cos\delta_i + F_{x,i}\sin\delta_i)l_i - (F_{x,i}\cos\delta_i - F_{y,i}\sin\delta_i)s_i\right) &= I_{zz}\dot{r}
\end{aligned}
\tag{B.2.8}
$$

The wheel and suspension geometry is shown in figure B.2.4. While the steering torque due to braking forces from the traditional brakes are a function of the scrub radius, the steering torque due to braking or traction forces from the motors are a function of the kingpin offset. This is because, when the motor is used to generate tractive or braking forces, the torque due to these wheel forces are reacted upon by the motor which is inboard on the chassis, not connected to the steering system. The wheel forces themselves then act on the steering system from the wheel center and hence the steering torque becomes a function of the kingpin offset.

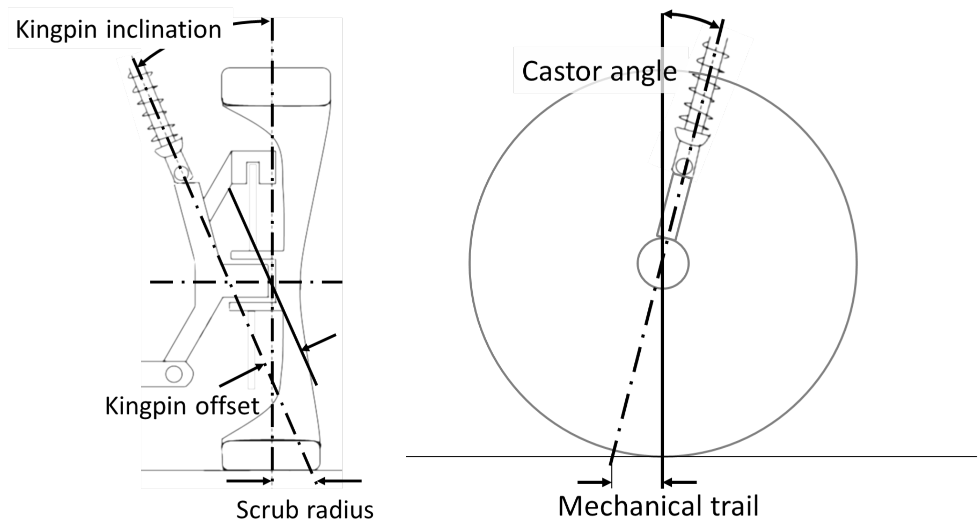

(a) *Kingpin offset, scrub radius and kingpin inclination*

(b) *Castor trail and castor angle*

Figure B.2.4: *Wheel and suspension geometry*

On the other hand, when the brakes are used, it locks the wheel and the steering system into one rigid unit (the brakes are mounted on the suspension on which is also the steering tie rod). Hence, the torques due to the wheel forces act directly on the steering system and are a function of the scrub radius.

The contribution of the longitudinal tyre force on one wheel to the steering torque can be expressed as shown in equation (B.2.9). Here, d_{kpo} is the kingpin offset, γ is the castor angle and β is the kingpin inclination.

$$
T_{str} = \frac{\cos\gamma}{\sqrt{\cos^2\beta + \cos^2\gamma - \cos^2\beta\cos^2\gamma}} d_{kpo} F_x
\tag{B.2.9}
$$

For the simulation, the `ode15s` solver was used. This is a stiff variable time-step solver that can handle singular mass matrices.

C Model based controllers

In this chapter, the work to be done in the future regarding the controller is described. In brief, proposals for new types of controllers are presented.

C.1 Model based controller I

In this model based controller, a steady state reference generator and an inverse model is used to determine the torque required.

Given the single track vehicle model, (eqn B.1.1) setting $\dot{v}$, $\dot{r}$ and ΔT to zero and solving for r, we get the steady state reference generator. This expression is differentiated to get the target yaw acceleration, $\dot{r}$, which will be a function of steering rate ($\dot{\delta}$).

These target states are then substituted in the inverse model to determine the required torque. The final expression for ΔT will still be a function of the vehicle lateral velocity. But since the inverse model runs continously as a dynamic model, the lateral velocity is also known.

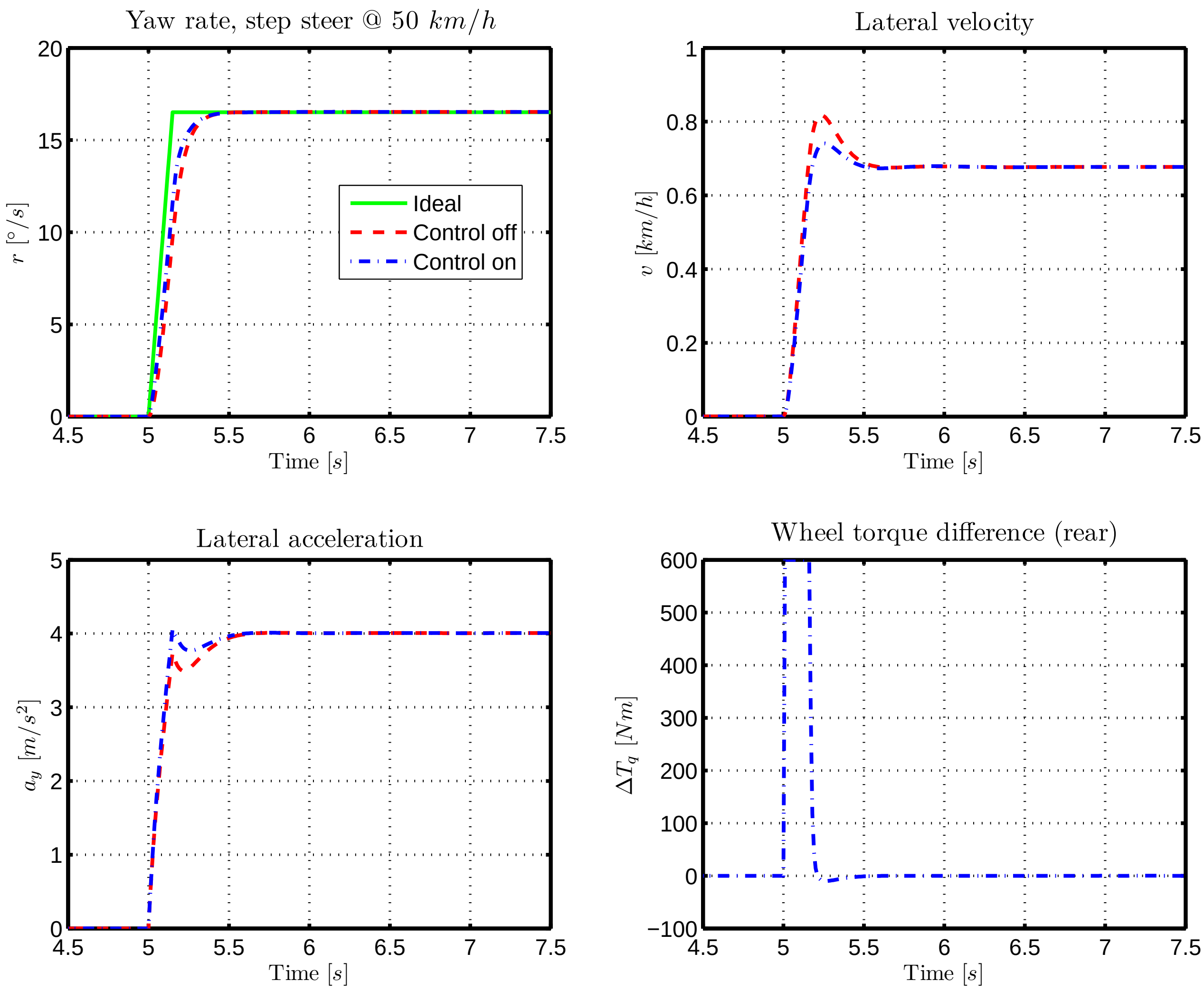

Figure C.1.1: *Vehicle performance at 50 km/h with model based controller 1*

Note that this controller has a steady state yaw rate as the target yaw rate and a target yaw acceleration derived from the target yaw rate. This controller was tested on both the linear bicycle model and the two track vehicle model. It was seen that while the controller performed reasonably well at low speeds, it was prone to yaw overshoot at higher speeds. This occured in the case of both the single track model and the two track model where the issue was exacerbated.

To counteract this problem, a limitation was added to the torque vectoring so as to reduce the maximum torque vectoring done at 150 km/h to 400 Nm from the usual value of 600. The torque limit and the speed was determined experimentally.

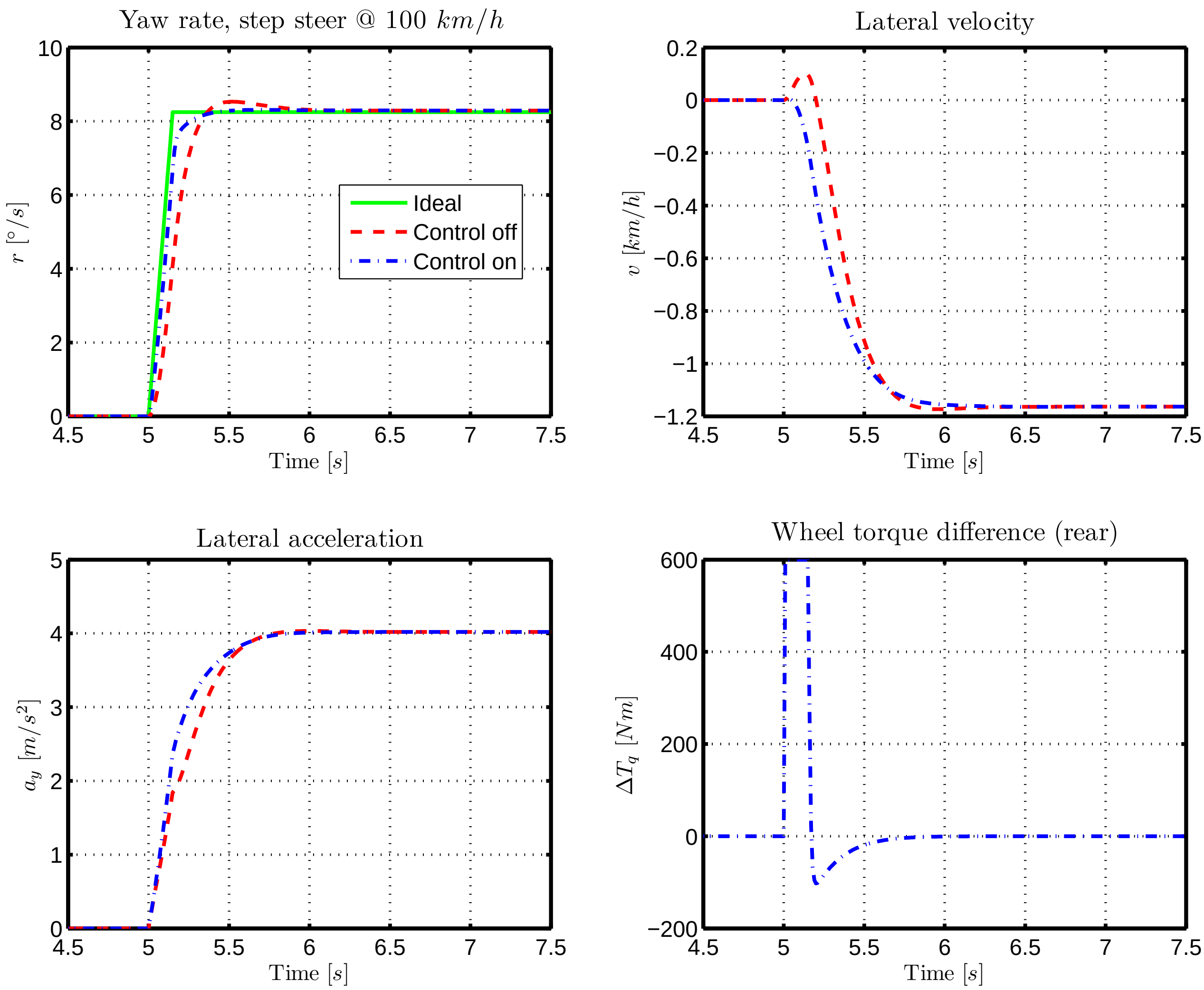

Figure C.1.2: *Vehicle performance at* 100 km/h *with model based controller 1*

Figures C.1.1, C.1.2 and C.1.3 show the controller performance with the two track model in the reference manoeuvres.

The controller performance is comparable to that of the empirical controller. At low speeds, the yaw response is slightly worse. At higher speeds, the model based controller performs better in terms of damping while losing out to the empirical controller in yaw response. With the empirical controllers it would be possible to adjust them so as to favour response over damping or vice-versa. However, it is not quite clear if the model based controllers can be tuned in the same way.

C.2 Model based controller II

This is another type of model based controller where the torque is determined not based on a reference yaw rate but instead based on a reference yaw acceleration.

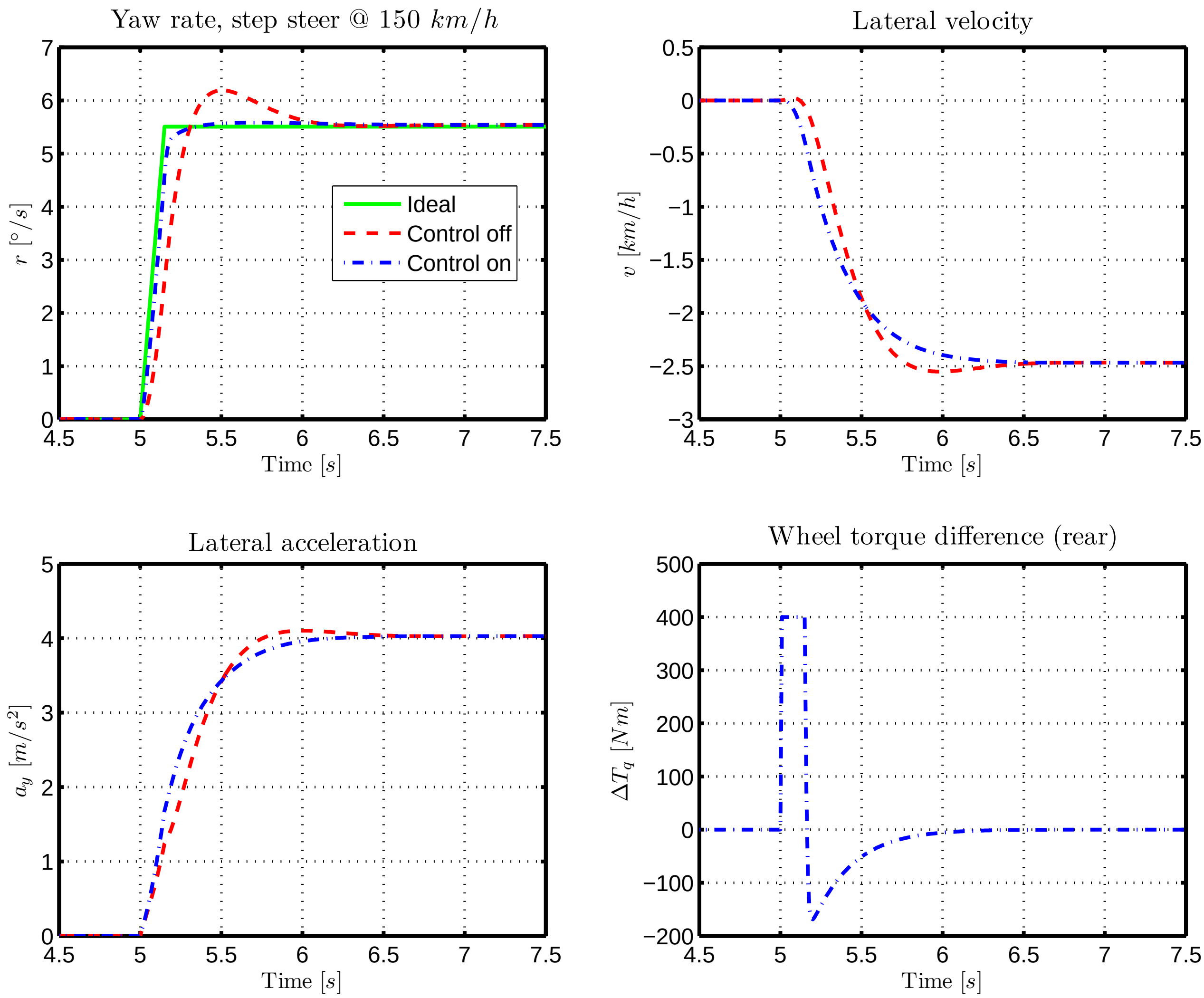

Figure C.1.3: *Vehicle performance at 150 km/h with model based controller 1*

Like in the other model based controller, this one involves a linear single track reference model that runs in the controller. This model generates the vehicle states which the controller believes the vehicle has at any point in time.

The controller also generates the expected steady state yaw rate for the current steering wheel angle. This is determined by the equation (C.2.1) where K_u is the understeer gradient for the vehicle.

$$r_{ss} = \frac{\delta}{\frac{l}{u} + K_u u} \tag{C.2.1}$$

This reference steady state yaw rate is used to generate the target yaw acceleration required for the actual vehicle as shown in equation (C.2.2).

$$\dot{r}_{tgt} = (r_{ref} - r_{lin})/\Delta t \tag{C.2.2}$$

This target acceleration is used in the yaw moment balance equation of the linear vehicle model equations of motion (equation B.1.1) to determine the required yaw moment torque.

This controller was once again tested with both the linear single track and the two track vehicle model. With the single track vehicle model, the controller made the vehicle yaw response close to ideal for all speeds.

However, with the two track model, while the performance was better than the previous model based controller, similar yaw overshoot problems were seen at higher speeds.

One possible explanation could be the non-linear nature of the tyres and the load transfer could be causing the tyre stiffnesses to differ significantly from the linear model and hence the difference in performance.

To test this, the load transfer and the non-linearity of the tyres were built into the single track linear vehicle model. Non-linearity of both the trye stiffness and the tyre-road friction coefficient were taken into account.

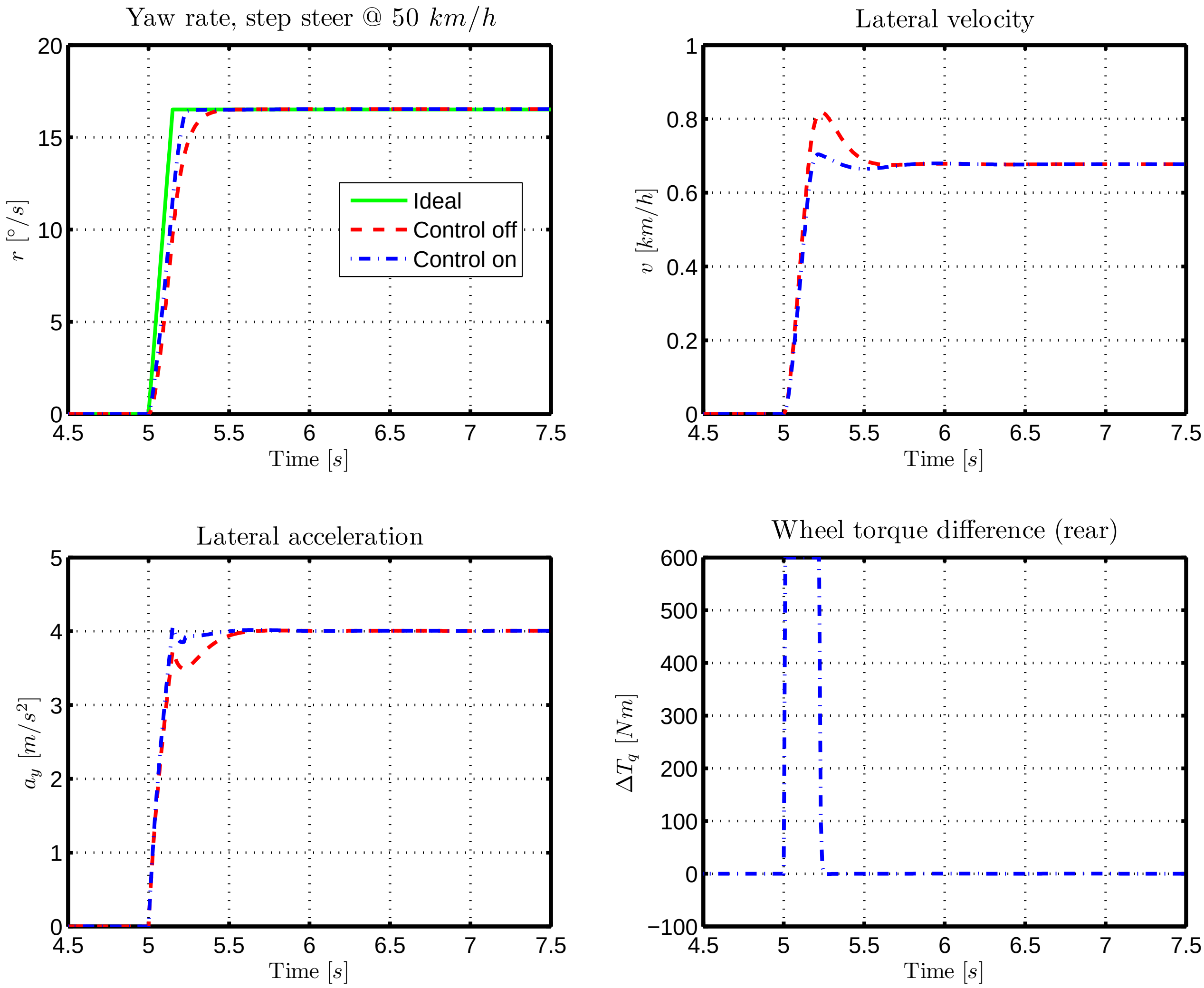

Figure C.2.1: *Vehicle performance at 50 km/h with model based controller 2*

Figure C.2.1 shows the performance of this controller at 50 km/h with the step steer manoeuvre. It can be seen that the yaw response of the vehicle is close to ideal. The small deviation from the ideal is most likely due to the fact that the torque limit has been hit.

The vehicle yaw response at 100 km/h is shown in figure C.2.2. Here, it can be seen that the vehicle yaw response is very close to the ideal. Even here, the controller makes full use to the torque vectoring capability available. The lateral acceleration and the lateral velocity plots show similar behaviour as in all other cases with the yaw controller.

Figure C.2.3 shows the yaw response at 150 km/h. Here, a small deviation from the ideal can be seen. This is initally a bit surprising since the torque vectoring limit is not reached either. It appears as though controller stops the torque vectoring too early.

This is because, at such high speed (150 km/h), there is quite a lot of drive torque going to the front wheels to maintain the speed and eating away at their lateral capacity. This causes the vehicle to respond slower than the controller expects and hence causes the deterioration in performance. This is not taken into account in the

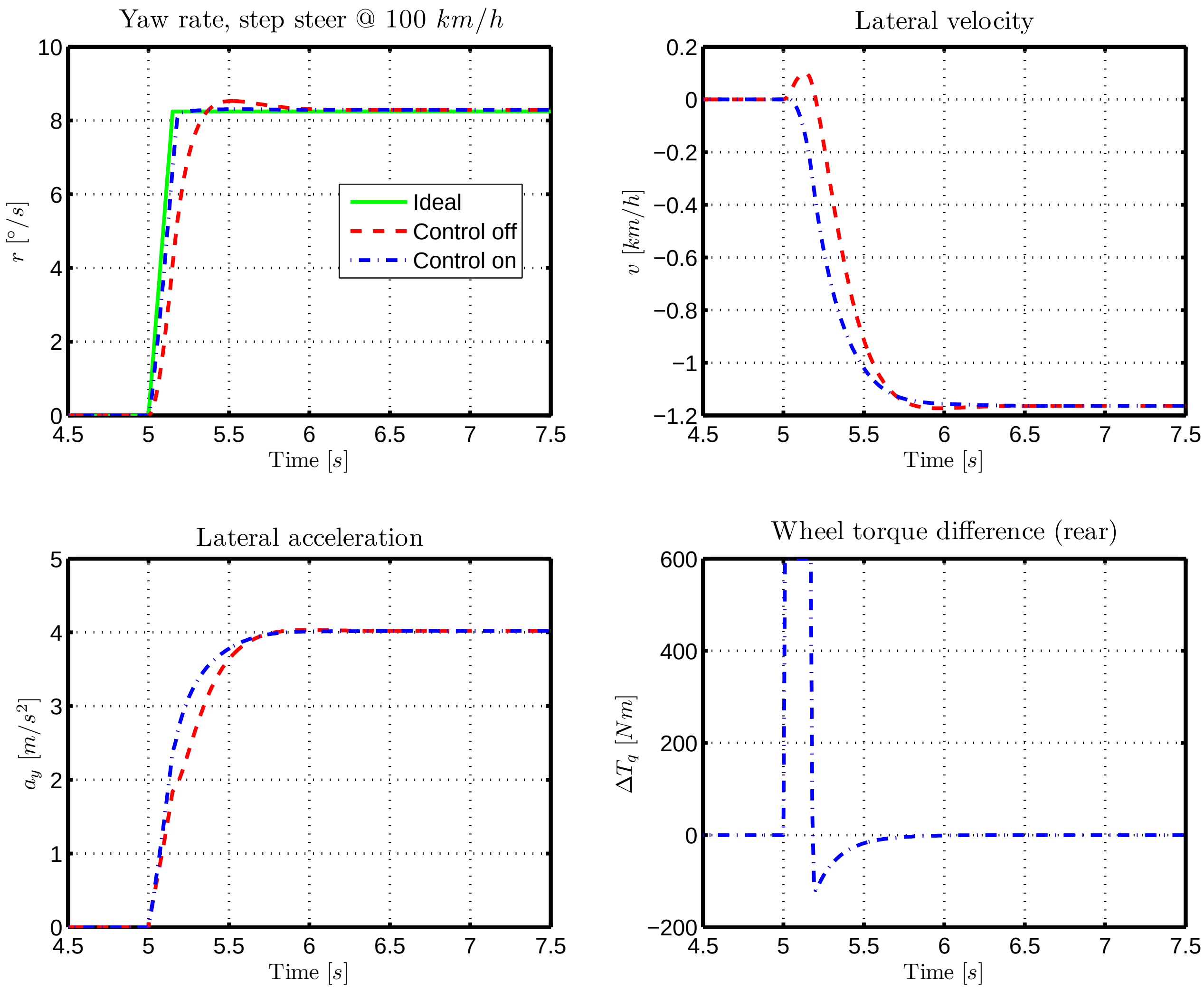

Figure C.2.2: *Vehicle performance at* 100 km/h *with model based controller 2*

controller as this information is not available with sufficient accuracy in a normal vehicle to be of use in the controller.

C.3 Validation

In this section, the model based controllers are evaluated and validated.

The frequency response and phase shift of the model based controller I is shown in figure D.2.5. The model based controller I performs nearly as well as the empirical controller. One of the minor differences is that the model based controller performs slightly worse in terms of increasing the frequency bandwidth and maintaining a flat frequency response curve while it is better at keeping the phase shift low. In other words, at higher frequencies of steering input, the model based controller seems to favour yaw reponse over damping.

Figure D.2.7 shows the frequency response and the phase shift of the vehicle at 7 m/s^2. In this case, there is neglible difference between the model based controller and the empirical controller in terms of frequency bandwidth. However, the model based controller still has a slight edge in keeping the phase shift low.

The frequency response and the phase shift of the second model based controller is shown in figure D.2.6. This model based controller again has a small advantage in terms of maintaining low phase shift. This controller however, while it does not maintain a flat frequency response curve, it does extend the frequency bandwidth.

Figure D.2.8 shows the frequency response and the phase shift at 7 m/s^2. In this case, the controller

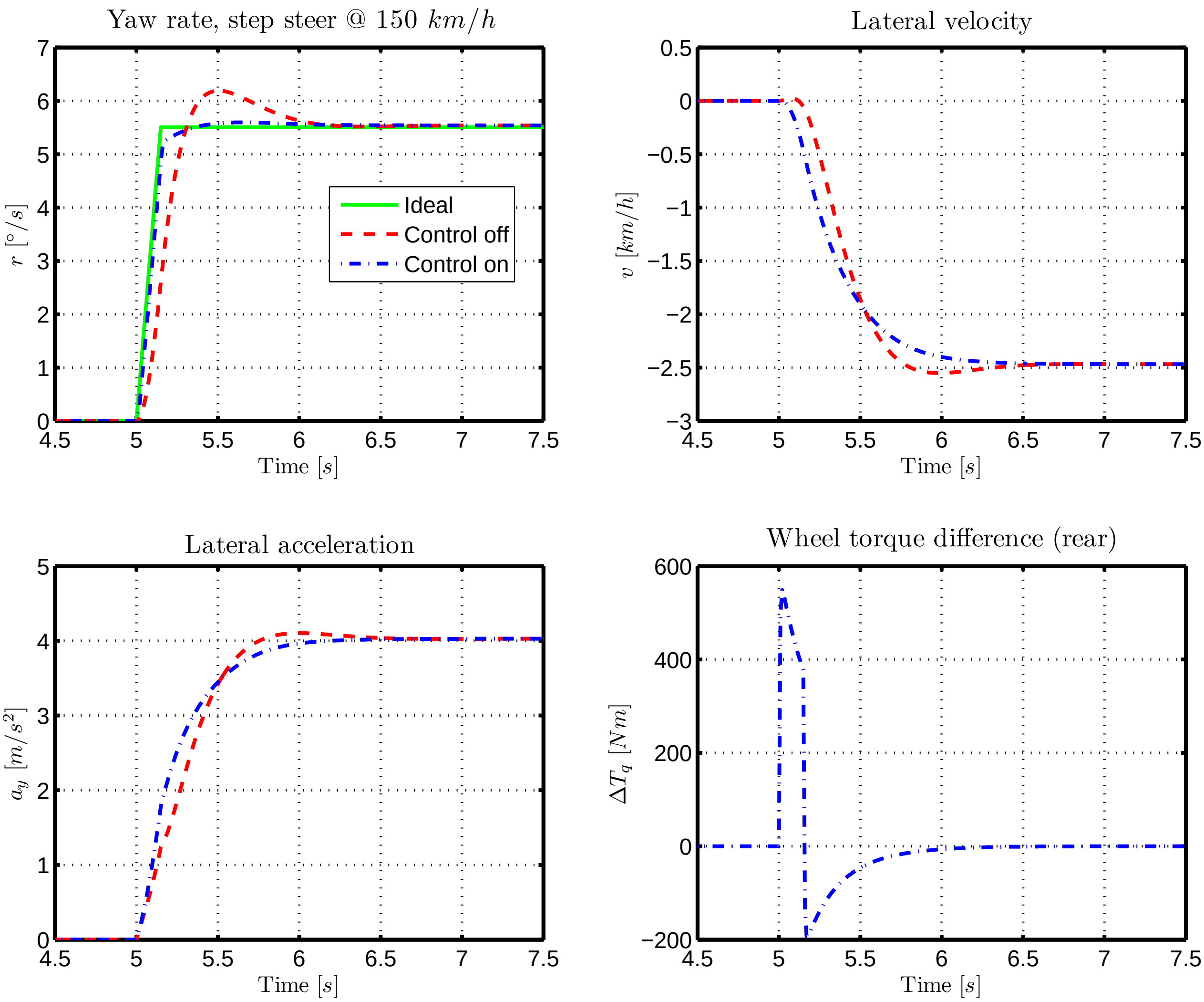

Figure C.2.3: *Vehicle performance at* 150 km/h *with model based controller 2*

performs slightly better than the empirical controller at low speeds in terms of phase shift while losing out at high speeds. Whereas with the frequency bandwith, the controller is clearly superior to the empirical one at high speeds but equivalent at low speeds. Once again a possible explanation for the difference could be that the model based controller does not account for the increased drive torque at the front wheels while the empirical controller, in a way, does. Since several tunings were obtained for the empirical controller which were analysed and the best one among them chosen, it is possible that the controller, in a way, compensates for this effect.

Figures D.2.1 and D.2.2 show the controller performance for the sine with dwell steering manoeuvre with 30° and 45° steering amplitudes respectively. This validation test was done mainly to verify that the controller does not make the situation worse with torque vectoring. As can be seen, the controller performs similarly to the empirical controller. There is very little difference between the two controllers in terms of performance. The model based controller however, does seem to utilise the torque vectoring more.

Figures D.2.3 and D.2.4 show the performance of the second model based controller in the sine with dwell manoeuvres. The controller performance once again is very similar to the empirical and the first model based controller. All the controllers seem to have similar drawbacks as well. Especially, in the case of 45° steering angle, the vehicle yaw rate plot shows the same fluctation just after the end of the manoeuvre. Since the model based controllers are based on the linear model, it is understandble that their torque request at this point changes significantly since the linear model being close to ideal, would follow the steering input closely.

Since the empirical model also shows the same behaviour (flaw), this indicates that the controller with the optimised parameters accurately capture the dynamic behaviour of the vehicle.

D Figures

D.1 Empirical controller

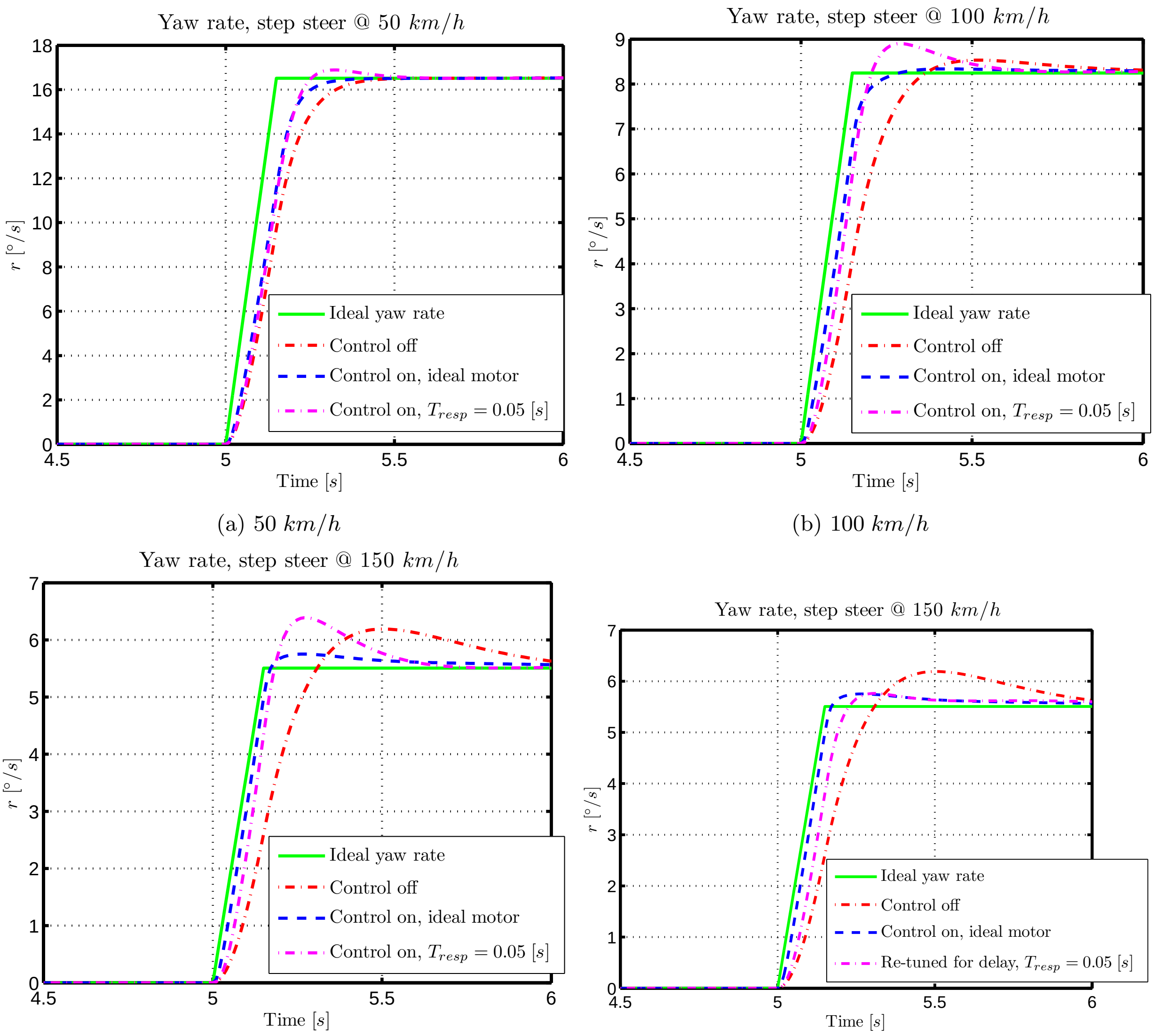

(a) 50 km/h

(b) 100 km/h

(c) 150 km/h

(d) 150 km/h, *tuned controller*

Figure D.1.1: *Vehicle performance with step steer and non-ideal motors*

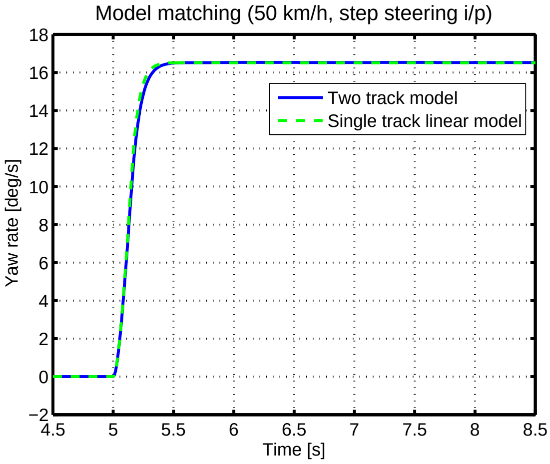

(a) *Step steer*, 50 km/h

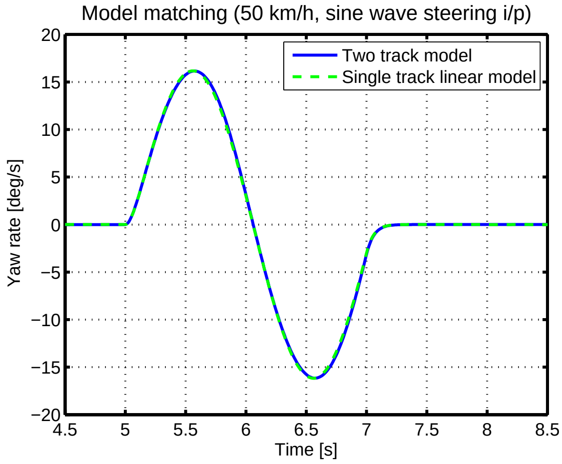

(b) *Sine steer*, 50 km/h

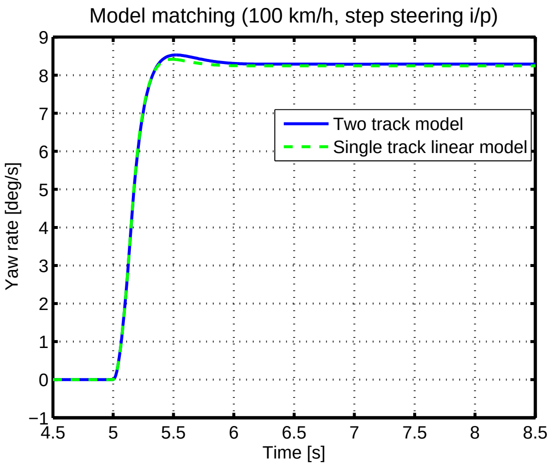

(c) *Step steer*, 100 km/h

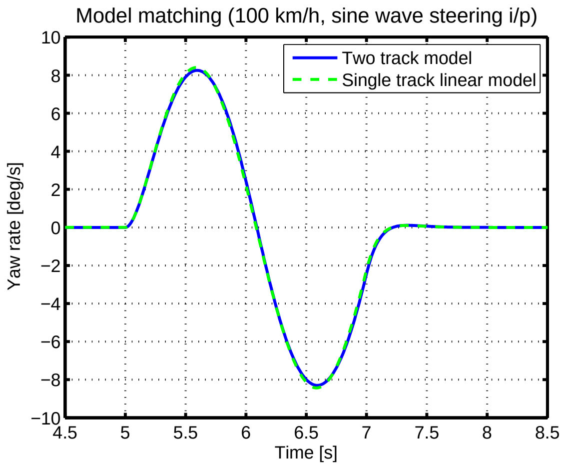

(d) *Sine steer*, 100 km/h

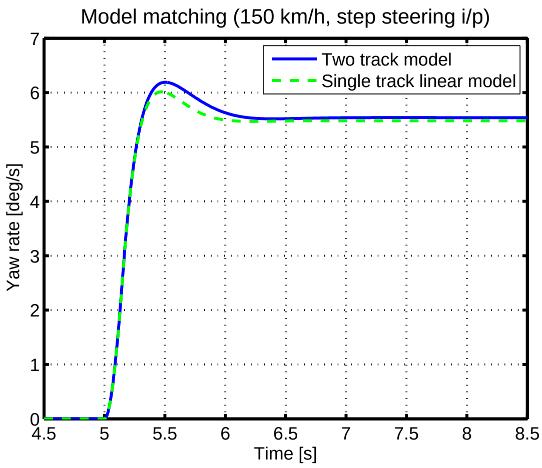

(e) *Step steer*, 150 km/h

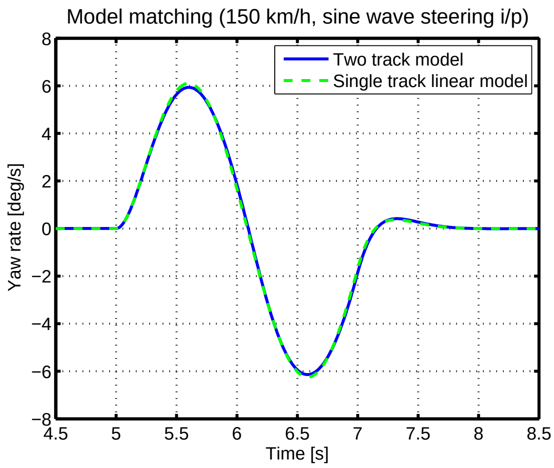

(f) *Sine steer*, 150 km/h

Figure D.1.2: *Model matching*

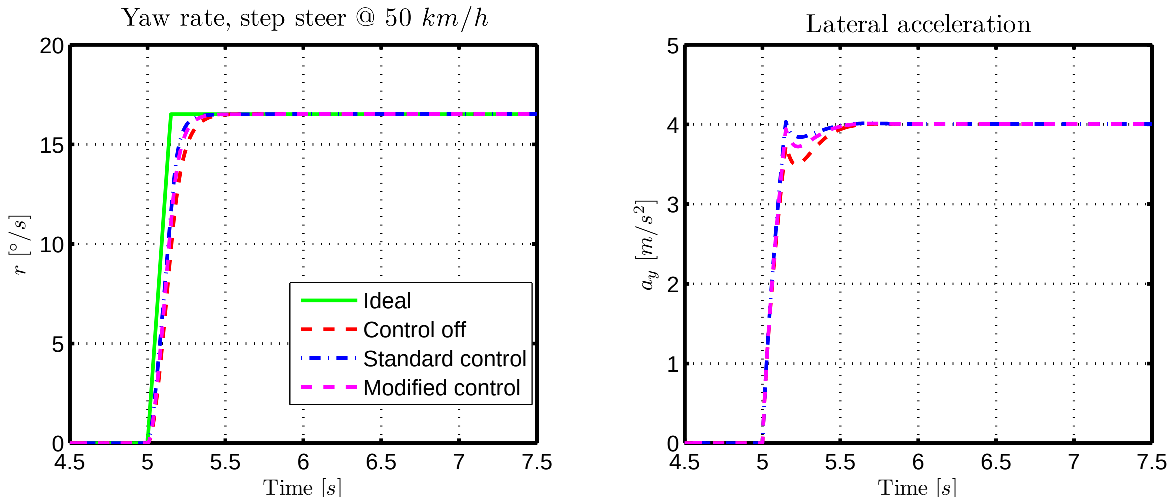

Figure D.1.3: *Reduced lateral acceleration overshoot at* 50 km/h

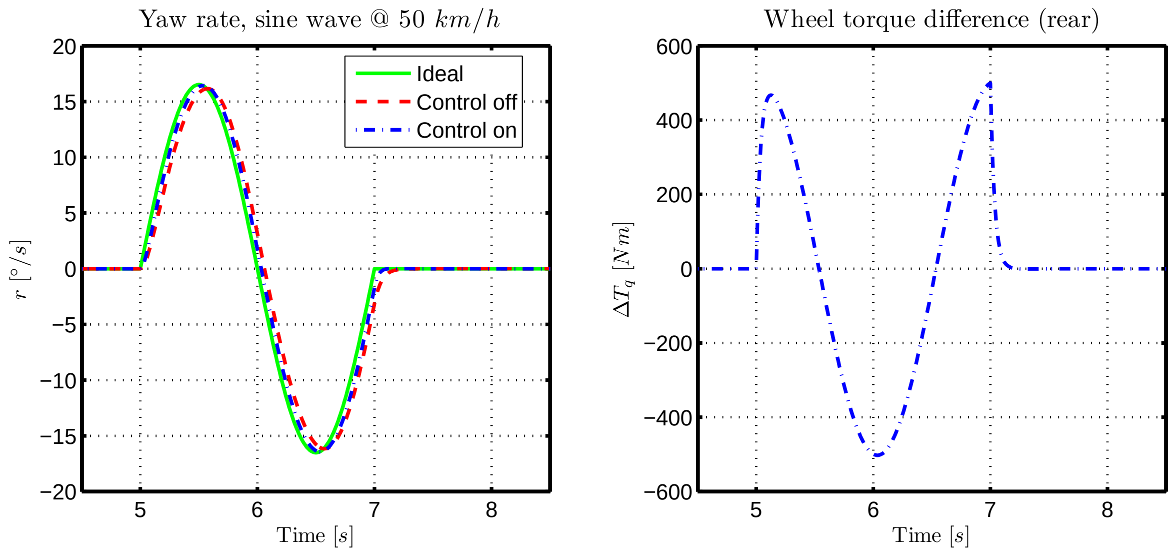

Figure D.1.4: *Vehicle performance at* 50 km/h*, sine wave steering input with empirical controller*

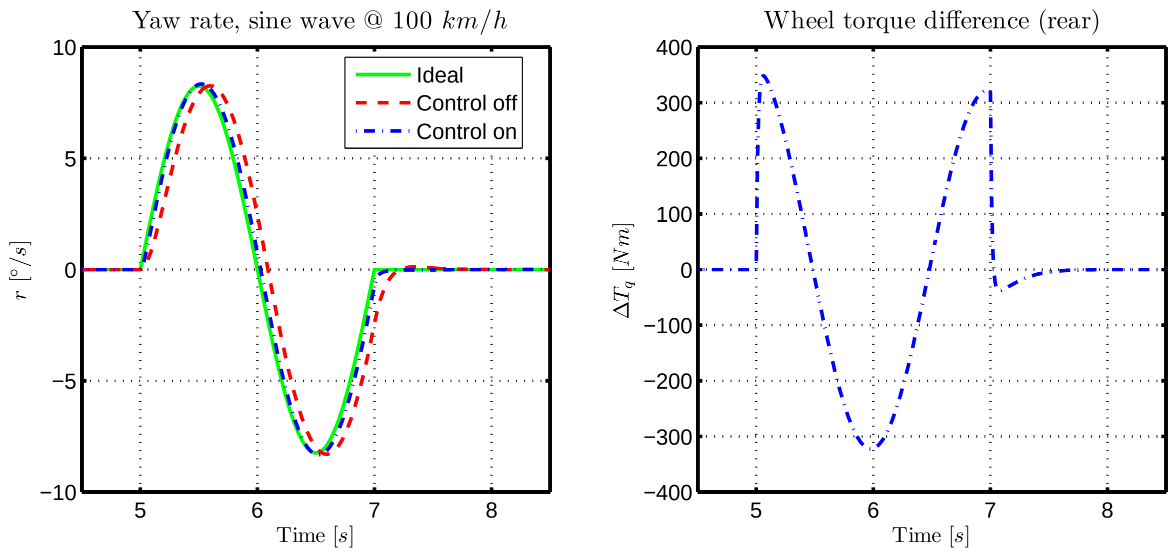

Figure D.1.5: *Vehicle performance at* 100 km/h*, sine wave steering input with empirical controller*

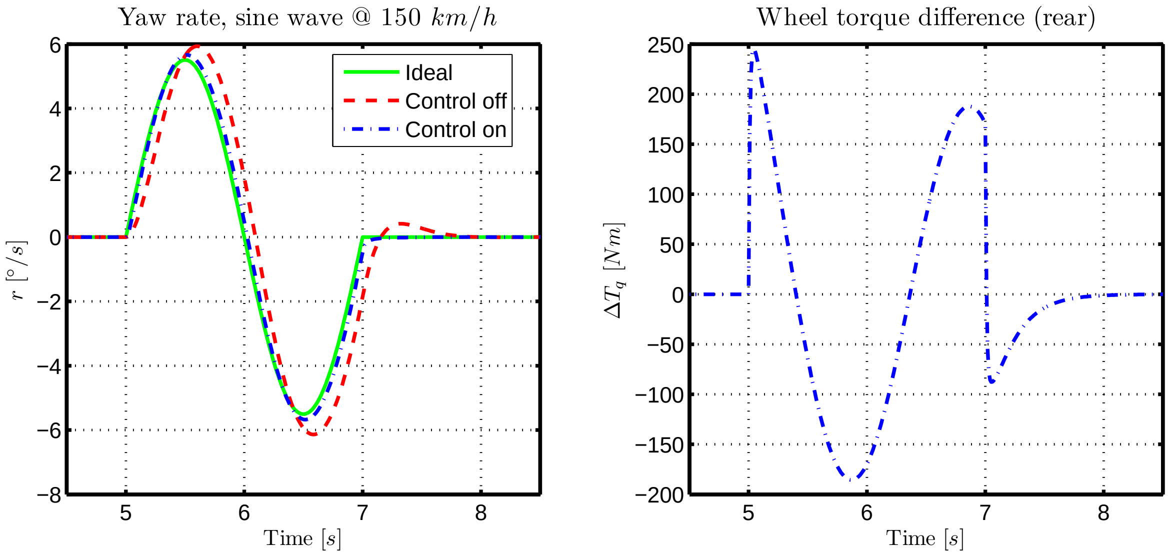

Figure D.1.6: *Vehicle performance at* 150 km/h*, sine wave steering input with empirical controller*

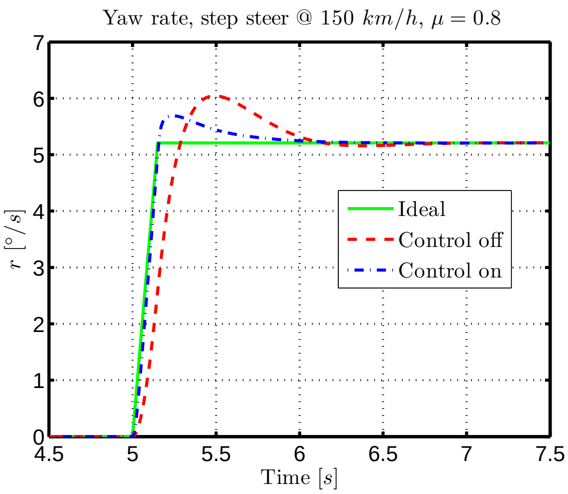

(a) *Step steer,* $\mu = 0.8$

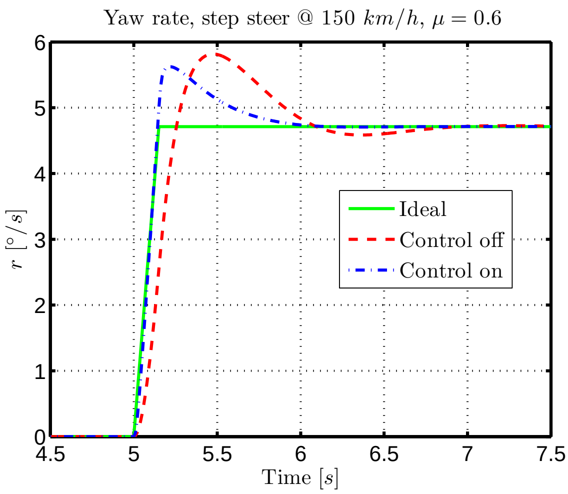

(b) *Step steer,* $\mu = 0.6$

Figure D.1.7: *Vehicle performance at* 150 km/h *on low* μ *surfaces*

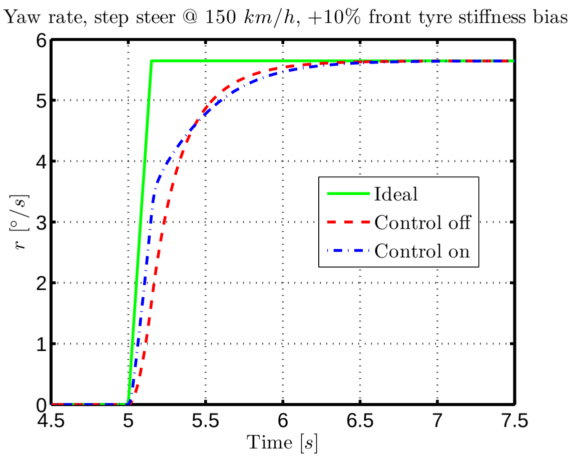

(a) *Step steer,* +10% *front tyre stiffness*

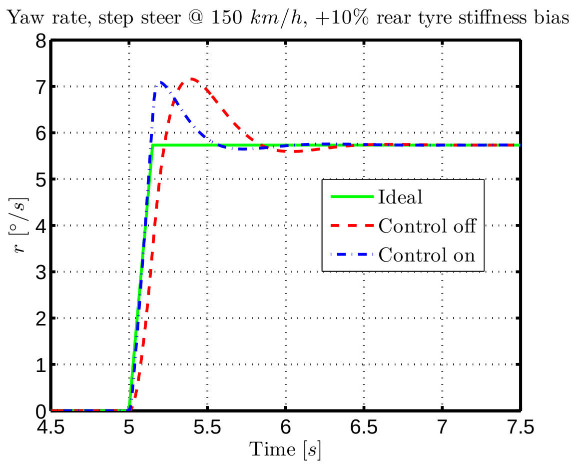

(b) *Step steer,* +10% *rear tyre stiffness*

Figure D.1.8: *Vehicle performance at* 150 km/h *with different tyre stiffness*

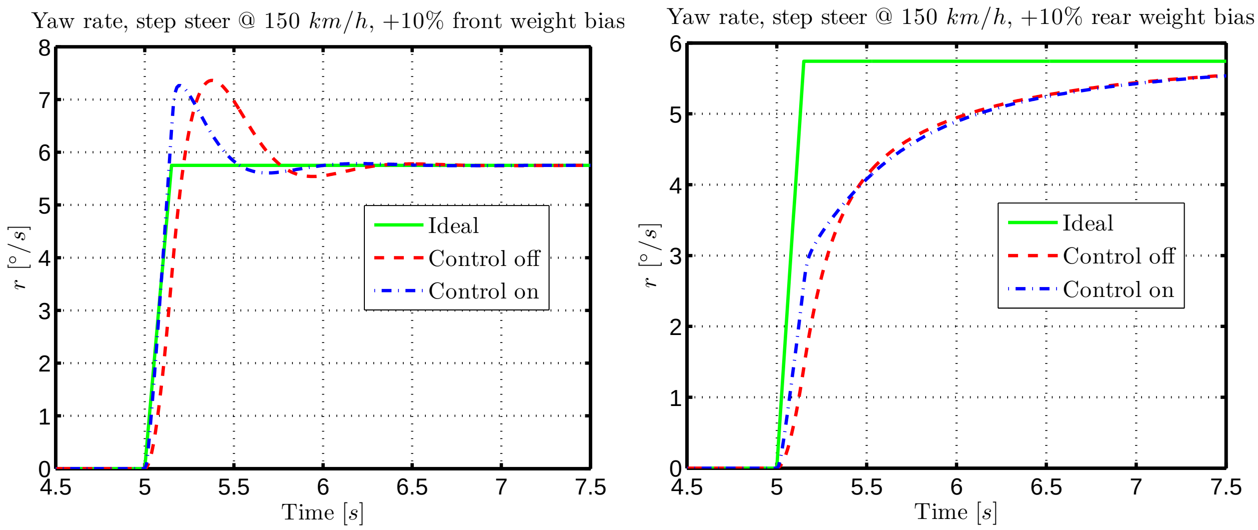

(a) *Step steer, +10% front weight bias* (b) *Step steer, +10% rear weight bias*

Figure D.1.9: *Vehicle performance at 150 km/h with different weight distribution*

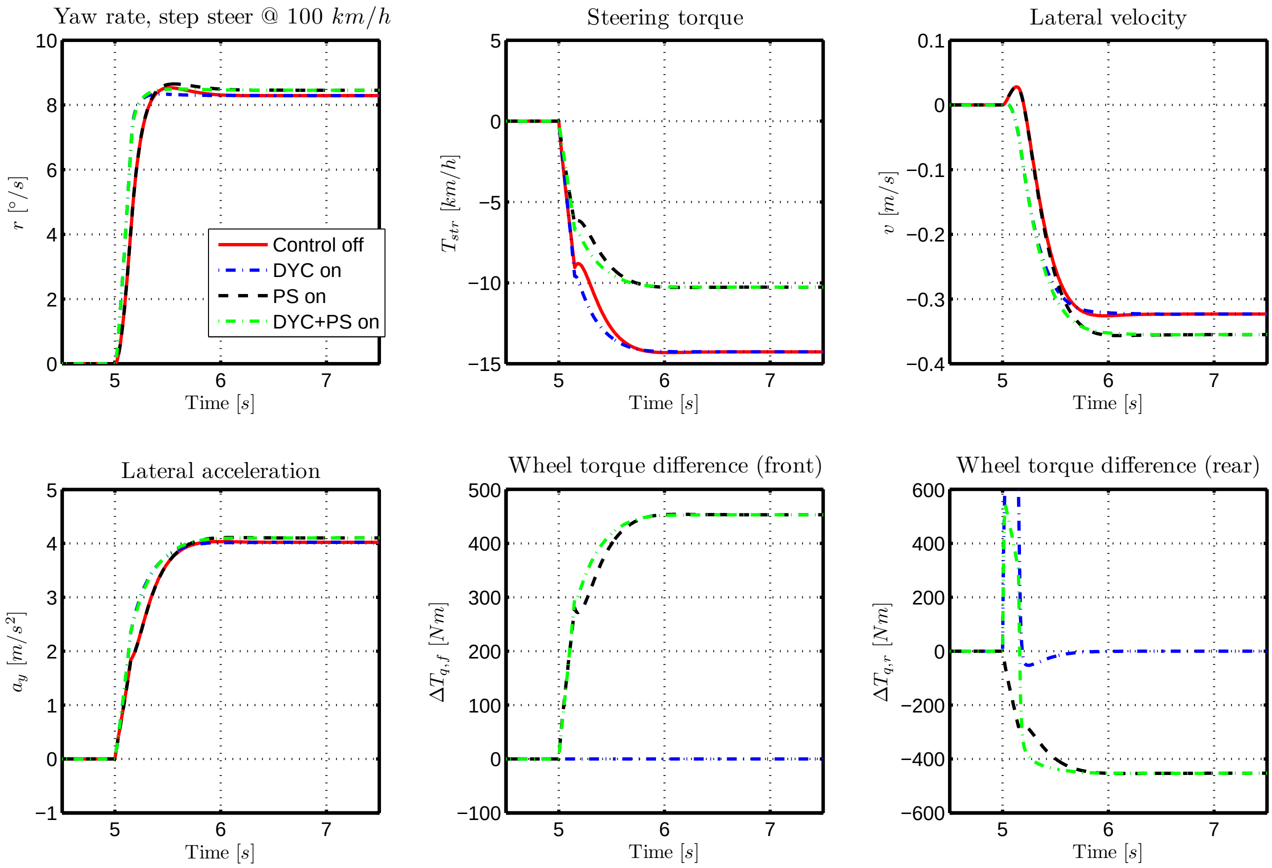

Figure D.1.10: *Steering torque assist and lateral dynamics at 100 km/h with step steer*

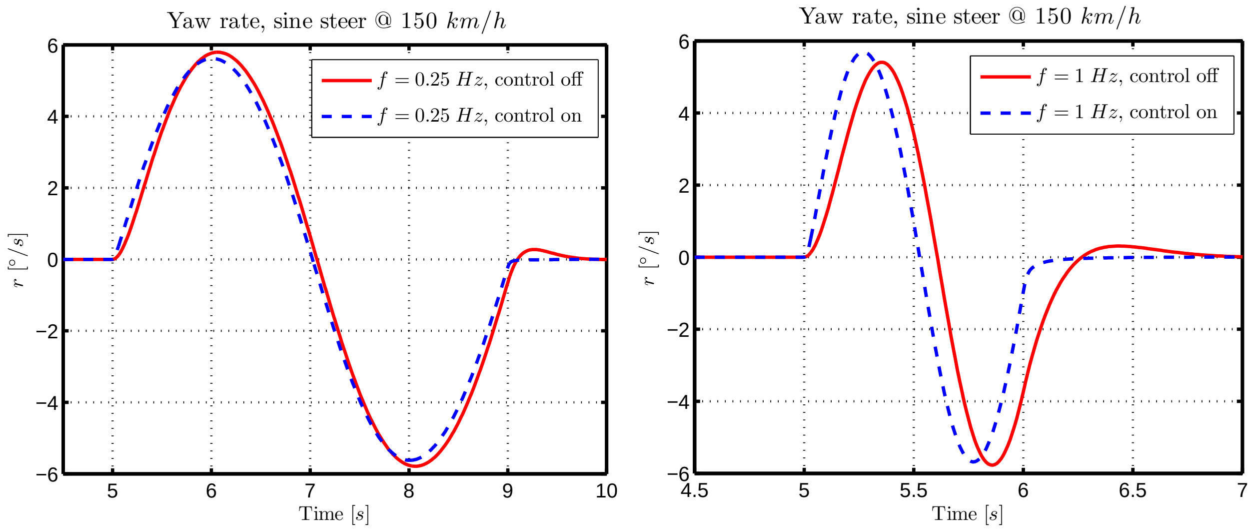

(a) *Sine wave* $0.25\ Hz$ (b) *Sine wave* $1\ Hz$

Figure D.1.11: *Validation of yaw controller at* $150\ km/h$ *for different sine frequencies*

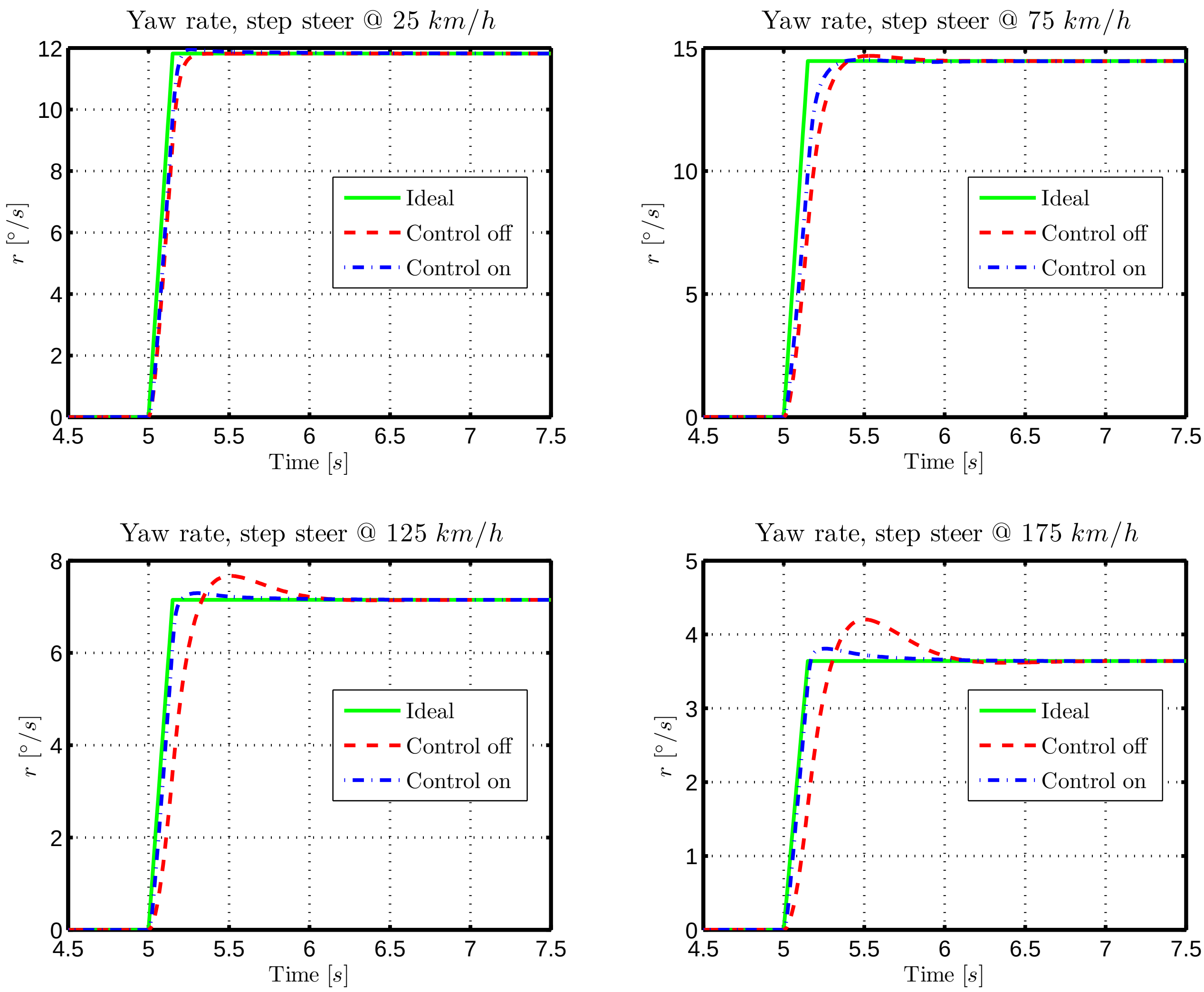

Figure D.1.12: *Validation of yaw controller for different speeds with the control parameters interpolated*

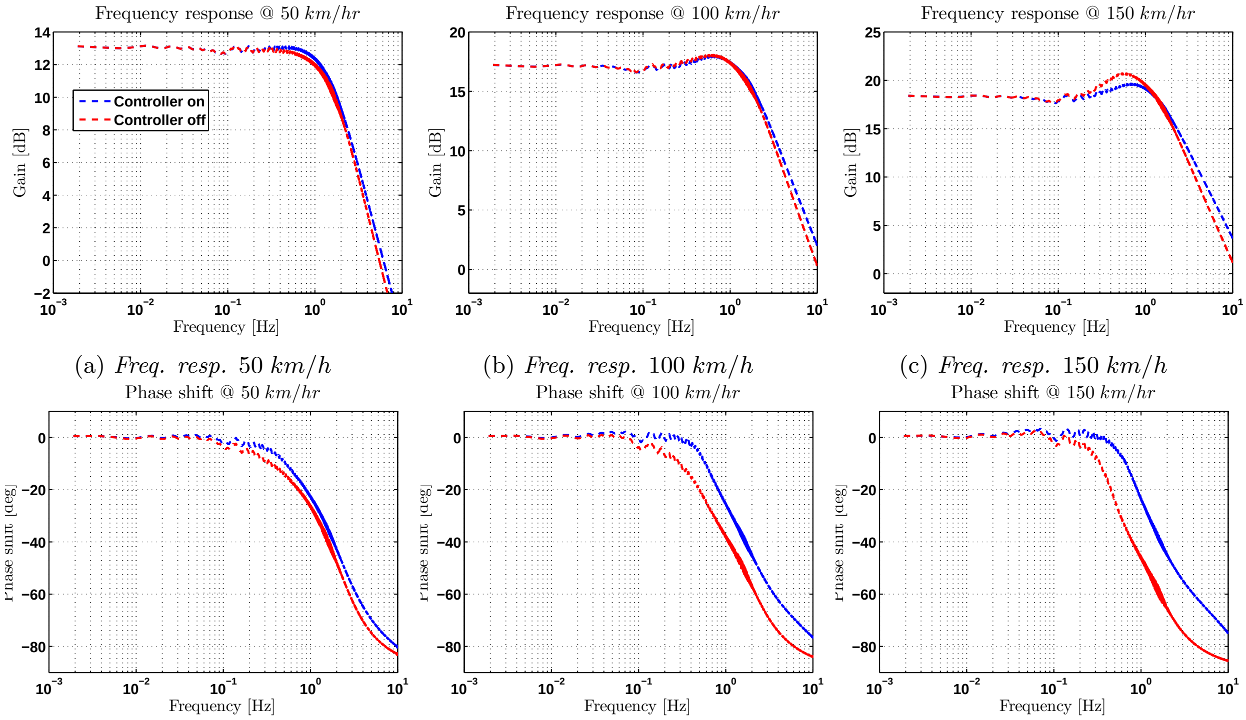

(a) *Freq. resp. 50 km/h* (b) *Freq. resp. 100 km/h* (c) *Freq. resp. 150 km/h*

(d) *Phase shift 50 km/h* (e) *Phase shift 100 km/h* (f) *Phase shift 150 km/h*

Figure D.1.13: *Frequency response and phase shift at 7 m/s^2*

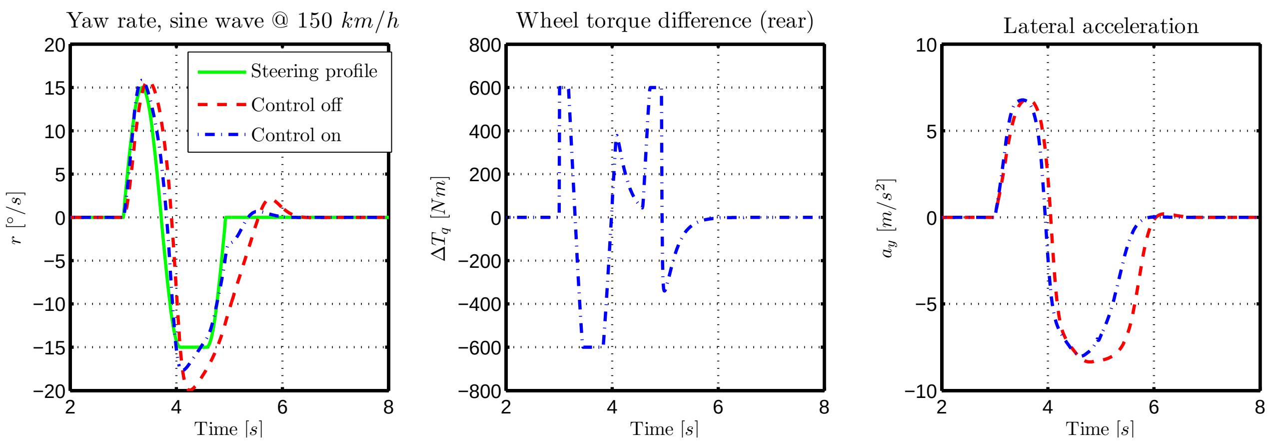

Figure D.1.14: *Controller performance in a sine with dwell steering manoeuvre at 150 km/h with 30° steering angle*

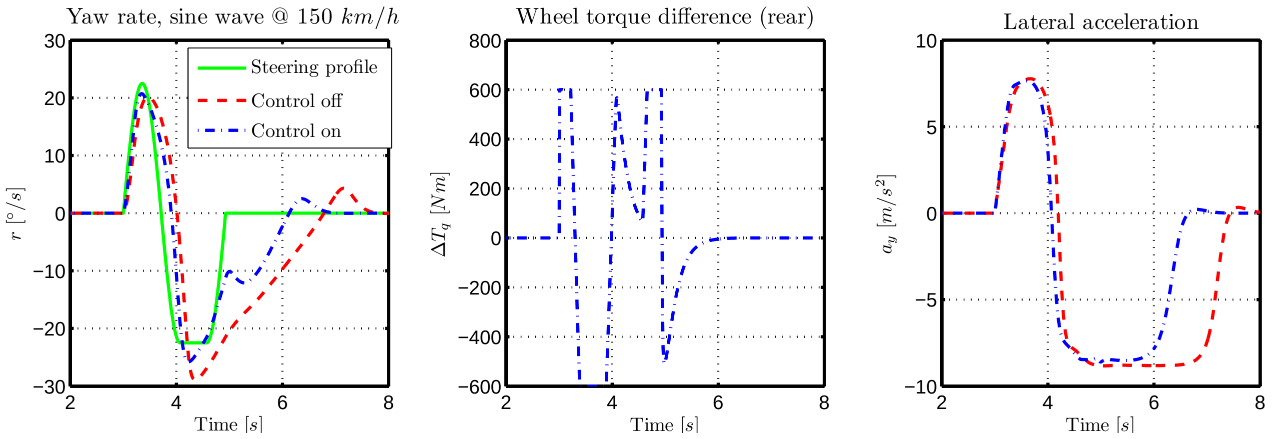

Figure D.1.15: *Controller performance in a sine with dwell steering manoeuvre at* 150 km/h *with* 45° *steering angle*

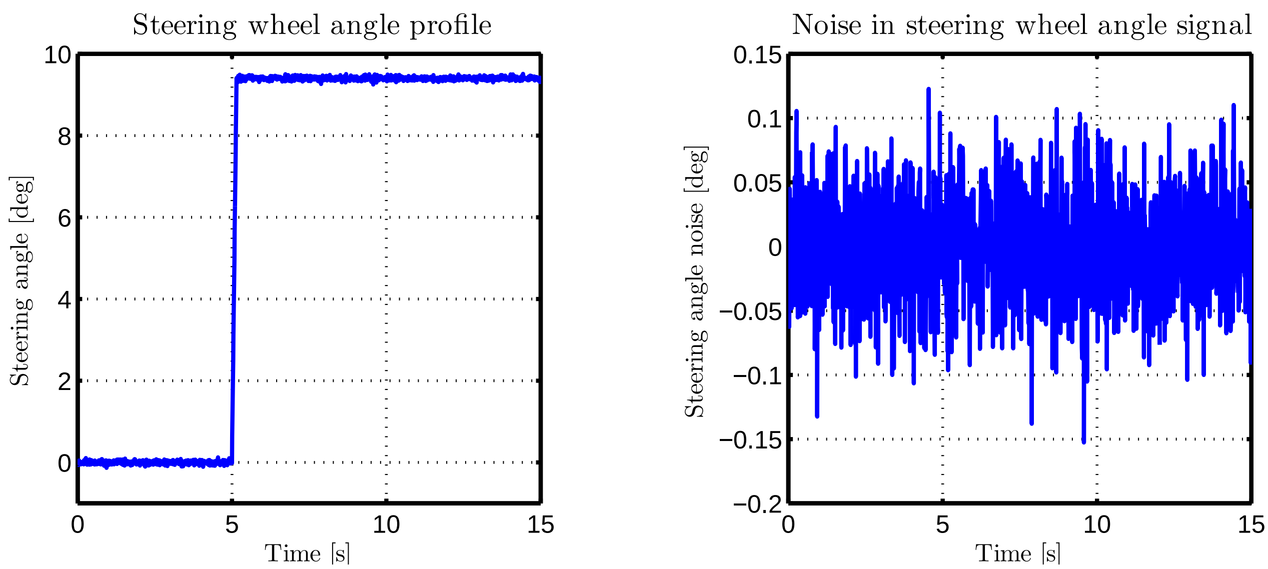

Figure D.1.16: *Steering angle profile with noise*

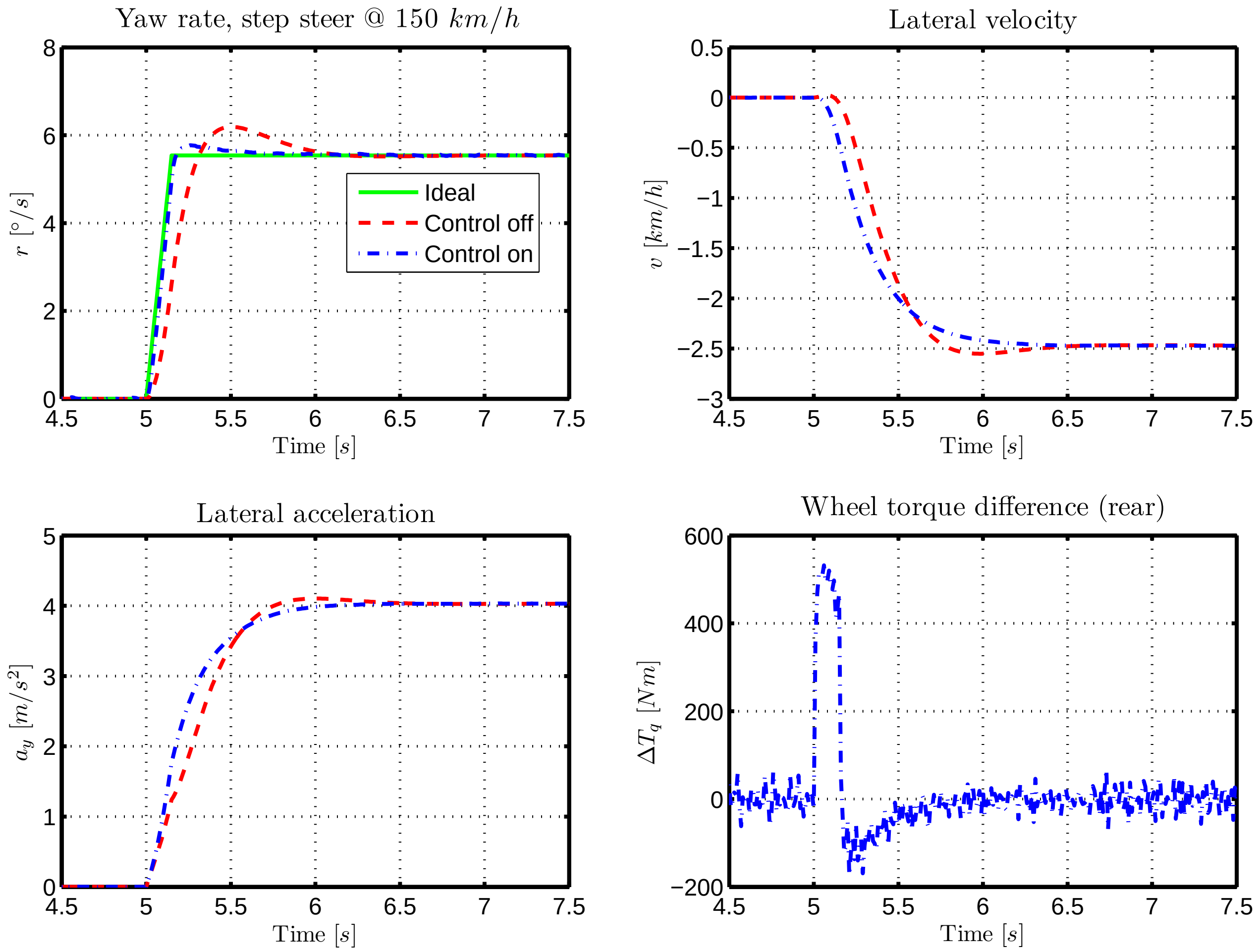

Figure D.1.17: *Performance of original controller in the presence of steering wheel angle noise*

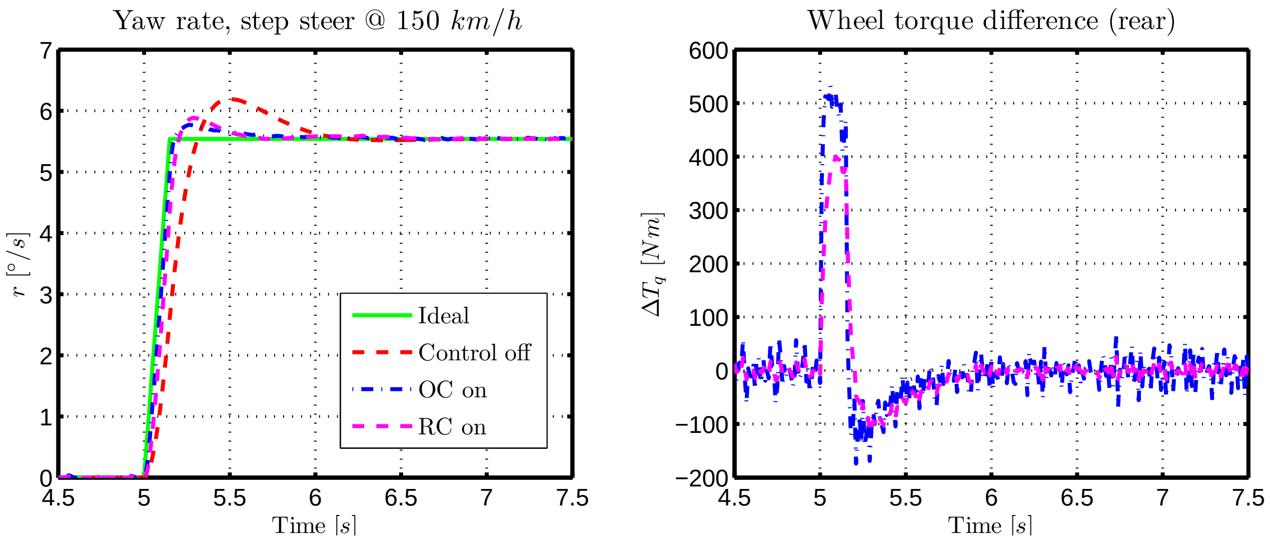

Figure D.1.18: *Performance of original controller (OC) and re-tuned controller (RC) in the presence of steering wheel angle noise*

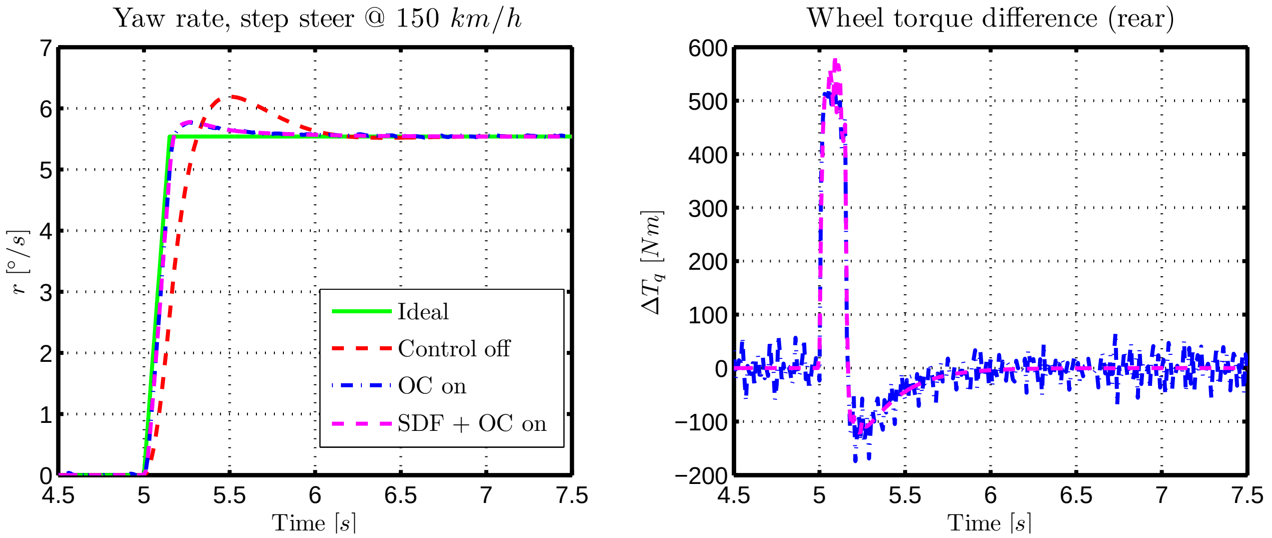

Figure D.1.19: *Performance of original controller (OC) with and without steering deadband filter (SDF) in the presence of steering wheel angle noise*

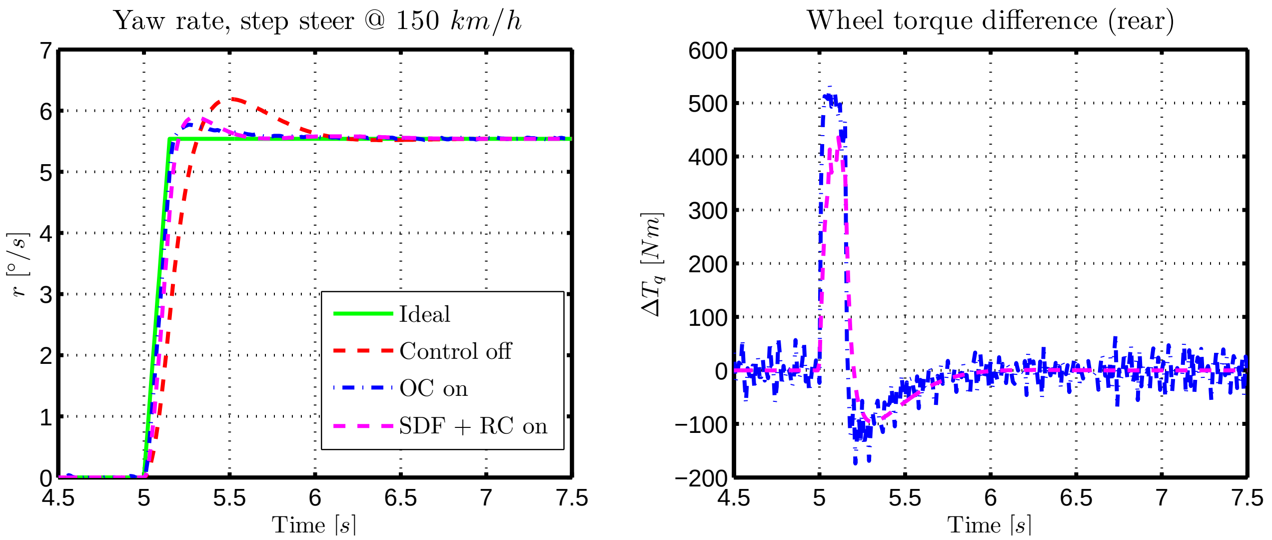

Figure D.1.20: *Performance of original controller (OC) and re-tuned controller (RC) with steering deadband filter (SDF) in the presence of steering wheel angle noise*

D.2 Model based controllers

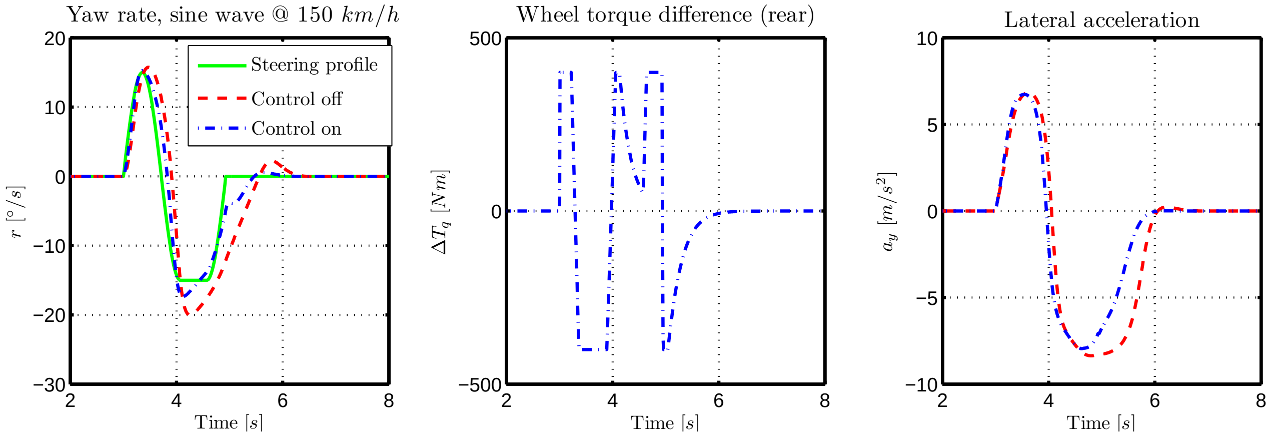

Figure D.2.1: *Performance of the model based controller I in a sine with dwell steering manoeuvre at* 150 km/h *with* 30° *steering angle*

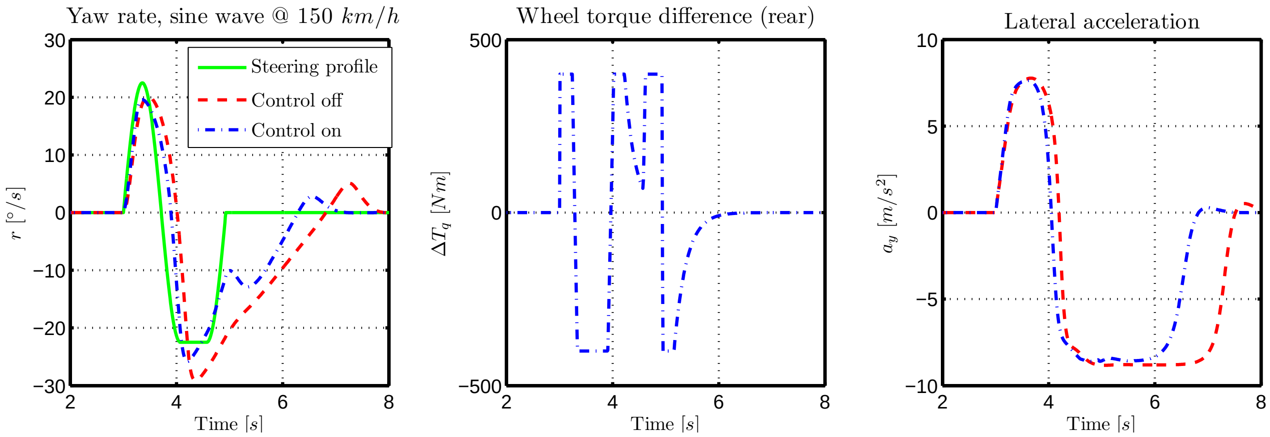

Figure D.2.2: *Performance of the model based controller I in a sine with dwell steering manoeuvre at* 150 km/h *with* 45° *steering angle*

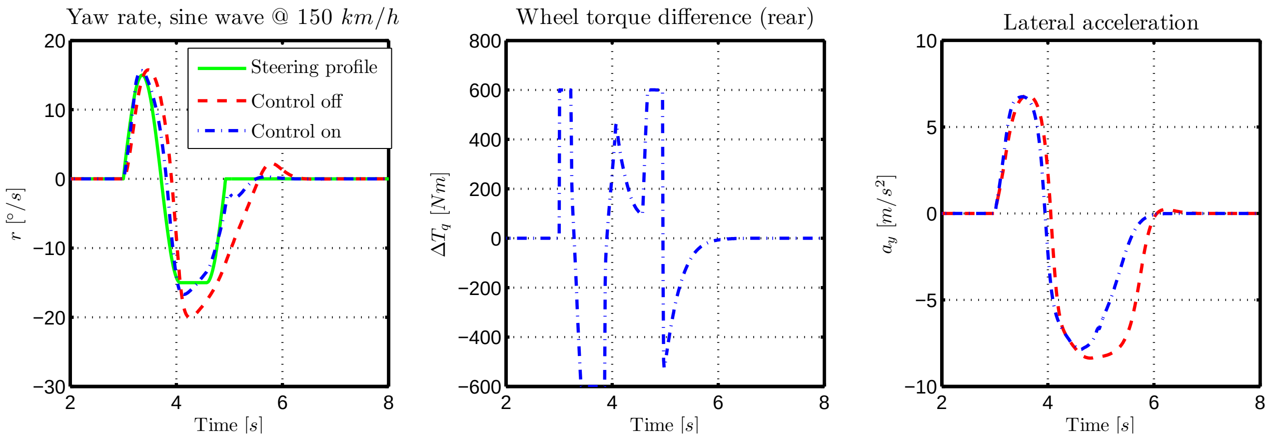

Figure D.2.3: *Performance of the model based controller II in a sine with dwell steering manoeuvre at* 150 km/h *with* 30° *steering angle*

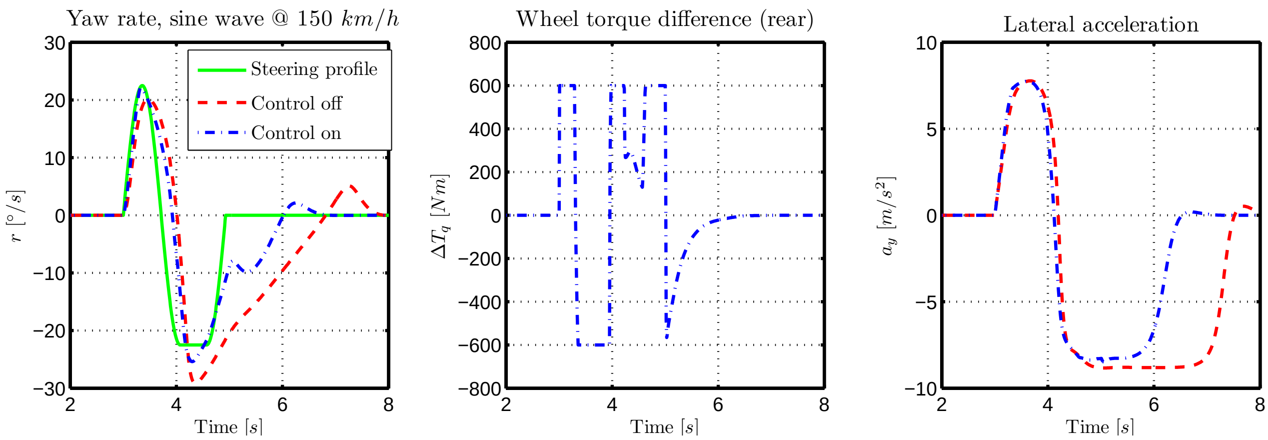

Figure D.2.4: *Performance of the model based controller II in a sine with dwell steering manoeuvre at* 150 km/h *with* 45° *steering angle*

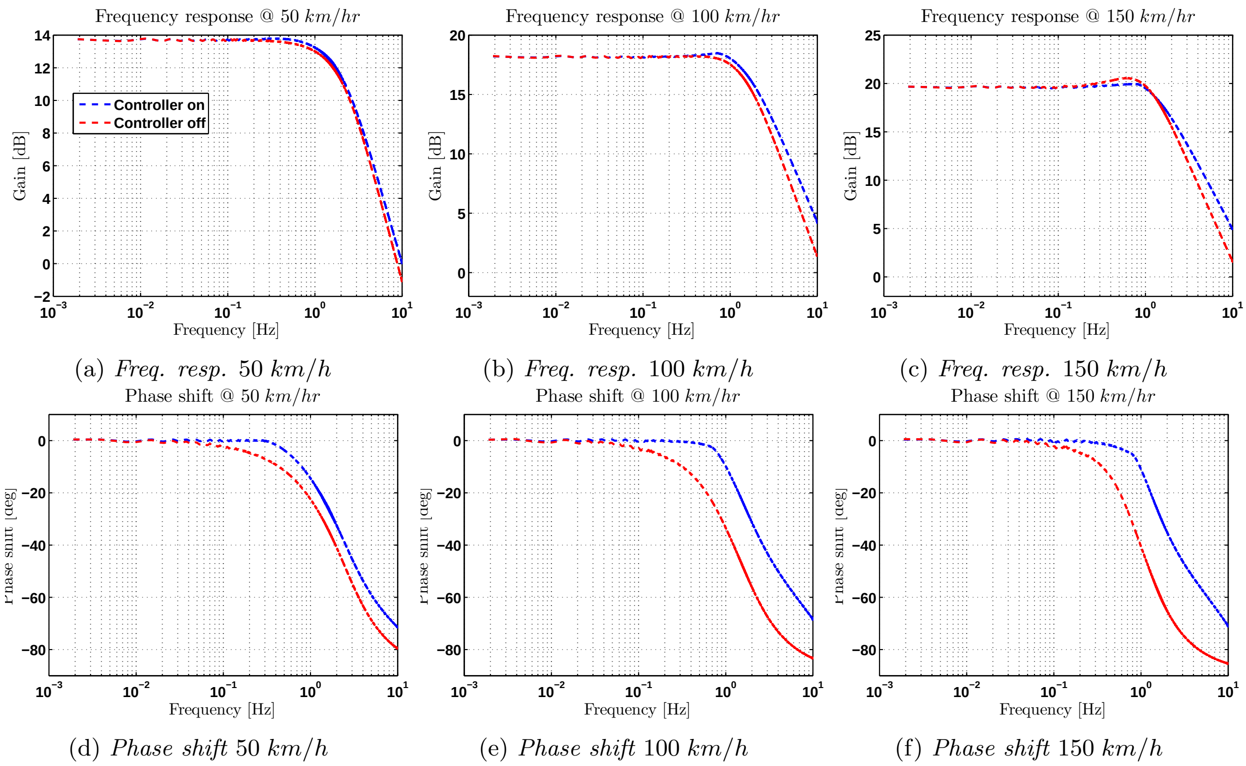

(a) *Freq. resp.* 50 km/h (b) *Freq. resp.* 100 km/h (c) *Freq. resp.* 150 km/h

(d) *Phase shift* 50 km/h (e) *Phase shift* 100 km/h (f) *Phase shift* 150 km/h

Figure D.2.5: *Frequency response and phase shift at* 4 m/s^2 *of the model based controller I*

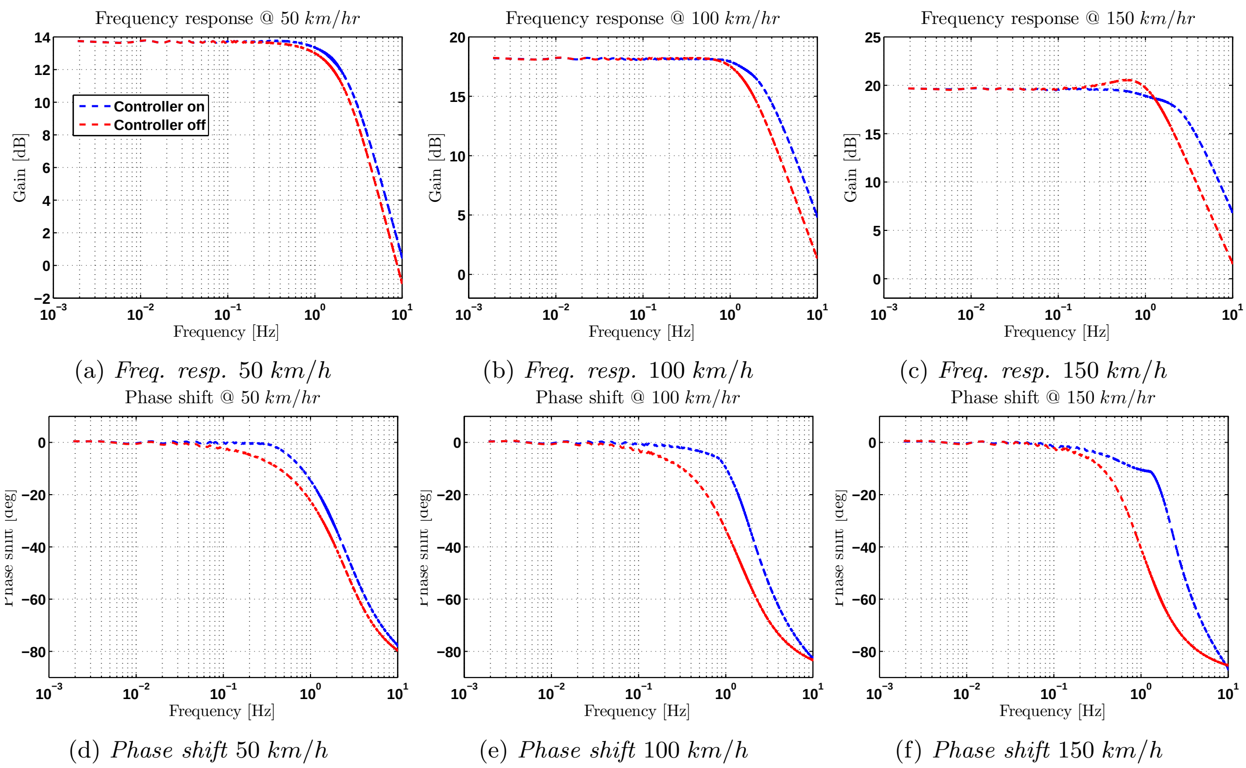

(a) *Freq. resp.* 50 km/h (b) *Freq. resp.* 100 km/h (c) *Freq. resp.* 150 km/h

(d) *Phase shift* 50 km/h (e) *Phase shift* 100 km/h (f) *Phase shift* 150 km/h

Figure D.2.6: *Frequency response and phase shift at* 4 m/s^2 *of the model based controller II*

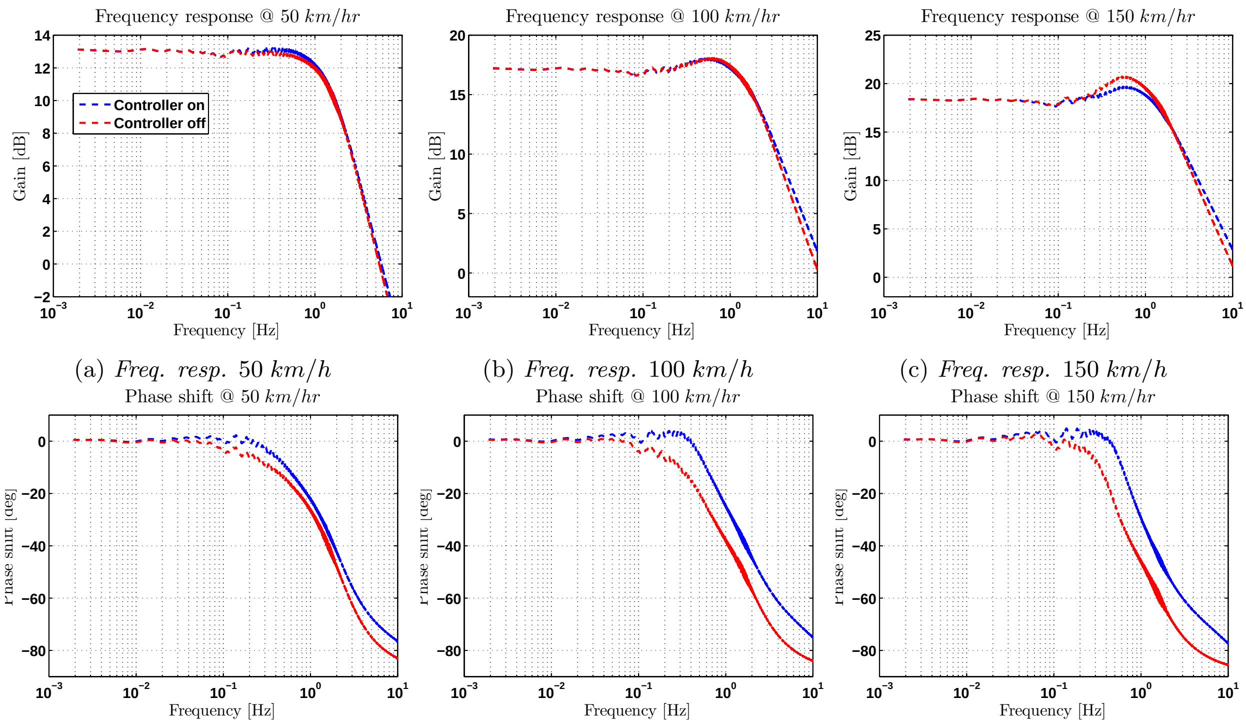

(a) *Freq. resp.* 50 km/h (b) *Freq. resp.* 100 km/h (c) *Freq. resp.* 150 km/h

(d) *Phase shift* 50 km/h (e) *Phase shift* 100 km/h (f) *Phase shift* 150 km/h

Figure D.2.7: *Frequency response and phase shift at* 7 m/s^2 *of the model based controller I*

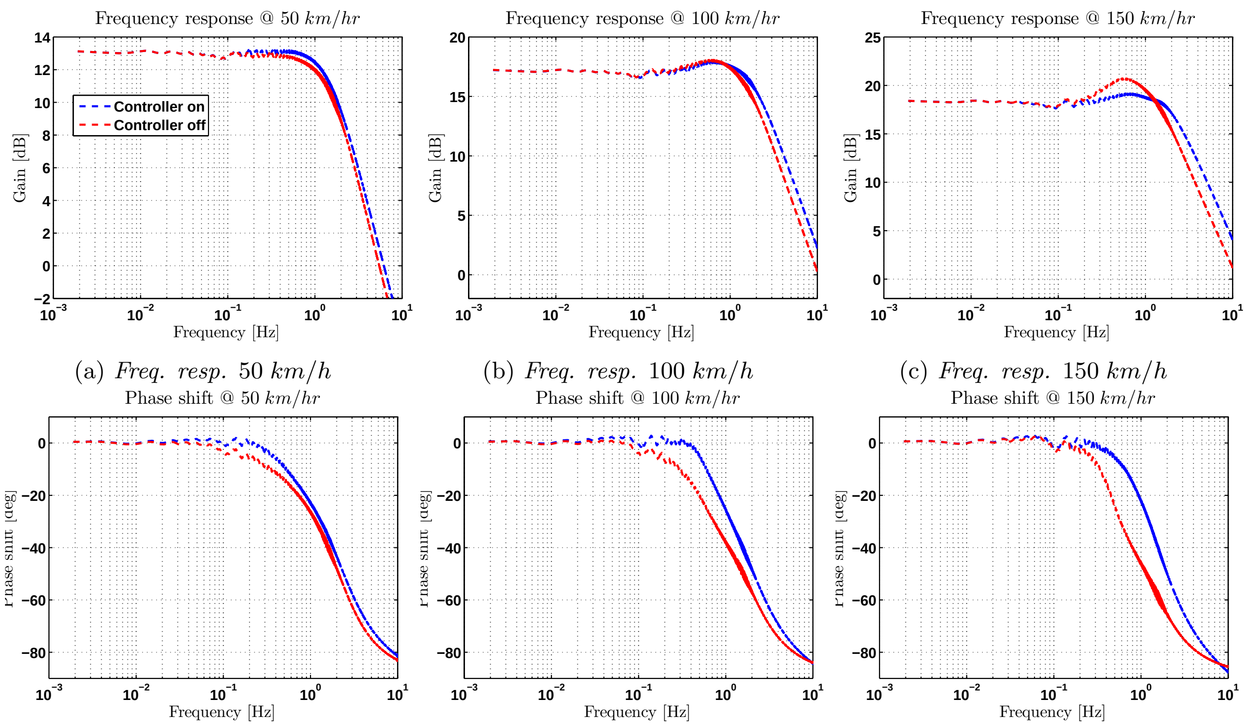

(a) *Freq. resp.* 50 km/h (b) *Freq. resp.* 100 km/h (c) *Freq. resp.* 150 km/h

(d) *Phase shift* 50 km/h (e) *Phase shift* 100 km/h (f) *Phase shift* 150 km/h

Figure D.2.8: *Frequency response and phase shift at* 7 m/s^2 *of the model based controller II*